Daniel Savitsky

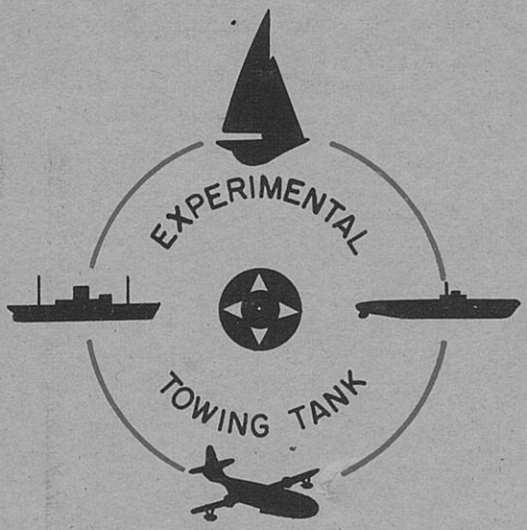

HYDRODYNAMIC DESIGN OF SEAPLANES II

S.I.T. GRADUATE SCHOOL COURSE F.D. 216

by

B. V. Korvin-Kroukovsky

Experimental Towing Tank
Stevens Institute of Technology
Hoboken, New Jersey

Table of Contents

1.	Introduction	page 1
2.	Fluid Flow	2
3.	Complex Variable	3
4.	Function of a Complex Variable	9
5.	Transformation	11
6.	Simple Transformations	13
7.	Theorem of Schwarz and Christoffel	15
8.	Application of the Schwarz-Christoffel Transformation to the flow in a right-angle corner.	17
9.	The Flow About a Submerged Plate	18
10.	Application to a Planing Surface	21
11.	Shape of the Wetted Area of a Vee Planing Surface	24
12.	Pressures Acting on the Wedge	25
13.	Discontinuous Fluid Flow	28
	The Function $\zeta = dz/dw$	29
	The Function $\Omega = \ln \zeta$	31
	Determination of the Constants P and Q	32
	Relation between w and t	33
	Definition and determination at the constant C	34
	Shape of the Free Streamlines	36
	Dynamic Pressures Acting on the Wedge in Weightless Fluid	37
14.	Flow in the spray root of a plate of infinite extent	40
	The transformation $(dz/dw) = f(t)$	42
	The transformation dw/dt	44
	The transformation dz/dt	46
	Flow Net	47
	Velocities and pressure distributions along solid boundary	48
15.	Comparison of Pressures from the Expanding Plate and from the Spray Root Theories	50

Table of Contents (Con't.)

16. The Flow at a Flat Planing Surface

Determination of γ_n

The Transformation dw/dt

Transformation dz/dt

Shape of the Free Boundary

Velocity and Pressure Distribution

on the Solid Boundary (the Planing Surface)

HYDRODYNAMIC DESIGN OF SEAPLANES II

S.I.T. Graduate School Course F. D. 216

B. V. Korvin-Kroukovsky

1. Introduction

In the first semester course, FD-215, we considered all aspects of the hydrodynamics of seaplane design, essentially in descriptive form. Such quantitative data as were given were based on the empirical study of the experimental data. We have referred to the spray root, or to the virtual mass, but did not go into the details of their definition. In this course we will concentrate specifically on the details of the fluid flow induced by a planing surface, treating the subject by the methods of mathematical physics. We will start by making a brief review of the parts of hydromechanics and of mathematics which we will need for this purpose.

The motion of a fluid, in our case of water, near the free surface on which the planing occurs, is governed by forces which have their origin in three properties of the fluid: inertia, weight (gravity forces) and viscosity. The complete solution, taking all three of these properties into account, is impossible, and it is always necessary to make approximations by considering the properties most important to the problem, and neglecting the less important ones. The choice of which properties to consider is governed primarily by the magnitude of the velocities involved, since inertial forces depend on the square of the speed, viscous forces are proportional to speed, and gravitational forces are constant and are independent of speed. Thus, for instance, in the case of the fluid seepage through porous soils, the velocities are very low and inertial forces can therefore be neglected in comparison with the predominating viscous forces, while the effect of gravity takes the simple form of the gravity potential, which causes the motion. In our immediate field of interest--the planing of a seaplane, the velocities are sufficiently high so that inertial forces strongly predominate over the viscous or gravity forces. We will proceed therefore on the assumption that only inertial forces will have to be considered, and will

neglect the viscosity and the gravity, i.e., we will deal with the weightless perfect fluid.

We can introduce from the outset a further simplification in our work by assuming the fluid motion in space to take place in two dimensions in a series of parallel planes, and by assuming that there is no flow from plane to plane. This we did already in the first part of the course in Fig. 34, in connection with the analysis of the impact. Confining the analysis to two-dimensional motion permits the use of functions of complex variables, as we shall see later, and this both simplifies and increases the power of the analysis.

2. Fluid Flow

Let us consider the simple motion of a fluid in a tube produced by the motion of the piston A (Fig. 1). The velocity U can be resolved into the component u parallel to the x axis and the component v parallel to the y axis. The motion can be considered as having been started initially by the force P normal to the face of the piston. The walls of the tube do not contribute any force, because the assumption of a perfect fluid implies that all tangential forces are equal to zero. Such a motion, which can be considered as having been started from rest by the action of the normal forces only, and in the absence of tangential forces, is called the "potential motion". We define the potential function ϕ as a function such that:

$$u = \frac{\partial \phi}{\partial x} \quad \text{and} \quad v = \frac{\partial \phi}{\partial y}. \qquad (1)$$

Strictly speaking, by comparison with the electric potential and the gravity potential, the definition should be:

$$u = -\frac{\partial \phi}{\partial x} \qquad v = -\frac{\partial \phi}{\partial y}.$$

This definition is used mostly by English writers (Lamb, Milne-Thomson). The minus sign, however, is omitted by many writers (Durand, Glauert), and we will follow this practice.

Since ϕ is a function of x and y, it will be expressed on Fig. 1

by a series of "equipotential lines" ϕ_1 , ϕ_2 , ϕ_3 , etc. For the straight tubes, these lines are straight and are equally spaced, since u and v are constant, but for a curved divergent flow they become a series of curves as shown on Fig. 2.

It will be noted that value of the potential at each equipotential line is obtained by integration of the equations (1), which involves the addition of an arbitrary constant. In the solution of any problem of hydrodynamics we obtain, therefore, only the relative spacing of the equipotential lines, but have free choice in designating any particular line as $\phi = 0$, the designations of all other lines immediately being determined by their distances from the line $\phi = 0$.

Equations (1) express the components of the velocity as the gradient of the potential in the x or y direction, or for the total velocity we can write:

$$U = \frac{\partial \phi}{\partial n}.$$

The potential is a scalar function, but the gradient is a vector function, since it involves the specification of a direction. In particular the gradient $\partial\phi/\partial n$ indicates the velocity vector which is normal to the equipotential line. The curves ψ_1, ψ_2, ψ_3 ... etc., on Figs. 1 and 2, drawn so that velocity vector at any point in a potential flow is tangent to the curve, are called streamlines. The streamlines ψ_1, ψ_2 ... etc., form therefore a family of curves orthogonal to the equipotential lines ϕ_1 , ϕ_2 ... etc., that is at each point of space the ψ curve is normal to the ϕ curve. The system of ϕ and ψ lines is called the flow net.

We will designate by s the distance measured along equipotential lines, and normal to streamlines, and we will designate by the name "flux" the quantity U x s, which represents the volume per second of the flowing fluid (for a "slice" of unit thickness). We start with an arbitrary point at which we call s = 0 and then designate by $\psi = 0$ the streamline for which the flux U x s = U x 0 = 0. Then the subsequent streamlines will be marked with the corresponding values of the flux $\psi_1 = Us_1$, $\psi_2 = Us_2$, etc. The flow net is constructed by taking equal increments of the flux U x Δs so that $\psi_1 = (\psi_2 - \psi_1) = (\psi_3 - \psi_2)$

etc. The function ψ defining the value of the flux, and defining the arrangement of the streamlines is called the "stream function".

Applying these definitions to the curvilinear flow net of Fig. 2, in which U is variable, we can write:

$$U = \frac{\partial \psi}{\partial s}.$$

On the basis of Fig. 3, for equal increments of ψ we can substitute $U = u/\cos\theta$ and $\Delta s = \Delta y \cos\theta$, so that

$$\frac{u}{\cos\theta} = \lim_{\Delta \to 0} \frac{\Delta \psi}{\Delta y \cos\theta}$$

or

$$u = \frac{\partial \psi}{\partial y} \qquad (2a)$$

Likewise substituting $U = v/\sin\theta$ and $s = -\Delta x \sin\theta$ gives

$$\frac{v}{\sin\theta} = \lim_{\Delta \to 0} \frac{\Delta \psi}{-\Delta x \sin\theta}$$

or

$$v = -\frac{\partial \psi}{\partial x}.$$

Equating equations (1) and (2) we obtain the Cauchy-Riemann Equations:

$$\left.\begin{aligned} u &= \frac{\partial \phi}{\partial x} = \frac{\partial \psi}{\partial y} \\ v &= \frac{\partial \phi}{\partial y} = -\frac{\partial \psi}{\partial x} \end{aligned}\right\}. \qquad (3)$$

By differentiating the first of equations (3) with respect to x and the second with respect to y, and by transposing, we obtain the two-dimensional form of the Laplace equation:

$$\left.\begin{aligned} \frac{\partial^2 \phi}{\partial x^2} + \frac{\partial^2 \phi}{\partial y^2} &= 0 \\ \text{and} \\ \frac{\partial^2 \psi}{\partial x^2} + \frac{\partial^2 \psi}{\partial y^2} &= 0 \end{aligned}\right\} \qquad (4)$$

It will be noted that both ϕ and ψ separately satisfy the Laplace equation. The Laplacian operator

$$\frac{\partial^2}{\partial x^2} + \frac{\partial^2}{\partial y^2}$$

is usually designated by ∇^2 or Del squared and Laplace's equation is written as

$$\nabla^2 \phi = 0 \quad \text{and} \quad \nabla^2 \psi = 0 \qquad (5)$$

It will be observed that the Cauchy-Riemann equations (3) and Laplace's equations (4) or (5) were derived above as a direct result of the initial assumption that the motion of the fluid was generated from rest under action of the normal pressures only, and that tangential forces are equal to zero (no viscosity, i.e., the perfect fluid), together with the definition of the potential function ϕ. The orthogonality of the curves ϕ = const. and ψ = const. immediately led to equations (3) and (4), which are in fact mathematical definitions of this orthogonality.

Conversely, if the functions describing a fluid flow are found to satisfy equations (3) or (5), the flow is the potential one, i.e. could have been generated from rest by the action of normal forces.

As you know from your course on theoretical hydrodynamics, Laplace's equation can also be derived from the equation of continuity

$$\frac{\partial u}{\partial x} + \frac{\partial v}{\partial y} = 0$$

which expresses the equality of the fluid flowing into and out of an infinitesimal volume of space in two-dimensional flow. In the particular case of potential motion, also known as irrotational, we can substitute $u = \partial\phi/\partial x$ and $v = \partial\phi/\partial y$, immediately obtaining the Laplace equation.

3. Complex Variables.

The Cauchy-Riemann and Laplace equations are also satisfied by a certain class of functions of a complex variable, which become very useful in the presentation of two-dimensional flow problems. We will proceed, therefore, with a brief review of the functions of a complex variable. We define the complex number z such that:

$$z = x + iy \tag{6}$$

where $i = \sqrt{-1}$, or $i^2 = -1$. Here x is called the real part and y the imaginary part. (The letter j is often used instead of i.) Referring to Fig. 4, known as the "Argand Diagram," we can interpret a complex number geometrically as the pair of real numbers which define the point P by measuring the distance x horizontally and the distance y vertically. Using polar coordinates, we can write $x = R\cos\theta$ and $y = R\sin\theta$, and therefore

$$z = R(\cos\theta + i\sin\theta) \tag{7}$$

where $R = (x^2 + y^2)^{1/2}$ and $\theta = \tan^{-1} y/x$.

Expanding $\cos\theta$ and $i\sin\theta$ in Taylor's Series, we obtain:

$$\cos\theta = 1 - \theta^2/2! + \theta^4/4! - \cdots$$

$$i\sin\theta = i\theta - i\theta^3/3! - i\theta^5/5! - \cdots$$

and

$$\cos\theta + i\sin\theta = 1 + i\theta - \theta^2/2! - i\theta^3/3! + \theta^4/4! - \cdots$$

The last series is identical with the expansion of

$$e^x = 1 + x + x^2/2! + x^3/3! + x^4/4! - \cdots$$

if we let $x = i\theta$, and remember that $i^2 = -1$, $i^3 = i \times i^2 = -i$, $i^4 = (-1)(-1) = 1$ etc. Therefore we have Euler's Theorem:

$$\cos\theta + i\sin\theta = e^{i\theta} \tag{8}$$

and

$$z = Re^{i\theta} \tag{9}$$

In this form R is called the Modulus and θ the argument or the amplitude. Equations 6, 7 and 9 show three ways of defining a point on the Argand diagram, or three equivalent forms of expressing a complex number, one or another of which may be used most conveniently in any given problem.

Equality of two complex numbers z_1 and z_2 implies the identity of the radius vectors R and therefore if $z_1 = z_2$, $x_1 = x_2$ and $y_1 = y_2$, i.e. both the real parts and the imaginary parts are equal.

Since two complex quantities z_1 and z_2 are represented on the Argand Diagram of Fig. 5 by radius vectors R_1 and R_2, the sum $z = z_1 + z_2$ must be obtained by the rule of vector addition, from which it follows (using the notation of Equation 6) that

$$z_1 + z_2 = (x_1 + iy_1) + (x_2 + iy_2) = (x_1 + x_2) + i(y_1 + y_2), \tag{10}$$

i.e. the real parts and the imaginary parts of complex numbers are added separately.

The multiplication of two complex numbers can be accomplished most conveniently by using the notation of Equation 9:

$$z_1 z_2 = (R_1 e^{i\theta_1})(R_2 e^{i\theta_2}) = R_1 R_2 e^{i(\theta_1 + \theta_2)} \tag{11}$$

i.e. in multiplying two complex numbers the moduli are multiplied, and the arguments are added.

Two complex numbers differing only in the sign of i are called conjugate numbers. Thus:

$$\left.\begin{aligned} z &= x + iy = Re^{i\theta} \\ \text{and} \\ z &= x - iy = Re^{-i\theta} \end{aligned}\right\} \tag{12}$$

are conjugate numbers. If z is a complex number, its conjugate is denoted by the bar placed over the original symbol. It is clear from the above that the sum of a complex number and of its conjugate is a real number:

$$z + \bar{z} = 2x \tag{13}$$

and the difference is a pure imaginary number

$$z - \bar{z} = 2iy. \tag{14}$$

Using the notation of Equation 9, we find that the product of the real number and of its conjugate is real, and is equal to the square of the modulus:

$$z\bar{z} = (Re^{i\theta})(Re^{-i\theta}) = R^2 e^{i(\theta-\theta)} = R^2. \tag{15}$$

The ability to express a complex number in three equivalent forms gives great flexibility to the analysis. For this reason it is often desirable to carry out an analysis of real functions in terms of complex numbers. This can be done either by designating that only real part of the complex numbers involved is to be taken into account, as for instance:

$$\phi = Re\,[f(z)]$$

or by expressing a real number as a sum of a complex number and of its conjugate.

The division of one complex number by another in the notation of Equation (6) is accomplished by multiplying the nominator and the denominator by the conjugate of the denominator:

$$\frac{z_1}{z_2} = \frac{x_1 + iy_1}{x_2 + iy_2} = \frac{(x_1+iy_1)(x_2-iy_2)}{(x_2+iy_2)(x_2-iy_2)} = \frac{(x_1+iy_1)(x_2-iy_2)}{x_2^2+y_2^2}. \tag{16}$$

In many problems in fluid flow the Laplace equation, which has two roots, is satisfied by a complex number, and by its reciprocal, and therefore it is of interest to consider the meaning of this reciprocal $1/z = \frac{1}{R} e^{-i\theta}$. Let Fig. 6 be the Argand Diagram, on which the circle of the modulus R = 1 is drawn. Consider the point P, out-

side of this unit circle, given by the complex number $z = R e^{i\theta}$. Consider the point A, inside of the circle such that $OQ_1 \cdot OP = 1$, or $OQ_1 = 1/OP$. Thus if $R = OP$ is the modulus of z corresponding to the point P, $1/R$ is the modulus of the complex number corresponding to the point Q_1. The argument $-i\theta$ corresponds to its conjugate Q.

Since many solutions of flow problems will involve logarithms, we will now write the expression for the logarithm of a complex number.

The form of Equation (9) is evidently most suitable for this purpose:

$$\log z = \log R e^{i\theta + 2ni\pi} = \log R + i\theta \times 2n\pi = \frac{1}{2}\log(x^2+y^2) + i\tan^{-1}\frac{y}{x} + 2n\pi \quad (17)$$

Multiplication by i is equivalent to the rotation of a vector by 90°, since $i = \cos\frac{\pi}{2} + i\sin\frac{\pi}{2}$ and

$$iz = Re^{i\theta} e^{i\pi/2} = Re^{i(\theta+\pi/2)}.$$

Also the reciprocal:

conjugate No.

$$1/i = \cos\frac{\pi}{2} - i\sin\frac{\pi}{2} = -i. \quad (18)$$

4. Functions of a Complex Variable.

The Argand diagram representing the function z, with axes x and y is called the "z plane". It is the plane of the physical dimensions of the space in which we operate. Since the fluid flow is represented by the network of orthogonal lines ϕ = const. and ψ = const., we can also represent it as a complex number $w = \phi + i\psi$, which is called the "complex potential." The solution of a flow problem will consist in establishing the functional relation between w and z, i.e by expressing $w = w(z) = w(x + iy)$ or inversely $z = z(w) = z(\phi + i\psi)$.

We shall limit our discussions to the functions $w = w(z)$ such that within a certain range of values of z, defined by the contour C on Fig. 7, the following conditions are satisfied:

a. To each value of z there corresponds one, and only one, finite value of f(z). In other words, f (z) is finite and single-valued within the contour C.

b. For each value of z within the contour C there exists a single-valued and finite derivative of (z) with respect to z. The functions satisfying these two conditions are called "analytic", "holomorphic" or "regular".

We shall proceed now with a detailed examination of the second of conditions--that the function shall possess a finite derivative.

By definition, the derivative d w (z)/d z is

$$\frac{dw(z)}{dz} = \lim_{\Delta z \to 0} \frac{w(z+\Delta z) - w(z)}{\Delta z}$$

In this case z, w and Δ z are vectors, and Δ z has both magnitude and the direction, as shown on Fig. 8. In order that the derivative may have a unique value it must be independent of the manner in which Δ z approaches zero. In particular it must have the same value for the vector Δ z parallel to the x axis or parallel to the y axis, i.e., whether the point z + Δ z approaches z with y = const. and x variable, or x = const. and y variable. In the first case we have Δ z = Δ x, and

LOOK INTO

$$\frac{w(z+\Delta z)-w(z)}{\Delta z} = \frac{\phi(x+\Delta x, y)-\phi(x,y)}{\Delta x} + i\,\frac{\psi(x+\Delta x, y)-\psi(x,y)}{\Delta x}$$

and in the limit

$$\frac{dw(z)}{dz} = \frac{\partial \phi}{\partial x} + i\,\frac{\partial \psi}{\partial x}. \qquad (19)$$

In the second case Δ z = i Δy, and

$$\frac{w(z+\Delta z)-w(z)}{\Delta z} = \frac{\phi(x, y+\Delta y)-\phi(x,y)}{i\Delta y} + i\,\frac{\psi(x, y+\Delta y)-\psi(x,y)}{i\Delta y}$$

or in the limit

$$\frac{dw(z)}{dz} = -i\,\frac{\partial \phi}{\partial y} + \frac{\partial \psi}{\partial y}. \qquad (20)$$

In order that the function w (z) may have a unique derivative, it is necessary that (19) be equal to (20), and therefore that

equating real and imaginary parts.

$$\frac{\partial \phi}{\partial x} = \frac{\partial \psi}{\partial y} \quad ; \quad \frac{\partial \phi}{\partial y} = -\frac{\partial \psi}{\partial x}. \qquad (21)$$

These are the same Cauchy-Rieman equations (3) which were derived originally as the direct consequence of the orthogonality of ϕ and ψ functions in a potential fluid flow. In the present case they were derived as a direct consequence of the postulate that the functions, defined as holomorphic, have a unique derivative. Thus the "holomorphic" or "regular" functions of a complex variable represent possible patterns of a potential, or irrotational, fluid flow.

The Cauchy-Riemann equations represent a necessary, but not a sufficient, condition for potential flow. In addition, it is necessary that all the partial derivatives $\partial\phi/\partial x$, $\partial\phi/\partial y$, $\partial\psi/\partial x$ and $\partial\psi/\partial y$ be continuous. In application to fluid flow, these derivatives represent the components of the fluid velocity, which are necessarily continuous, except at certain exceptional points (Ref. 1, Art. 5.30).

More rigorous treatment of the derivative, and of the Cauchy-Riemann equations will be found on page 448 of Ref. 2 and an excellent detailed treatment is given on pages 377-385 of Ref. 3.

5. Transformation

The relation between two real variables, say x and y, can be expressed on a single diagram by plotting $y = y(x)$ as ordinates vs. x as abscissae. However, the complex number $z = x + iy$ requires the entire two dimensional diagram for its presentation. If $z = x + iy$ is taken to be an independent variable and $\zeta = \xi + i\eta$ to be the dependent variable $\zeta = \zeta(z)$, two diagrams are required to show the relation between z and ζ. The definition of $\zeta = \zeta(z)$ by means of two Argand diagrams is known as the "conformal transformation" or "conformal mapping". The word "conformal" emphasizes the fact that in the process of transformation all angles between sections of lines of infinitesimal length are identical on the two diagrams, and that infinitesimally small figures are of identical proportions. We will proceed with a demonstration of these properties of conformal transformations.

Let Fig. 9 represent the functional relation $\zeta = \zeta(z)$ by means of two Argand diagrams--a z plane and a ζ plane. Let the complex numbers z, z_1 and z_2 be represented by the points P, P_1 and P_2 of the z plane,

and the numbers ζ, ζ and ζ_2 by the points Q, Q_1 and Q_2 of the ζ plane. Form the ratios

$$\frac{\zeta_1 - \zeta}{z_1 - z} = \frac{f(z_1) - f(z)}{z_1 - z}$$

and

$$\frac{\zeta_2 - \zeta}{z_2 - z} = \frac{f(z_2) - f(z)}{z_2 - z}.$$

If the vectors $z_1 - z$ and $z_2 - z$ be made vanishingly small, the above ratios will represent derivatives, i.e.

$$\frac{\zeta_1 - \zeta}{z_1 - z} = \frac{d\zeta}{dz} = f'(z)$$

and

$$\frac{\zeta_2 - \zeta}{z_2 - z} = \frac{d\zeta}{dz} = f'(z).$$

Since the derivative of a holomorphic function has the same value for any direction of the vanishing vector Δz, the above ratios are equal, i.e.

$$\frac{\zeta_1 - \zeta}{z_1 - z} = \frac{\zeta_2 - \zeta}{z_2 - z} = \frac{d\zeta}{dz}$$

or, expressing the vectors $\zeta_1 - \zeta$, $z_1 - z$, etc. in exponential form,

$$\frac{r_1 e^{i\theta_1}}{R_1 e^{i\Theta_1}} = \frac{r_2 e^{i\theta_2}}{R_2 e^{i\Theta_2}},$$

where r_1 is the modulus of the vector QQ_1, i.e. the length of it, r_2 the length of the vector QQ_2 etc. Equality of two complex numbers indicates the equality of the moduli and of the arguments, and therefore $\frac{r_1}{R_1} = \frac{r_2}{R_2}$, or $\frac{QQ_1}{PP_1} = \frac{QQ_2}{PP_2}$, and

$$\frac{e^{i\theta_1}}{e^{i\Theta_1}} = \frac{e^{i\theta_2}}{e^{i\Theta_2}}.$$

Since the arguments are equal the angles are also equal, i.e.

$$\angle P_1 P P_2 = \angle Q_1 Q Q_2.$$

Thus, in the process of the transformation, angles are preserved and lengths remain proportional to each other, i.e. the figure changes its size, but retains its proportions. The particularly important part of these properties is that the right angles between the curves x = const.

and y = const. in the z plane remain right angles between the curves ξ = const. and η = const. in the ζ plane, i.e. the orthogonal set of curves in the z plane is mapped as an orthogonal set on the ζ plane.

6. Simple Transformations

Assume that in taking on a number of values the independent variable z traces the continuous contour C_1 in the z plane of Fig. 10. The dependent variable $\zeta = \zeta(z)$ will likewise trace a continuous contour in the ζ plane. The transformation consisting of the addition of a real constant,

$$\zeta = z + a = (x+a) + iy \qquad (22)$$

will map the contour C_1 in the z plane into the contour C_2 in the ζ plane, i.e. will consist of a horizontal displacement. The addition of an imaginary number

$$\zeta = z + ib = x + i(y+b) \qquad (23)$$

will result in a vertical displacement, i.e. the contour C_3, and the addition of a complex number

$$\zeta = z + (a+ib) = (x+a) + i(y+b) \qquad (24)$$

will result in a combined displacement in both directions.

Multiplication by a real constant,

$$\zeta = az = ax + iay = (aR)e^{i\theta}, \qquad (25)$$

results in a change of scale of the figure, retaining the same proportions, as in contour 4 on Fig. 11,

Multiplication by a complex number,

$$\zeta = zre^{i\phi} = (Re^{i\theta})(re^{i\phi}) = Rre^{i(\theta+\phi)} \qquad (26)$$

represents a change of the scale of the contour by the factor r and a rotation of it through the angle ϕ, as in Fig. 12.

Any fluid flow is represented in the w plane--Fig. 12--by a series of equipotential lines parallel to the vertical axis and the streamlines parallel to the horizontal axis. This is merely the matter of definition of the complex potential $w = \phi + i\psi$. The problem consists in finding the form of the corresponding curves ϕ = const. and ψ = const. in the z plane. For instance consider the transformation

$$w = w(z) = z^2 \tag{27}$$

or

$$\phi + i\psi = x^2 - y^2 + 2ixy$$

and therefore:

$$\begin{aligned} \phi &= x^2 - y^2, \\ \psi &= 2xy. \end{aligned} \tag{28}$$

The equipotential lines ϕ = const. are rectangular hyperbolae constructed on the axes OX and OY as shown on Fig. 13 and the streamlines ψ = const. are rectangular hyperbolae with axes OX and OY as asymptotes. Fig. 13 shows therefore the flow of a fluid inside a rectangular corner.

As another example consider the transformation

$$w = f(z) = z + 1/z \tag{29}$$

or

$$\phi + i\psi = x + iy + \frac{1}{x+iy} = x + iy + \frac{x - iy}{x^2+y^2}$$
$$= \frac{x(x^2+y^2+1)}{x^2+y^2} + i\,\frac{y(x^2+y^2-1)}{x^2+y^2}.$$

Separating the real and imaginary parts,

$$\phi = \frac{x(x^2+y^2+1)}{x^2+y^2}$$

and (30)

$$\psi = \frac{y(x^2+y^2-1)}{x^2+y^2}.$$

For the particular streamline $\psi = 0$ we have two solutions:

$$y = 0 \qquad \text{and} \qquad x^2 + y^2 = 1.$$

The first represents the x axis, while the second represents a cylinder of unit radius. The transformation thus gives the flow about a cylinder immersed in a uniform stream, as shown in Fig. 14. For very large values of z, 1/z can be neglected and we have $\phi = x$ and $\psi = y$, which are the equations of a uniform stream of unit velocity parallel to the x axis.

7. Theorem of Schwarz and Christoffel

We have considered above two simple forms of transformation. Many other examples will be found in references 1, 2 and 3, and a mathematical physicist is supposed to be familiar with them. In general, however, it is difficult to determine the transformation formula which is needed for a particular problem. Often the problem of establishing the correspondence between the z plane and the w plane is facilitated by an intermediate step of introducing an auxiliary t plane, so that $z = f(t)$. Then $w = w(t)$ can be established more easily than the final expression $w = w(z)$. A particularly simple form of the complex t plane is chosen, represented by the real axis as on Fig. 15 (a), in which the region above this axis only is considered. The theorem of Schwarz and Christoffel provides the means of deriving the formula for transformation of the "upper half of the t plane" into the interior of a closed polygon in the z or w plane, so that the real t axis becomes the boundary of the polygon. We will see later how the solution of many problems will depend on this step.

It must be noted that as long as complex functions are dealt with, the Cauchy-Riemann and Laplace equations will be satisfied, and the particular solution will depend on the conditions at the boundaries. If a functional relation between two complex planes is found, such as to provide a correspondence between the boundaries in these planes, it is the transformation required for the solution of a particular problem.

The Schwarz-Christoffel theorem is expressed in the form of the differential equation

$$\frac{dz}{dt} = A(t-a)^{\frac{\alpha}{\pi}-1}(t-b)^{\frac{\beta}{\pi}-1}(t-c)^{\frac{\gamma}{\pi}-1} \cdots\cdots\cdots \quad (31)$$

where a, b, c.....are real quantities ranging from $-\infty$ to $+\infty$ so

that $a < b < c.....$, and α, β, γ .....are the internal angles of an n-sided polygon so that

$$\alpha + \beta + \gamma = (n-2)\pi.$$

Consider Fig. 15 (a) to represent the real axis of the t plane. The variable t, always remaining real, designates a point moving along the real axis in the t plane from $+\infty$ to $-\infty$. The constant coefficient A may be either real or complex. Fig. 15 (b) represents the corresponding polygon in the z plane, with corresponding vertices designated a, b, c.....

In order to understand the significance of Eq. 31, consider the variation with t of the complex quantity.

$$\delta z = A\,\delta t\,(t-a)^{\frac{\alpha}{\pi}-1}(t-b)^{\frac{\beta}{\pi}-1}(t-c)^{\frac{\gamma}{\pi}-1} \quad \text{---} \quad (32)$$

Consider the point t moving from right to left. As long as t lies to the right of the point c, i.e. $a < b < c < t$, all the variable factors in the expression (32) will remain real. This implies that only the modulus of δz will change in value with changes of t, while its argument, i.e. its inclination, will remain fixed. The representative point in the z plane will consequently move in a straight line.

After passing through the point $t = c$, $(t - c)$ becomes negative, and a negative quantity raised to a fractional power usually becomes complex. Transpose the negative term $(t - c)$ as follows:

$$(t-c)^{\frac{\gamma}{\pi}-1} = (c-t)^{\frac{\gamma}{\pi}-1}(-1)^{\frac{\gamma}{\pi}-1}$$

and note that

$$(-1)^{\frac{\gamma}{\pi}-1} = (\cos\pi - i\sin\pi)^{\frac{\gamma}{\pi}-1} = e^{-i\pi(\frac{\gamma}{\pi}-1)}$$
$$= e^{-i(\gamma-\pi)} = \cos(\pi-\gamma) + i\sin(\pi-\gamma). \quad (33)$$

Since the argument of the product of two complex numbers is the sum of the arguments of the two constituents, the argument of δz after passing through the point A has increased by $\pi - \gamma$, and from then onward maintains a constant angle until it arrives at the point b. The corresponding figure in the z plane, Fig. 15 (b), clearly

consists of two sides of a polygon with a difference of the angles of inclination of $\pi - \gamma$.

The final formula for the transformation is derived by the integration of Eq. (31):

$$z = A\int (t-a)^{\frac{\alpha}{\pi}-1} (t-b)^{\frac{\beta}{\pi}-1} (t-c)^{\frac{\gamma}{\pi}-1} \ldots dt + B, \quad (34)$$

where B is the constant of integration.

In the above paragraphs, an attempt was made to explain (not to prove) the Schwarz-Christoffel theorem in the simplest and most concise way, essentially following Ref.(5). For a more complete and more rigorous treatment the reader is referred to Article 10.2 of Ref. 1 and Article 85 of Ref. 4. Since the latter was used in the prerequisite course FD-204, and is readily available, Articles 85 to 92 inclusive will be considered as a part of the present course.

8. Application of the Schwarz-Christoffel Transformation to the flow in a right-angle corner.

We wish to construct the flow net for the flow of fluid in a right-angle corner, which we will take as the first quadrant bounded by positive y and x axes, designated as the z plane on Fig. 16 (a). Fig. 16 (b) designates, as usual, the real axis of the t plane, and Fig. 16 (c) the w plane. One of the streamlines will follow the boundary, and we will designate it by $\psi = 0$. This streamline is intersected by a number of equipotential lines, and we designate by $\phi = 0$ the equipotential line passing through the corner 0. We have to take three distinct steps:

a. Establish the transformation $z = z(t)$.

b. Establish the transformation $w = w(t)$.

c. Eliminate t from these relations to get $w = w(z)$.

For the first step we let the origin 0 of the t plane correspond to the origin 0 of the z plane, and let $t = \infty$ to correspond to $z = \infty$. We have one vertex of the closed polygon at 0 with an internal angle of $\pi/2$ and all other vertices at infinity. Application of the Schwarz-Christoffel theorem gives:

$$z = A\int (t-0)^{\frac{\pi}{2\pi}-1}\,dt + B$$
$$= A\int t^{-1/2}\,dt + B = 2At^{1/2} + B.$$

The constant B = 0 since z = 0 when t = 0,
and we have

$$z = 2At^{1/2} \qquad \text{or} \qquad t = \frac{z^2}{4A^2}. \tag{35}$$

For the second step we observe that the streamline hugging the boundary $\psi = 0$ is the real axis of the w plane, which can be associated directly with the real axis of the t plane. The transformation $w = w(t)$ is therefore merely an adjustment of the scale, and we can write

$$w = kt \qquad \text{or} \qquad t = w/k \tag{36}$$

where k is a real constant.

Equating expressions (35) and (36) gives:

$$w = Cz^2 \tag{37}$$

where all the constants have been lumped under C.

This equation is identical with Eq. (27) for C = 1, and separation of the variables gives Eqs. (28). Since the real values of w correspond to real values of z (in the flow along the x axis), the constant C is real. It is therefore a proportionality factor depending on scale, and the data of the present problem are not sufficient for its evaluation.

9. The flow about a submerged plate.

We will consider now a more practical problem of the fluid flow about a thin plate in a uniform stream. Let Fig. 17 represent the z plane, in which CC' is the plate, placed normal to the x axis, and assume the uniform fluid velocity V at infinity parallel to the x axis. Designate by $\psi = 0$ the streamline ABCDA', and since the flow is symmetrical consider only the upper half of it, which can be associated with the upper half of the w plane, which is the same as in Fig. 16 (c).

As a first step we map the upper half of the z plane in Fig. 17 onto the upper half of the t plane. We associate various values of t with the corners of the closed polygon on z plane as follows:

Vertex A--corresponds to $t = -\infty$ (at infinity)

Vertex B--corresponds to $t = -1$

Vertex C--corresponds to $t = 0$

Vertex D--corresponds to $t = +1$

Vertex A'--corresponds to $t = +\infty$ (at infinity)

The internal angles of the polygon are:

$\pi/2$ at B and D (i.e. at $t = 1$ and $t = -1$)

2π at C (i.e. at $t = 0$).

Applying the Schwarz-Christoffel theorem:

$$\frac{dz}{dt} = A(t+1)^{-1/2}\, t\, (t-1)^{-1/2} = At(t^2-1)^{-1/2} \qquad (38)$$

$$\therefore \quad z = A(t^2-1)^{1/2} + B. \qquad (39)$$

Let the origin of the z plane be taken at B (or D) so that $z = 0$ for $t = \pm 1$. This determines $B = 0$. At the point C, $Z = iL$, where L is the half breadth of the plate and $t = 0$.

$$z = iL = A(-1)^{1/2} = iA$$

which gives $A = L$, so that we have

$$z = L(t^2-1)^{1/2} \qquad (40)$$

As in the previous example, the upper half of w plane is associated with the upper part of the t plane, and the real axis $\psi = 0$ with the real axis of the t plane. Again, if $\phi = 0$ is assigned to the equipotential line passing through the point C (i.e. $t = 0$), we have

$$w = kt. \qquad (41)$$

The constant k is again real, and this time it can be evaluated, since the statement of the problem provides a sufficient number of boundary conditions. It depends on the conditions at infinity where the fluid has a uniform horizontal velocity V. Therefore, from (38) and (41)

$$V = \frac{dw}{dz} = \frac{dw}{dt}\frac{dt}{dz} = k\,\frac{(t^2-1)^{1/2}}{Lt};$$

for $|t| \to \infty$, $V = k/L$,

i.e. $$k = LV, \tag{42}$$

so that we have two parametric equations in t:

$$\left.\begin{aligned} w &= LVt \\ \text{and} \quad z &= L(t^2-1)^{1/2} \end{aligned}\right\} \tag{43}$$

or $$z^2 = L^2(t^2-1) = \frac{w^2 - L^2V^2}{V^2}$$

and $$w^2 = V^2(z^2+L^2). \tag{44}$$

The transformation is now completed, and all that remains is to separate the variables:

$$\phi^2 - \psi^2 + 2i\phi\psi = V^2(x^2 - y^2 + 2ixy + L^2)$$

and therefore:

$$\left.\begin{aligned} \phi^2 - \psi^2 &= V^2(x^2 - y^2 + L^2) \\ \phi\psi &= V^2 xy \end{aligned}\right\} \tag{45}$$

and solving these equations for ϕ and ψ gives:

$$\left.\begin{aligned} \phi^4 - V^2(x^2 - y^2 + L^2)\phi^2 - V^4x^2y^2 = 0 \\ \psi^4 + V^2(x^2 - y^2 + L^2)\psi^2 - V^4x^2y^2 = 0 \end{aligned}\right\} \tag{46}$$

The flow is completely determined by two parameters: the velocity V at infinity, and the half breadth of the plate L. The flow is symmetrical, both in regards to the centerline, or the dividing streamline $\psi = 0$, and about the plate, which coincides with the equipotential line $\phi = 0$. Equations (46) are satisfied therefore for either positive or negative values of ϕ and ψ.

On the surface of the plate $\psi = 0$ and x = 0 and the first of Eqs. (45) becomes

$$\phi^2 = V^2 (L^2 - y^2)$$

or

$$\phi = \pm V (L^2 - y^2)^{1/2} \qquad (46a)$$

and the velocity

$$v = \frac{\partial \phi}{\partial y} = \mp \frac{V y}{(L^2 - y^2)^{1/2}}. \qquad (46b)$$

The velocity is zero at the points B and D when y = 0, and these points are called "stagnation points". The velocity approaches infinity at the edges of the plate, as y approaches L.

In the subsequent problem we will be interested in the horizontal component of velocity U for the points in line with the plate and outside of it, for which $\chi = 0$, $\phi = 0$ and $\psi = 0$. Eq. (45) for this case becomes

$$-\psi^2 = V^2 (-y^2 + L^2)$$

or

$$\psi = V (y^2 - L^2)^{1/2}$$

$$\therefore \quad u = \frac{\partial \psi}{\partial y} = V \frac{y}{(y^2 - L^2)^{1/2}}. \qquad (47)$$

10. Application to a Planing Surface

We shall proceed with the application of the above to the analysis of a Vee planing surface, as formulated by H. Wagner (Ref.6). Let Fig. 18 represent a Vee surface planing with the horizontal velocity V and the angle of trim τ. Resolve the velocity V into components parallel and normal to the keel. Assume the fluid divided into a number of slices by the planes normal to the keel. To an observer situated between any two planes, the passage of the planing surface will appear identical with the penetration of the wedge as shown on Fig. 19.

H. Wagner assumed that the fluid flow caused by an immersing wedge of wetted width 2c is identical with the lower half of the flow about a flat plate of the same width, as shown on Fig. 20. In the previous chapter the plate was considered to be vertical, and the flow to be horizontal, merely for the convenience of stating the velocity as V, rather than iV. For the horizontal plate having a vertical velocity v_o and half breadth c, Eq. (47) becomes:

$$v = v_0 \frac{x}{(x^2 - c^2)^{1/2}} \qquad (48)$$

The rise η of the water surface in the time t is

$$\eta = \int_0^t v\,dt = \int_0^t v_0 \frac{x}{(x^2 - c^2)^{1/2}}\,dt. \qquad (49)$$

The time variable t is inconvenient and can be eliminated by noting that the wetted half breadth c increases with time, so that

$$t = t(c) \quad \text{and} \quad dt = \frac{1}{dc/dt}\,dc = \frac{1}{\dot{c}}\,dc,$$

where $\dot{c}$ is the rate of expansion of the plate, i.e. the horizontal velocity of the edge of the wetted area. Eq. (49) now becomes

$$\eta = \int_0^c \frac{v_0}{\dot{c}} \frac{x}{(x^2 - c^2)^{1/2}}\,dc. \qquad (50)$$

This is the rise η, when the half breadth of the wetted area attains the value $c < x$; as c increases with time, the rise η at the point x continuously increases.

Consider first the case of a simple wedge formed by two flat surfaces placed at an angle of deadrise β, as on Fig. 19. In this case $\dot{c}$ is constant and the integration can be carried out without difficulty (remembering that c is variable, and x is constant) giving:

$$\eta = x \frac{v_0}{\dot{c}} \sin^{-1} \frac{c}{x} \Big|_0^c = x \frac{v_0}{\dot{c}} \sin^{-1} \frac{c}{x} \qquad (51)$$

Consider now the instant when the rise η of a particle on the water surface is such as to bring it into the contact with the wedge. At this instant we have:

$$\eta = y = x \tan \beta,$$

and $$c = x.$$

Evaluating the limits in Eq. 51:

$$\chi = \tan\beta = \chi \frac{v_o}{\dot{c}} \frac{\pi}{2}$$

and finally:

$$\dot{c} = \frac{\pi}{2} \cdot \frac{v_o}{\tan\beta} . \qquad (52)$$

For the simple wedge $\dot{c}$ is constant for constant v_o, and the time of penetration is determined by the depth of penetration $h = c_o \tan\beta$, and the velocity v_o. It follows as a corollary that:

$$c = \frac{\pi}{2} c_o \qquad (53)$$

where c_o is the half-breadth of the intersection of the wedge with the undisturbed water surface.

For a wedge of arbitary cross section, as on Fig. 21, for instance, Wagner defines the shape by the power series

$$y = B_o x + B_1 x^2 + B_2 x^3 + \cdots\cdots B_n x^{n+1} \qquad (54)$$

where the coefficients are chosen so as to represent the bottom shape.

Likewise the ratio $\lambda = v_o/\dot{c}$ is defined by the power series (Ref. 6):

$$\lambda = a_o + a_1 c + a_2 c^2 + a_3 c^3 + \cdots\cdots a_m c^m \qquad (54a)$$

Substitution of this series into Eq. (50) allows the integral to be evaluated term by term (since x is constant and c the variable):

$$\eta = \int_o^c \left[\frac{a_o \chi}{(\chi^2 - c^2)^{1/2}} + \frac{a_1 \chi c}{(\chi^2 - c^2)^{1/2}} + \frac{a_2 \chi c^2}{(\chi^2 - c^2)^{1/2}} + \cdots + \frac{a_m \chi c^m}{(\chi^2 - c^2)^{1/2}} \right] dc \qquad (55)$$

and

$$\eta = a_o \chi \sin^{-1}\frac{c}{\chi} - a_1 \chi^2 \left(1 - \frac{c^2}{\chi^2}\right)^{\frac{1}{2}} + a_2 \chi^3 \left[\frac{-c}{2\chi}\left(1 - \frac{c^2}{\chi^2}\right)^{1/2} + \frac{1}{2}\sin^{-1}\frac{c}{\chi} \right] \cdots \Bigg|_o^c$$

when x = c and y = N. Equating the terms of like powers of series (54) and (55) determines

$$\lambda = \frac{v_o}{\dot{c}} = \frac{2}{\pi} B_o + B_1 c + \frac{4}{\pi} B_2 c^2 + \frac{3}{2} B_3 c^3 + \frac{16}{3\pi} B_4 c^4 + \cdots \qquad (56)$$

For the simple straight sided wedge $B_o = \tan \beta$, all other coefficients are zero, and the series reduces to Eq. (52).

11. Shape of the Wetted Area of a Vee Planing Surface.

Eq. (53), which defines the width of the wetted area in terms of the width of intersection of the wedge with the undisturbed water surface, now can be used to define the plan form of the wetted area.

In the case of a Vee-shaped planing surface, the intersection of the surface with the calm-water level takes place along two oblique lines, designated by A on Figure 22. It appears that there is no noticeable rise of the water level at point D, where the keel first comes into contact with water, and that this point can be conveniently taken as a point of reference. Aft of the first point of contact D, the rise of the water surface is along the line E located ahead of the line of the calm-water intersection A.

The length L_2 (from point D to the intersection of the calm-water lines A with the chine which is projected onto the keel) depends on the angle of trim τ and the angle of deadrise β, and is defined by:

$$L_2 = \frac{b}{2} \frac{\tan \beta}{\tan \tau}$$

where b is the beam of the planing surface.

The rising surface of water meets the surface of the wedge at the distance c from the centerline of the wedge, which is greater than the distance c_o from the centerline of the wedge to calm-water intersection. For the case of the wedge formed by two planes, it is found that

$$\frac{c}{c_o} = \frac{\pi}{2}$$

and the ratio L_1/L_2 can be written with reference to Figure 22 as:

$$\frac{L_1}{L_2} = \frac{fg}{fc} = \frac{2}{\pi}.$$

Thus,

$$L_1 = \frac{b}{\pi} \frac{\tan \beta}{\tan \tau}.$$

The values obtained from the above formula are found to agree very well with experimental values. For convenience of reference, the data computed for several deadrises and angles of trim are tabulated below:

Table I

Deadrise β	Trim	Length L_1
10°	4°	.80
	8°	.40
	12°	.26
20°	4°	1.66
	8°	.84
	12°	.53
30°	4°	2.63
	8°	1.31
	12°	.84

12. Pressures Acting on the Wedge.

In the previous article the data of Art. 10 were used to determine the shape of the wetted area. In the present article, the pressures acting on the wedge will be determined.

The pressure acting on a plate of constant width in a uniform stream can be obtained simply by Bernoulli's equation:

$$p + \frac{\rho U^2}{2} = \text{Constant} = p_\infty + \frac{\rho V^2}{2} \qquad (57)$$

where p and U denote the pressure and the velocity at a particular point, and p_∞ and V are the pressure and the velocity at infinity. The velocity of the fluid flowing along the plate can be obtained from Eq. (46b), which for the case of the horizontal plate will be rewritten as:

$$U = u = \frac{v_0 x}{(c^2 - x^2)^{1/2}}. \qquad (58)$$

Substituting this into Eq. (57) gives:

$$p - p_\infty = \frac{\rho v_0^2}{2}\left(1 - \frac{x^2}{c^2 - x^2}\right). \tag{59}$$

In the center of the plate, where x = 0, this gives the usual stagnation pressure

$$p - p_\infty = \frac{\rho v_0^2}{2}. \tag{60}$$

In the present problem, however, the half-breadth of the plate, c, is variable and is a function of time, so that potential function of the flow is also variable and is a function of time. It is necessary therefore to use the general form of Bernoulli's equation (Ref. 9):

$$\frac{p}{\rho} = -\frac{\partial \phi}{\partial t} - \Omega - \frac{U^2}{2} + F(t) \tag{61}$$

where Ω represents extraneous forces, which in this case will be assumed to be zero, and F (t) corresponds to the Bernoulli constant and may be a function of time. It is determined by the conditions at a great distance where $d\phi/dt$ due to the plate is insignificant. For the present case it becomes

$$F(t) = \frac{v_0^2}{2} + \frac{p_\infty}{\rho}. \tag{62}$$

At the plate U = u, and Eq. (61) becomes

$$\frac{p - p_\infty}{\rho} = -\frac{\partial \phi}{\partial t} - \frac{u^2}{2} + \frac{v_0^2}{2}, \tag{63}$$

where u is defined by Eq. (58).

To obtain $\partial\phi/\partial t$, Eq. (46a) is rewritten:

$$\phi = -v_0 \left(c^2 - x^2\right)^{1/2}. \tag{64}$$

Remembering that in this case c is variable and x is constant, and assuming v_0 to be variable (as in the case of impact):

$$\frac{\partial \phi}{\partial t} = -\left(c^2 - x^2\right)^{1/2} \frac{dv_0}{dt} - \frac{v_0 c}{\left(c^2 - x^2\right)^{1/2}} \frac{dc}{dt}. \tag{64a}$$

Introducing the designation $\lambda = v_o/c$, or $dc/dt = v_o/\lambda$, inserting Eq's. (58), (62) and (64) into Eq. (63), and letting $p_\infty = 0$:

$$\frac{p}{\rho} = \sqrt{c^2 - x^2}\,\frac{dv_o}{dt} + \frac{v_o^2 c}{\lambda\sqrt{c^2-x^2}} - \frac{v_o^2 x^2}{2(c^2-x^2)} + \frac{v_o^2}{2}. \qquad (65)$$

For the particular case of the constant penetration velocity v_o, $dv_o/dt = 0$, and we obtain

$$p = \frac{\rho v_o^2}{2}\left[\frac{2c}{\lambda(c^2-x^2)^{1/2}} - \frac{x^2}{(c^2-x^2)} + 1\right]. \qquad (66)$$

The first term within the brackets gives the effect of the expansion of the wetted width, the second term, similar in form to Eq. 59, the reduction of pressure due to the flow along the surface of the plate, and the third term adds the stagnation pressure of the fluid due to velocity v_o at infinity. The contribution of each term, and the total pressure p are plotted vs. x on Fig. 22a.

The pressure in the center, obtained by letting x = 0 in Eq. (66) is:

$$p_c = \frac{\rho v_o^2}{2}\left(\frac{2}{\lambda} + 1\right). \qquad (67)$$

For instance, in the case of the straight-sided wedge of deadrise $\beta = 20^\circ$,

$$\lambda = \frac{2\tan\beta}{\pi} = .232$$

and

$$\left(\frac{2}{\lambda} + 1\right) = 9.7,$$

i.e. in the case of the vee-shaped wedge of 20° deadrise, the pressure in the center is 9.6 times greater than the pressure in the center of a plate of fixed width, or in the center of the same wedge, after its edges become immersed. The most conspicuous part of Fig. 22a, however, is the sharp pressure peak near the edge of the wetted area, the intensity of which, for a 22.5° deadrise, is shown to be about 16-1/2 times the stagnation pressure $\rho v_o^2/2$. It will be noted that terms I and II approach $+\infty$ and $-\infty$ at the edge of the plate x = 0, but the rate of approach to infinity is such that a peak of maximum pressure is formed at x = .965 c.

It will be noted further that pressures increase with decreasing λ, i.e. with the decrease of the deadrise β, becoming infinite for the flat plate $\beta = 0$, to which this method of analysis is not applicable.

Whenever the mathematical analysis indicates that some quantity, such as velocity or pressure, becomes infinite, Nature makes some adjustment of the type of the flow or of the parameters involved to avoid such a condition. It is not surprising, therefore, to find that experimental pressures check well with the ones calculated by Eq. 66, and illustrated by Fig. 22, for deadrises of the order of 20 or 30 degrees, but that for smaller deadrises, such as 10°, the experimental pressures fall well below the theoretical.

13. Discontinuous Fluid Flow.

In Art. 9 and Fig. 17, the pattern of the fluid flow about a flat plate was developed. In the three subsequent articles, this knowledge was used to yield useful information on the shape of the wetted area of a planing surface, and on the pressure distribution in each of the transverse slices of which it was assumed to be composed. This pressure distribution is well confirmed by experiment. Good agreement was obtained because only half of the entire field of flow was considered, on the side on which the fluid impinges on the plate, and in this half the theoretical and the actual flow patterns are very similar. This is not the case on the other side of the plate. Equations (45a) and (47) indicate that the velocity becomes infinite at the edge of the plate where $y = L$. Since infinite velocity and the infinite acceleration required for the fluid to flow around the edge cannot actually occur, the flow breaks away at the edge and assumes the form shown on Fig. (23a). Once the type of flow is visualized, certain simplifying assumptions can be made and a suitable theory formulated. This theory is known as the Helmholtz-Kirchoff theory of free jets. It makes use of the Schwarz-Christoffel transformation, but instead of transforming the z plane directly into the t plane, it applies first two intermediate stages of transformation, based upon the physical nature of the problem.

We will now apply this theory to a wedge of deadrise β immersed in the fluid. The flat plate is a particular case of the wedge for which $\beta = 0$.

Following the Helmholtz-Kirchhoff theory, consider Figure 23a to represent the upward flow of water against the wedge A-O-B, and consider two streamlines initially infinitely close to the plane of symmetry I-O. After impinging on the surface of the wedge these streamlines separate, follow the surface of the wedge along O-A and O-B, break off at the chines A and B, and continue as free surfaces along A-C and B-D. Since these free surfaces are exposed to the air, the pressure at any point of the free streamline is the same, and is equal to the atmospheric pressure. Since the pressure is uniform, the velocity also is uniform by virtue of Bernoulli's theorem, and is equal to the velocity at infinity, i.e. to the field velocity V. For simplicity of the analytical work, this velocity will be assumed equal to 1. The branches of the streamlines A-C and B-D are characterized therefore by the constant velocity V, and by the continuously changing direction of the streamline. This direction will be designated by the angle θ between the tangent to the streamline and the positive normal to the initial flow direction, or to the plane of symmetry I-O, as shown on Figures 23a and b.

For the sections O-A and O-B of the streamlines, on the other hand, the velocity is continuously changing from U = 0 at the stagnation point O, to U = V = 1 at the chines A and B, while the direction remains constant ($\theta = \beta$ and $\theta = \pi - \beta$). The object of the following two transformations is to represent the properties of these two regions of the flow by horizontal and vertical lines, forming a polygon (a rectangle) suitable for the application of the Schwarz-Christoffel theorem.

The Function $\zeta = dz/dw$:

First we formulate the function $\zeta = dz/dw$, and investigate its physical meaning.

Expanding dw/dz gives:

$$\frac{dw}{dz} = \frac{d(\phi + i\psi)}{d(x+iy)} = \frac{\partial \phi}{\partial x} + i\frac{\partial \psi}{\partial x} = \frac{\partial \psi}{\partial y} - i\frac{\partial \phi}{\partial y} \qquad (67)$$

By properties of analytic function derivative is independent of path.

where

$\frac{\partial \phi}{\partial x} = \frac{\partial \psi}{\partial y} = u$, the velocity component parallel to the x axis, and

$-\frac{\partial \psi}{\partial x} = \frac{\partial \phi}{\partial y} = v$, the velocity component parallel to the y axis.

Substituting these expressions into Eq. (67) gives

$$\frac{dw}{dz} = u - i v,$$

which is known as the complex velocity.

A new designation ζ is now introduced:

$$\zeta = \frac{dz}{dw} = \frac{1}{u - iv} = \frac{u}{u^2 + v^2} + i \frac{v}{u^2 + v^2}$$

or, since $u^2 + v^2 = U^2$, where U is the resultant velocity in any direction:

$$\zeta = \frac{dz}{dw} = \frac{1}{U}\left(\frac{u}{U} + i \frac{v}{U}\right). \qquad (68)$$

Furthermore,

$$u/U = \cos\theta, \qquad v/U = \sin\theta$$

and

$$\zeta = \frac{1}{U}(\cos\theta + i \sin\theta) = \frac{1}{U} e^{i\theta}. \qquad (69)$$

An interesting property of this function, shown on Figure 23b, is that the vector drawn from the origin of a polar diagram to any point of the ζ plane will agree in direction with, and be in magnitude the reciprocal of, the velocity at the corresponding point of the z plane. Thus for the sections O-A and O-B of the streamline $\psi = 0$ the directions of the velocity vectors are $\theta = \beta$ and $\theta = (\pi - \beta)$. At the keel O, the velocity U = 0, and its reciprocal $1/U = \infty$. For the sections of the free streamline A-C and B-D, the velocity and its reciprocal have the uniform value of 1, while the direction changes from $\theta = \beta$ or $\theta = (\pi - \beta)$ at the points A and B to $\theta = \pi/2$ at the points C and D at infinity. These sections are represented therefore on Figure 23b by the circular arc ACDB.

The Function $\Omega = \ln \zeta$

Figure 23c, which is the graphical representation of the function Ω can now be constructed on the basis of Eq. (69) as follows:

$$\Omega = \ln \zeta = \ln\left(\frac{1}{U}\right) + i\theta. \qquad (70)$$

Here the symbol ln is used to denote the logarithm to the base e. For the sections A-C and B-D of the streamline we have $1/U = 1$, and $\ln 1 = 0$. These are represented, therefore, on Figure 23c by the vertical line ACDB, the ends of which are located at $\theta = \beta$ and $\theta = (\pi - \beta)$. The horizontal lines, drawn from these points to infinity, are the lines of θ = Constant and log $1/U$ varying from 0 to ∞. For convenience of reference these relations are tabulated below:

Point	U	ln 1/U	θ
A	1	0	β
B	1	0	$\pi - \beta$
C	1	0	$\pi/2$
D	1	0	$\pi/2$
O	0	∞	β and $\pi - \beta$

Plotting Ω for the streamline DBOA on the basis of Eq. (70) gives a figure consisting of three straight lines forming two internal angles of $\pi/2$ at the points A and B. Two corresponding corners located at infinity can be imagined, completing a closed polygon (a rectangle). The area enclosed by this polygon can be transformed to occupy the entire upper half of the t plane— Fig. 23d, so that the polygon itself is developed into the real axis of the t plane. In this case, there are two corners giving two finite points at A and B to which the values of $t_1 = +1$ and $t_2 = -1$ can be conveniently assigned, and two equal internal angles $\alpha = \beta = \pi/2$, so that by the Schwarz-Christoffel theorem:

$$\Omega = P\int (t-1)^{-1/2}(t+1)^{-1/2}\,dt = P\int (t^2-1)^{-1/2}\,dt$$

or, after integration:

$$\Omega = \ln \frac{dz}{dw} = P\ln\left(t + \sqrt{t^2-1}\right) + Q = P\cosh^{-1} t + Q \qquad (71)$$

Determination of the Constants P and Q.

The next step is to determine the constants P and Q. This is done by substitution of the values of the variables t and θ, which are known at the chine points A and B of Figure 23.

Thus at the chine A we have 1/U = 1, ln 1 = 0 and from Eq. (70) $\Omega = i\theta = i\beta$. Since at this point t = 1 and $\cosh^{-1}(1) = 0$, substituting these values into Equation (71) gives the value of Q:

$$Q = i\beta$$

Similarly at the chine point B:

$$\Omega = i\theta = i(\pi - \beta), \qquad t = -1,$$

and

$$\cosh^{-1}(-1) = i\pi.$$

Hence,

$$i(\pi - \beta) = i\pi P + Q = i\pi P + i\beta$$

$$\therefore \quad P = \frac{\pi - 2\beta}{\pi}$$

Finally, substituting these values into Eq. 71 gives

$$\ln \zeta = \frac{\pi - 2\beta}{\pi} \cosh^{-1} t + i\beta \qquad (72)$$

or in the alternate form:

$$\ln \zeta = \frac{\pi - 2\beta}{\pi} \ln\left(t + \sqrt{t^2 - 1}\right) + i\beta. \qquad (73)$$

The above equation is perfectly general and applies to any point in the field. Considering now the free boundary A-C, it follows from Equation (70) that $\ln \zeta = i\theta$. Hence, Equation (72) becomes:

$$i\theta = \frac{\pi - 2\beta}{\pi} \cosh^{-1} t + i\beta$$

or

$$\cosh^{-1} t = i \frac{(\theta - \beta)\pi}{\pi - 2\beta}.$$

or, since cosh ix = cos x,

$$t = \cos \bar{\theta} \qquad (74)$$

where a new designation $\bar{\theta}$ was introduced, defined as:

$$\bar{\theta} = \frac{(\theta-\beta)\pi}{\pi-2\beta}. \qquad (75)$$

At the point A: $\theta = \beta$, $\bar{\theta} = 0$ and $t = 1$.
At the point B: $\theta = \pi-\beta$, $\bar{\theta} = \pi$ and $t = -1$.
At the points C and D: $\theta = \pi/2$, $\bar{\theta} = \pi/2$ and $t = 0$.
For the flat plate: $\beta = 0$, $\bar{\theta} = \theta$

Eq. (75) can be considered as a transformation function giving the flow about a straight-sided wedge in terms of the flow about a flat plate. It was introduced by Bobyleff in 1881 (Ref 9-b).

Relation between w and t

In the previous section, a relation was obtained between t and the direction θ of the tangent to the free streamline ($\psi = 0$). The relationship between w and t will now be established. By using 1/w instead of w, a convenient correspondence between the 1/w and t variables is obtained, both becoming zero at the points C and D, as shown on Figures 23-d and 23-e. Inspection of these figures shows that the Schwarz-Christoffel theorem is now applicable. There is only one angle at CD, i.e. at $t = 0$, and this must be considered to be the "internal angle" having the value of 2π, since the area "enclosed" by the polygon is the entire area of the w^{-1} plane. (It should be remembered that lines O-A and O-B of Fig. 1-e in reality coincide). Hence, by the Schwarz-Christoffel theorem,

$$\frac{dw^{-1}}{dt} = E\,(t-0)^{\frac{2\pi}{\pi}-1}$$

or

$$\frac{dw^{-1}}{dt} = Et$$

where E is a constant.

Integrating:

$$w^{-1} = \frac{1}{2}Et^2 + F.$$

At t = 0, $w^{-1} = 1/\infty = 0$; hence F = 0, and

$$w^{-1} = \pm E t^2$$

or, if the constant 2/E is denoted by C:

$$w = \frac{C}{t^2}. \tag{76}$$

Definition and Determination of the Constant C

For the particular streamline $\psi = 0$,

$$w = \phi + i\psi = \phi$$

and Equation (76) can be rewritten as

$$\phi = \frac{C}{t^2}. \tag{77}$$

Since $t^2 = 1$ at the chine points A and B, it can be seen that the constant C is the value of the potential ϕ at the chine. In order to evaluate C, it is necessary to consider Eq. (73) which gives the relation between $\zeta = dz/d\phi$ (for $\psi = 0$ and $w = \phi$) and t, and Equation (77) which gives the relation between ϕ and t in terms of C, eventually eliminating ϕ and establishing the value of C in terms of z, i.e. in terms of x and y. First the term $i\beta$ in Equation (73) is put in the form

$$i\beta = \ln e^{i\beta} = \ln(\cos\beta + i\sin\beta). \tag{78}$$

Substituting this into Equation (73) and taking antilogarithms gives the expression:

$$\zeta = \left(t + \sqrt{t^2-1}\right)^n (\cos\beta + i\sin\beta) \tag{80}$$

where

$$n = \frac{\pi - 2\beta}{\pi}. \tag{81}$$

On the other hand, ζ along the streamline $\psi = 0$ is defined as

$$\zeta = \frac{dz}{dw} = \frac{dz}{d\phi} = \frac{dx}{d\phi} + i\frac{dy}{d\phi}. \tag{82}$$

For the parts OA and OB of the streamline $\psi = 0, |t| > 1$, and $(t^2 - 1)^{1/2}$ is real. Furthermore, the streamline $\psi = 0$ is represented by the real axis of the t plane, i.e., t itself is real. Therefore, the real and imaginary parts of Eqs. (80) and (81) can be readily separated, giving:

$$dx = \left(t + \sqrt{t^2-1}\right)^n \cos\beta \, d\phi \qquad (83)$$

and

$$dy = \left(t + \sqrt{t^2-1}\right)^n \sin\beta \, d\phi. \qquad (84)$$

Equation (77) gives the following relation between $d\phi$ and dt:

$$\frac{d\phi}{dt} = \frac{-2C}{t^3}. \qquad (85)$$

Substituting the value of $d\phi$ from Equation (85) into Equation (83):

$$dx = \frac{-2C\left(t + \sqrt{t^2-1}\right)^n}{t^3} \cos\beta \, dt. \qquad (86)$$

Since at the keel $t = \infty$ and at the chine $t = 1$, the half beam b/2 can be expressed by integrating dx for all values of t from ∞ to 1:

$$\frac{b}{2} = \int_0^{b/2} dx = -2C\cos\beta \int_\infty^1 \frac{\left(t + \sqrt{t^2-1}\right)^n}{t^3} dt. \qquad (87)$$

From this the value of the constant C can be computed in terms of the beam b and the angle of deadrise β.

It will be convenient to express the constant C as

$$C = b\,k \qquad (88)$$

where

$$\frac{1}{k} = 4\cos\beta \int_1^\infty \frac{\left(t + \sqrt{t^2-1}\right)^n}{t^3} dt. \qquad (89)$$

In order to carry out the integration, it is necessary to change the variable, letting

$$t = \frac{1}{\cos\gamma} \quad \text{and} \quad dt = \frac{\sin\gamma}{\cos^2\gamma} d\gamma \qquad (90)$$

The Equation (89) then becomes

$$\frac{1}{k} = 4\cos\beta \int_0^{\pi/2} (1+\sin\gamma)^n (\cos\gamma)^{1-n} \sin\gamma \, d\gamma. \qquad (91)$$

In the case of the flat plate, $\beta = 0$, $n = 1$, and Eq. (91) becomes

$$\frac{1}{k} = 4\int_0^{\pi/2} (1 + \sin\gamma)\sin\gamma\, d\gamma = 4 + \pi \quad (92)$$

In the more general case $\beta \neq 0$, Equation (91) can be integrated numerically, yielding, for the commonly used values of the deadrise β, the values of $1/k$ given in table II:

TABLE II

Deadrise β in degrees	Constant $1/k$
0.0	7.14
10.0	5.92
15.0	5.35
20.0	4.73
22.5	4.54
25.0	4.27
30.0	3.80

Shape of the Free Streamline

Along the free streamlines A-C and B-D, the magnitude of the velocity is constant and was taken as 1. Therefore

$$V = 1 = d\phi/ds \quad (93)$$

and

$$ds = d\phi$$

where s denotes the distance along the free streamline. Substituting the value of C from Eq. (88) into Eq. (85) gives

$$ds = d\phi = -2kbt^{-3}\,dt$$

and evaluating t on the basis of Eq. (74) gives:

$$ds = 2kb\tan\bar{\theta}\sec^2\bar{\theta}\,d\bar{\theta}, \quad (94)$$

$$\left.\begin{aligned} dx &= ds\cos\theta, \\ \text{and}\quad dy &= ds\sin\theta, \end{aligned}\right\} \quad (95)$$

For the particular case of the flat plate $\beta = 0$, $\bar{\theta} = \theta$, and Eq. (94) becomes:

$$\left.\begin{aligned} dx &= 2kb\tan\theta\sec\theta\,d\theta \\ dy &= 2kb\tan^2\theta\sec\theta\,d\theta \end{aligned}\right\} \qquad (96)$$

or, in a form more convenient for integration

$$dy = 2kb\left(\frac{d\theta}{\cos^3\theta} - \frac{d\theta}{\cos\theta}\right). \qquad (97)$$

Integrating Equations (96) and (97) between the limits 0 and θ gives

$$\left.\begin{aligned} x &= 2kb(\sec\theta - 1) \\ y &= kb\left[\tan\theta\sec\theta - \ln(\tan\theta + \sec\theta)\right] \end{aligned}\right\} \qquad (98)$$

or in the alternate form:

$$y = kb\left[\tan\theta\sec\theta - \ln\tan\left(\frac{\theta}{2} + \frac{\pi}{4}\right)\right]. \qquad (99)$$

In the above equations x and y are measured from the chines A and B outward and upward. For $\theta = 0$, x and y are equal to zero; they become infinite for $\theta = \pi/2$.

For the general case $\beta \neq 0$ and $\bar{\theta} \neq \theta$, Eq. (95) cannot be integrated analytically. The shape of the free streamline can be obtained, however, from Eq. (97) by replacing ds and $d\theta$ by Δs and $\Delta\bar{\theta} = f(\Delta\theta)$, and by carrying out step-by-step calculations of the increments of θ. Equations (95) can then be applied, and the free streamlines plotted. This has been done for several values of the deadrise β, and the results are given on Figure 24.

Dynamic Pressure Acting on the Wedge in Weightless Fluid

Let p designate the unit pressure in excess of atmospheric acting on the faces of the wedge. In the ideal non-viscous fluid this pressure acts along the normal to the surface. From Bernoulli's theorem, it is known that changes of unit pressure are equal in absolute value to the changes of the dynamic head. At the chine, the velocity is $U = V = 1$, the dynamic head is $\rho U^2/2 = \rho/2$, while the pressure is equal to atmospheric, i.e. $p = 0$. At the keel the velocity U is equal to zero and the pressure $p = pV^2/2 = p/2$. At any point between keel and chine,

the velocity $0 < U < 1$, and the pressure is:

$$p = \rho(1 - U^2)/2. \tag{100}$$

The velocity U can be obtained by combining Eqs. (69) and (80):

$$\zeta = \frac{dz}{dw} = \frac{1}{U} e^{i\theta} = \left(t + \sqrt{t^2-1}\right)^n e^{i\beta}. \tag{101}$$

Since $\theta = \beta$ along the faces of the wedge, the exponential may be cancelled, giving

$$U = \left(t + \sqrt{t^2-1}\right)^{-n}. \tag{102}$$

Substituting this into Eq. (100) gives the expression for p:

$$p = \frac{\rho}{2}\left[1 - \left(t + \sqrt{t^2-1}\right)^{-2n}\right]. \tag{103}$$

From Equations (86) and (88)

$$x = 2kb\cos\beta \int_t^\infty \left(t + \sqrt{t^2-1}\right)^n \frac{dt}{t^3}. \tag{104}$$

Equations (103) and (104) give simultaneous values of p and x in terms of the parameter t. For practical computations, it will be more convenient to change the variable t to the angle γ, using Eq. (90). Making this substitution and inserting the velocity at the chine V, heretofore set equal to 1, gives the following equations for p and x:

$$\left.\begin{aligned} p &= \frac{\rho V^2}{2}\left[1 - \left(\frac{\cos\gamma}{1+\sin\gamma}\right)^{2n}\right] \\ x &= 2kb\cos\beta \int_\gamma^{\pi/2} (1+\sin\gamma)^n (\cos\gamma)^{1-n} d\gamma \end{aligned}\right\} \tag{105}$$

In Eqs. (105) the parameter γ can be assigned arbitrary values in the range $0 < \gamma < \pi/2$ and corresponding values of p and x can be computed. Since the values $\gamma = \pi/2$ or $t = \infty$ correspond to the keel, x is measured from the centerline of the wedge.

For the flat plate, $\beta = 0$, $n = 1$, and Eq. (105) becomes:

$$\left.\begin{aligned} p &= \frac{\rho V^2}{2}\left[1 - \left(\frac{\cos\gamma}{1+\sin\gamma}\right)^2\right], \\ x &= 2kb\left(\frac{\pi}{4} - \frac{\gamma}{2} + \cos\gamma + \frac{\sin 2\gamma}{4}\right) \end{aligned}\right\} \tag{106}$$

The pressure distribution p = f (x), as computed by Eqs. (105) and (106), is plotted on Figure 25 for $\beta = 0$ and $\beta = 20^\circ$, as the ratio $p/p_{max.}$ vs. x/b.

The force acting on an element of the bottom, ds, is p ds, and the vertical component of this force is p ds cos β = p dx. The total vertical force acting on the wedge is therefore:

$$P = 2\int_0^{b/2} p\,dx \tag{107}$$

and, from Equation (105),

$$dx = -2kb\cos\beta\,(1+\sin\gamma)^n(\cos\gamma)^{1-n}\sin\gamma\,d\gamma \tag{108}$$

Substituting the values of p from Eq. 105 and dx from Eq. (108) into Eq. (107) gives the expression for the total force:

$$P = 2\rho kbV^2\cos\beta\int_0^{\pi/2}\left[\left(\frac{1+\sin\gamma}{\cos\gamma}\right)^n - \left(\frac{1+\sin\gamma}{\cos\gamma}\right)^{-n}\right]\cos\gamma\sin\gamma\,d\gamma \tag{109}$$

or

$$P = 2\rho kbV^2\cos\beta\, f(\gamma) \tag{110}$$

where $f(\gamma)$ denotes the value of the integral.

The ratio of the mean pressure over the wedge, P/b, to the dynamic pressure $\rho V^2/2$ is:

$$C_p = \frac{P}{b(\rho V^2/2)} = 4k\cos\beta\, f(\gamma). \tag{111}$$

For the flat plate, $\beta = 0$ and n = 1, and $f(\gamma)$ can be integrated:

$$f(\gamma) = 2\int_0^{\pi/2}\sin^2\gamma\,d\gamma = \pi/2.$$

The total pressure P acting on the flat plate of unit length is obtained by substitution of the above value of $f(\gamma)$ and of k from Table II into Eq. 110:

$$P = \rho bV^2\frac{\pi}{4+\pi}. \tag{112}$$

For $\beta \neq 0$, the integral $f(\gamma)$ can be evaluated by numerical integration. The results for several values of the deadrise are given in Table III.

TABLE III

β	$2f(\gamma)$	C_p	C_{p_β}/C_{p_o}
0	3.141	0.880	1.000
10	2.490	0.818	0.941
20	2.005	0.796	0.905
30	1.604	0.732	0.832

The last column of Table III compares the mean pressure or the load acting on the Vee-shaped surface or wedge with that acting on a flat plate plate of the same beam, defined as the horizontal distance between chines.

14. Flow in the spray root at a plate of infinite extent.

Now the technique of the free jet theory, developed in the previous article, will be applied to the spray root of a planing surface. This treatment was developed by H. Wagner, and is presented here as elaborated by J. D. Pierson and S. Leshmover in Ref. 12.

Fig. 26 shows the immersing wedge, the rise of water surface, and the pressure distribution as developed in Art. 10 on the basis of the expanding plate theory. A very high peak pressure is shown to exist very near the edge of the wetted area and very close to the free water surface. In reality, the severe pressure gradient, from the peak pressure at 96.5% of the wetted width to the atmospheric pressure at the edge of it, causes a rapid acceleration of the fluid particles along the surface of the wedge. A thin, rapidly moving sheet of water is formed, which separates at the chine and forms the spray. This thin sheet of water will be referred to as the "spray root." The formation of the spray root extends slightly the area of the pressure diagram on Fig. 26, as shown by the dotted line.

It has not been possible to apply the mathematical analysis to the entire field of flow, including the spray root, and the analysis

is applied first only to the region of the spray root itself, disregarding other boundaries. For this purpose the coordinate system is taken with the origin on the surface of the plate at the stagnation point (to be defined later) of the spray root, the x axis along the surface, and y axis normal to it. In the notation of Art. 10 therefore, these axes are moving with the velocity $\dot{c}$ with respect to the fluid at infinity. Considering only the spray root region, we can superpose an equal and opposite velocity $V = \dot{c}$ on the entire system, so that the axes can be considered as stationary, and the fluid as flowing from right to left with the velocity V.

The fluid, approaching the stagnation point with the initial velocity V, will create the pressure $\rho V^2/2$, and this pressure will accelerate the fluid in the spray again to the velocity V in the opposite direction. The entire spray root structure can be compared to a bucket of the Pelton Wheel. In the case of the actual wedge, with the stagnation point moving with velocity $\dot{c}$, the spray velocity becomes $2\dot{c}$, if cos β be taken as unity.

In order to carry out the analysis, the further simplification is made in assuming the angle β to be zero, and assuming the plate on which the flow impinges to be infinite, both in length and in breadth (doubly infinite), finally taking the form shown on Fig. 27. While such a flow evidently cannot generate itself, it may be considered as existing, if the plate was previously at an angle of attack, which was subsequently and gradually reduced to zero, without disrupting the flow. For easier visualization when establishing certain mathematical conventions, the entire configuration shown in Fig. 27 is rotated through 180° about the line of the solid boundary, and the remainder of analysis will refer to Fig. 28.

It has been explained before that part of the fluid is deflected forward (to the right on Fig. 28) by the high pressure gradient at the edge of the wetted area, while the bulk of the fluid is flowing to the left. There must exist, therefore, a dividing streamline, or a pair of streamlines located infinitely close together at infinity, impinging on the plate at right angle, and dividing so that one branch is directed forward, and the other branch aft along the plate. The point at which

the dividing streamline contacts the plate is called the stagnation point, and the origin of the axes of coordinates is taken as coinciding with it. On Fig. 28 this streamline is designated by $\psi = -\delta V$, where δ is the thickness of the spray sheet. The streamline forming the free surface is designated $\psi = 0$. It has two branches for the flow on the two sides of the dividing streamline.

Figure 29 represents the w plane corresponding to the z plane represented by Fig. 28. The streamline $\psi = 0$, representing the free surface, is the real axis. The dividing streamline $\psi = -\delta V$, in following the rigid boundary, has two branches of opposite direction on the z plane, but of the same direction—that of increasing values of ϕ in the w plane. It is represented therefore by the line defg folded on itself. It will be remembered that the solution of a hydrodynamic problem always depends on the establishment of the conditions at the boundaries, and that in this case, as in the previous article, we are concerned with the free boundary bc and the surface of the plate or the solid boundary defg.

The Transformation (dz/dw) = f (t)

As in the previous case, the function

$$\zeta = \frac{dz}{dw} = \frac{1}{U} e^{i\theta} = \frac{1}{U}(\cos\theta + i \sin\theta)$$

is defined, and the ζ plane is constructed, as in Fig. 30. At the points f and e on the solid boundary the velocity U = 0 and $\zeta = \infty$. The velocity at infinity will again be taken as 1, i.e. V = 1, so that for the points d and g, 1/U = 1/V = 1, i.e. on the solid boundary ζ varies from 1 to ∞. The directions of the velocity on the solid boundary are $\theta = \pi$ and $\theta = 2\pi$. On the free boundary b-c the velocity is constant U = V = 1, by Bernoulli's equation, since the atmospheric pressure is constant everywhere, while θ varies from π to 2π. It is represented therefore on the ζ plane by the semicircle of unit radius terminating at b and c coincident with g and d. It will be noted that the ζ plane is the hodograph plane, on which the vectors representing the reciprocal of the velocity are plotted from the origin by their magnitude and direction. The location of the vectors on the z plane, however, is in no way represented on the ζ plane.

The function

$$\Omega = \ln \zeta = \ln\left(\frac{1}{U}\right) + i\theta$$

is then formed, and the Ω plane is drawn on Fig. 31. On the solid boundary θ is constant, and $\ln \frac{1}{U}$ varies from 0 to ∞. The solid boundary is therefore represented by two horizontal lines de and gf. On the free boundary $\ln \frac{1}{U} = 0$, while θ varies from $\theta = \pi$ to $\theta = 2\pi$. The free boundary is represented therefore by the vertical line bc.

The Schwarz-Christoffel theorem is now applied, with the values of $t = 0$ associated with the point c and d, and $t = -1$ with the point e and f. Quoting from Reference (12): "The transformation is visualized by considering the straight sided figure b c d e f g in Fig. 31 to be 'split open' at the point b, g, after which the figure is unfolded into a straight line and placed on the real axis of the t plane." Since all internal angles are equal to $\pi/2$, we have

$$\frac{d\Omega}{dt} = A\,(t-0)^{-1/2}(t+1)^{-1/2}(t+1)^{-1/2} = At^{-1/2}(t+1)^{-1}.$$

The integral of the above can be conveniently represented in the form

$$\Omega = \ln \frac{dz}{dw} = A' \ln \frac{\sqrt{t} - i}{\sqrt{t} + i} + B \qquad (113)$$

as can be readily verified by differentiation. Here the symbol A' is used to denote A/i.

In order to evaluate the additive constant B, substitute into Eq. (113) the data corresponding to the point b, i.e.

$U = 1$ $\qquad \ln \frac{1}{U} = 0$

$\theta = +\pi$ $\qquad t = \infty$

$\Omega = \ln\left(\frac{1}{U}\right) + i\theta$

$\Omega_B = 0 + i\theta$

$$\lim_{t\to\infty}\left(\frac{\sqrt{t} - i}{\sqrt{t} + i}\right) = 1$$

$$\therefore\ i\pi = A'(0) + B \quad \text{or} \quad B = i\pi.$$

Thus, Eq. (113) now becomes

$$\ln \frac{dz}{dw} = A' \ln \frac{\sqrt{t} - i}{\sqrt{t} + i} + i\pi. \qquad (114)$$

In order to evaluate the coefficient A', the data corresponding to the point c or d will be substituted:

$$U = 1 \qquad \ln \frac{1}{U} = 0$$

$$\theta = 2\pi \qquad t = 0$$

$$\left(\frac{\sqrt{t} - i}{\sqrt{t} + i}\right)_{t=0} = -1 = e^{-i\pi}$$

$$\log\left(\frac{\sqrt{t} - i}{\sqrt{t} + i}\right)_{t=0} = -i\pi$$

$$\therefore\ i\,2\pi = A'(-i\pi) + i\pi \quad \text{and} \quad A' = -1.$$

Substitute this value of A' into Eq. (114) and observe that

$$B = i\pi = \ln e^{i\pi} = \ln(-1)$$

Then

$$\ln \frac{dz}{dw} = -\ln \frac{\sqrt{t} - i}{\sqrt{t} + i} + i\pi$$

$$= \ln \frac{\sqrt{t} + i}{\sqrt{t} - i} + \ln(-1)$$

$$= \ln\left(-\frac{\sqrt{t} + i}{\sqrt{t} - i}\right).$$

The anti-logarithm of both sides gives

$$\frac{dz}{dw} = -\frac{\sqrt{t} + i}{\sqrt{t} - i}. \qquad (115)$$

The Transformation dw/dt

The lower half of the w plane on Fig. 29 is to be mapped onto the upper half of the t plane on Fig. 32, so that the bounding polygon bcdefg is mapped onto the real axis of the t plane. The points c and d at infinity can be considered as coinciding, and the internal angle at this vertex is 0, while the corresponding value of t is t = 0. At the vertex ef, the internal angle is 2π, and t = -1. By the Schwarz-Christoffel theorem

$$\frac{dw}{dt} = C(t-0)^{\frac{0}{\pi}-1}(t+1)^{\frac{2\pi}{\pi}-1} = C\frac{t+1}{t} \qquad (116)$$

∞ SPRAY ROOM ∞

and integration gives

$$w = C(t + \ln t) + D \tag{117}$$

In order to determine the coefficient C, consider the points b and c. At the point c on the free streamline

$$w \overset{\phi=0}{=} 0 = C\left(0 + \lim_{+t \to 0} \ln|t|\right) + D. \tag{118}$$

At the point d on the solid boundary

$$w \overset{\phi=0}{=} -i\delta = C\left(0 + \lim_{-t \to 0} \ln|t|\right) + D. \tag{119}$$

Observe that $\ln(-t) = \ln(t)(-1)$

$$= \ln t + i\pi$$

and Eq. (119) becomes:

$$w \overset{\phi=0}{=} -i\delta = C\left(0 + \lim_{t \to 0} \ln|t| + i\pi\right) + D. \tag{120}$$

Subtract Eq. (118) from Eq. (120)

$$-i\delta = i\pi C$$

and

$$C = -\delta/\pi$$

The coefficient D is determined by substitution of this value of C into Eq. 117, together with the values of variables corresponding to the point ef, i.e. $t = -1$, $\phi = 0$, $\psi = -\delta$:

$$w = \phi + i\psi = -i\delta = \frac{-\delta}{\pi}\left[-1 + \ln(-1)\right] + D$$

$$-i\delta = \frac{\delta}{\pi} - \frac{\delta}{\pi}(i\pi) + D$$

or $$D = \frac{-\delta}{\pi}.$$

Eq. (116) now becomes

$$\frac{dw}{dt} = -\frac{\delta}{\pi}\,\frac{t+1}{t} \tag{121}$$

and Eq. (117) becomes

$$w = -\frac{\delta}{\pi}(t + \ln t + 1). \tag{122}$$

The Transformation dz/dt

$$\frac{dz}{dt} = \frac{dz}{dw}\,\frac{dw}{dt}.$$

Substitute dz/dw from Eq. (115) and dw/dt from Eq. (121):

$$\frac{dz}{dt} = \frac{\delta}{\pi}\left(\frac{\sqrt{t}+i}{\sqrt{t}-i}\right)\left(\frac{t+1}{t}\right).$$

Multiply both the numerator and the denominator of the first expression in brackets by the complex conjugate of the denominator:

$$\frac{dz}{dt} = \frac{\delta}{\pi}\left(\frac{t+2i\sqrt{t}-1}{t+1}\right)\left(\frac{t+1}{t}\right)$$
$$= \frac{\delta}{\pi}\left(\frac{t+2i\sqrt{t}-1}{t}\right)$$

or

$$\frac{dz}{dt} = \frac{\delta}{\pi}\left(1+i\,\frac{2}{\sqrt{t}}-\frac{1}{t}\right). \qquad (123)$$

Integration of Eq. (123) gives

$$z = \frac{\delta t}{\pi}+i\,\frac{4\delta}{\pi}\sqrt{t}-\frac{\delta}{\pi}\ln t+E. \qquad (124)$$

In order to determine the constant E, substitute the values corresponding to the point ef, i.e. z = 0, t = -1. Eq. (124) then becomes (remembering that $\ln(-1)=i\pi$)

$$0 = -\frac{\delta}{\pi}-\frac{4\delta}{\pi}-i\delta+E$$

or

$$E = \frac{5\delta}{\pi}+i\delta$$

and Eq. (124) becomes, after factoring out δ/π

$$z = \frac{\delta}{\pi}\left(t+4i\sqrt{t}-\ln t+5+i\pi\right). \qquad (125)$$

Equations (122) and (125) now give the values of w and z in terms of the parameter t, which is real on the free and solid boundaries. In order to separate the variables, however, it is necessary to consider separately positive and negative values of t. For positive values of t, representing the free boundaries, it follows at once that

$$\left.\begin{aligned} x &= \frac{\pi}{\delta}(t-\ln t+5)\\ y &= \frac{\pi}{\delta}(4\sqrt{t}+\pi)\end{aligned}\right\}, \qquad (126)$$

∞ SPRAY ROOT ∞

and the curve of the free boundary can be determined by assigning to t a series of values, and computing and plotting the corresponding values of x and y.

For negative values of t, corresponding to the solid boundary, the substitution $\sqrt{t} = i\sqrt{\xi}$ is made where the notation ξ is introduced to denote $|t|$. Then $\ln t = \ln \xi + i\pi$, and Eq. 125 becomes:

$$\left.\begin{aligned} x &= \frac{\delta}{\pi}\left(-\xi - 4\sqrt{\xi} - \ln \xi + 5\right) \\ y &= 0 \end{aligned}\right\} \qquad (127)$$

For Solid Boundary

Flow Net

Real values of t correspond to the free and solid boundaries of the region. The points in the interior of the region are represented by complex values of t. In order to obtain the flow net, i.e. to construct two sets of orthogonal curves of equipotential lines $\phi = \phi(x,y)$ and streamlines $\psi = \psi(x,y)$, it is convenient to make use of the exponential form

$$t = re^{i\alpha} \qquad (128)$$

where r and α are respectively the modulus and argument of t. Eq. (125) then becomes

$$\begin{aligned} \frac{\pi}{\delta} z &= \frac{\pi}{\delta}(x + iy) \\ &= re^{i\alpha} + 4ir^{1/2}e^{i\alpha/2} - \ln r - i\alpha + 5 + i\pi \\ &= r(\cos\alpha + i\sin\alpha) + 4ir^{1/2}\left(\cos\frac{\alpha}{2} + i\sin\frac{\alpha}{2}\right) - \ln r - i\alpha + 5 + i\pi \end{aligned}$$

and separating the real and imaginary parts

$$\left.\begin{aligned} \frac{x\pi}{\delta} &= r\cos\alpha - 4r^{1/2}\sin\frac{\alpha}{2} - \ln r + 5 \\ \frac{y\pi}{\delta} &= r\sin\alpha + 4r^{1/2}\cos\frac{\alpha}{2} - \alpha + \pi \end{aligned}\right\}. \qquad (129)$$

Likewise Eq. 122 becomes

$$\frac{\pi}{\delta} w = \frac{\pi}{\delta}(\phi + i\psi) = -\left[r(\cos\alpha + i\sin\alpha) + \ln r + i\alpha + 1\right]$$

and

$$\left.\begin{aligned} -\frac{\pi}{\delta}\phi &= r\cos\alpha + \ln r + 1 \\ -\frac{\pi}{\delta}\psi &= r\sin\alpha + \alpha \end{aligned}\right\}. \qquad (130)$$

To get velocity at any point substitute $t = re^{i\alpha}$ into reciprocal of 115 + simplifying resulting equation

For each pair of values of r and x, the corresponding pair of values of x and y is computed by Eq. (129), and the pair of values for ϕ and ψ by Eq. (130). The flow net, computed in this way in Ref. 12, is given on Fig. 33. It will be observed that all values are given in terms of the parameter π/δ, i.e. in terms of the spray thickness δ. With the problem formulated for the doubly infinite plane, the spray thickness δ is the only linear dimension available as a parameter.

The quantities ϕ and ψ were computed for the unit velocity V = 1, and have to be multiplied by velocity for any other value.

Velocities and pressure distributions along solid boundary.

The angle α in Eq. 128 varies from 0 to π since only the upper half of the t plane is considered. Along the solid boundary, the t is real and negative, y = 0 and x varies from $-\infty$ to $+\infty$. These conditions are satisfied by taking $\alpha = \pi$ and by taking r (which is real by definition) to be positive, and to vary from 0 to ∞. Substitution of these values into Eqs. (129) and (130) yields:

$$\left.\begin{aligned} x &= -\frac{\delta}{\pi}(r + 4\sqrt{r} + \ln r - 5) \\ y &= 0 \end{aligned}\right\} \qquad (131)$$

and

$$\left.\begin{aligned} \phi &= \frac{\delta}{\pi}(r - \ln r - 1) \\ \psi &= -\delta \end{aligned}\right\} \qquad (132)$$

Differentiating with respect to r:

$$\frac{dx}{dr} = -\frac{\delta}{\pi}\left(1 + \frac{2}{\sqrt{r}} + \frac{1}{r}\right) = -\frac{\delta}{\pi}\left(\frac{r + 2\sqrt{r} + 1}{r}\right)$$

$$= -\frac{\delta}{\pi}\,\frac{(\sqrt{r}+1)^2}{r}$$

$$\frac{d\phi}{dr} = \frac{\delta}{\pi}\left(1 - \frac{1}{r}\right) = \frac{\delta}{\pi}\left(\frac{r-1}{r}\right)$$

whence

$$u = \frac{\partial\phi}{\partial x} = \frac{d\phi}{dr}\,\frac{dr}{dx} = -\frac{r-1}{(\sqrt{r}+1)^2} = -\left(\frac{\sqrt{r}-1}{\sqrt{r}+1}\right).$$

Velocities and pressure distributions along solid boundary.

The angle α in Eq. 128 varies from 0 to π since only the upper half of the t plane is considered. Along the solid boundary, the t is real and negative, y = 0 and x varies from $-\infty$ to $+\infty$. These conditions are satisfied by taking $\alpha = \pi$ and by taking r (which is real by definition) to be positive, and to vary from 0 to ∞. Substitution of these values into Eqs. (129) and (130) yields:

$$x = -\frac{\delta}{\pi}(r + 4\sqrt{r} + \ln r - 5) \qquad (131)$$
$$y = 0$$

and

$$\phi = \frac{\delta}{\pi}(r - \ln r - 1) \qquad (132)$$
$$\psi = -\delta$$

differentiate with respect to r:

$$\frac{dx}{dr} = -\frac{\delta}{\pi}\left(1 + \frac{2}{\sqrt{r}} + \frac{1}{r}\right) = -\frac{\delta}{\pi}\left(\frac{r + 2\sqrt{r} + 1}{r}\right) = -\frac{\delta}{\pi}\frac{(\sqrt{r}+1)^2}{r}$$

$$\frac{d\phi}{dr} = \frac{\delta}{\pi}\left(1 - \frac{1}{r}\right) = \frac{\delta}{\pi}\left(\frac{r-1}{r}\right)$$

therefore:

$$u = \frac{\partial\phi}{\partial x} = \frac{d\phi}{dr}\frac{dr}{dx} = -\frac{r-1}{(\sqrt{r}+1)^2} = -\left(\frac{\sqrt{r}-1}{\sqrt{r}+1}\right)$$

In the previous derivation the velocity V at infinity was assumed equal to 1. Since U is evidently proportional to V, the above can be rewritten in the final form:

$$u = +V\frac{\sqrt{r}-1}{\sqrt{r}+1} \qquad (133)$$

by assigning to r the values in the range $0 < r < \infty$, the velocity U can be computed by Eq. (133) and the corresponding value of x at which the velocity occurs by Eq. (131). The value of r = 1 gives x = 0 and u = 0, i.e. corresponds to the stagnation point.

The values of $r < 1$ give positive values of x, i.e. correspond to the spray sheet on basis of Fig. 28. For $r \to 0$, u = -V, i.e. the

action of the spray (i.e. the pressure gradients in the spray root) cause the reversal of the flow of fluid particles contained between the streamlines $\psi = 0$ and $\psi = -\delta V$, which form the spray sheet.

Since the flow is steady, the pressure at any point can be computed by Bernoulli's Equation

$$p_\infty + \frac{\rho}{2} V^2 = p + \frac{\rho}{2} U^2 \qquad (134)$$

in this case $V = 0$ and $U = u$. The pressure p can be conveniently expressed as the difference in the pressure at a given point and the pressure at infinity, i.e. p_∞ can be assumed equal to 0. Eq. (134) then becomes

$$p = \frac{\rho}{2} V^2 - \frac{\rho}{2} u^2$$

or

$$\frac{p}{\frac{1}{2}\rho V^2} = 1 - \left(\frac{u}{V}\right)^2 \qquad (135)$$

Substitute the value of u/v from Eq. 133:

$$\frac{p}{\frac{1}{2}\rho V^2} = 1 - \left(\frac{\sqrt{r} - 1}{\sqrt{r} + 1}\right)^2 \qquad (136)$$

At the stagnation point, $r = 1$, this gives the usual impact pressure

$$p = \frac{1}{2}\rho V^2$$

The pressure p expressed in terms of the impact pressure, i.e. $p/\frac{1}{2}\rho V^2$ is plotted vs. the length parameter $x\sqrt{\pi}/\delta$ on Fig. 34, taken from Ref. 12. The curve has the same general shape as the pressure distribution curve I + II + III on Fig. 22a computed by the expanding plate theory. Here is the same characteristic high pressure peak, the abrupt fall of the pressure towards the spray sheet, and more gradual fall of the pressure in the direction of the flow of the solid water. In the next article we will compare the magnitudes of the peak pressure as computed by two methods: the expansion plate - which considers the entire field, but neglects the details at the spray root, and the spray root theory—which considers these details, but neglects other boundary conditions of the field.

exp. press vs spray root

15. Comparison of Pressures from the Expanding Plate and from the Spray Root Theories.*

We return now to Section 12 dealing with the pressures acting on the wedge, as determined by the expanding plate theory, in order to extend it to get expressions convenient for comparison of pressures with those obtained by the spray root theory.

The pressure at any point of the immersing wedge was given by Eq. (66), which we restate now in a slightly modified form:

$$P = \frac{\rho v_0^2}{\lambda}\left(\frac{1}{\sqrt{1-x^2/c^2}} - \frac{\lambda}{2}\frac{1}{c^2/x^2-1} + \frac{\lambda}{2}\right) \quad (138)$$

where C is the semi-breadth of the wetted area, x the distance of the point under consideration from the centerline, and the non-dimensional number λ was defined as the ratio of the penetration velocity v_0 to the expansion velocity of the edge of the wetted area C, or

$$\lambda = v_0/\dot{C} \quad (139)$$

The pressure is maximum when the slope of the curve of p versus x/c is zero, i.e. when for any particular value of C $dp/dx = 0$. Differentiating Eq. 138 with respect to p:

$$\frac{dp}{dx} = \frac{\rho v_0^2}{\lambda}\left(\frac{x/c^2}{(1-x^2/c^2)^{3/2}} - \frac{\lambda}{2}\frac{2c^2/x^3}{(c^2/x^2-1)^2}\right) \quad (140)$$

It will be observed that the first term in brackets corresponds to the slope of the Curve I, and the second term to the slope of the Curve II on Fig. 22a, and the $dp/dx = 0$ when these two are equal in absolute magnitude:

$$\frac{dp}{dx} = 0 = \frac{\bar{x}/c^2}{(1-\bar{x}^2/c^2)^{3/2}} - \frac{\lambda}{2}\frac{2c^2/\bar{x}^3}{(c^2/\bar{x}^2-1)^2}$$

The symbol $\bar{x}$ was used above to denote the value of x at which $dp/dx = 0$ and p = max. Dividing the numerator and denominator of the second term by c^4/x^4 we obtain

$$\frac{\bar{x}}{c^2(1-\bar{x}^2/c^2)^{3/2}} = \frac{\lambda}{c^2}\frac{\bar{x}}{(1-\bar{x}^2/c^2)^2}$$

*Following Ref. 7 except for the concluding paragraphs.

from which it follows:

$$\lambda = (1-\bar{x}^2/c^2)^{1/2}$$

or

$$\bar{x}/c = \sqrt{1-\lambda^2} \qquad (141)$$

Substituting this value of $\bar{x}/c$ into Eq. (138):

$$p_{max.} = \frac{\rho v_0}{\lambda}\left[\frac{1}{\lambda} - \frac{\lambda}{2}\left(\frac{1-\lambda^2}{\lambda^2}\right) + \frac{\lambda}{2}\right]$$

or finally:

$$p_{max.} = \frac{\rho v_0^2}{2\lambda^2}(1+2\lambda^2) \qquad (142)$$

In case of the spray root theory, the pressure at stagnation point is given by $1/2\,\rho V^2$, where V is the relative velocity of the fluid with respect to the stagnation point. In application to the wedge penetrating into still water, the stagnation point can be assumed to coincide with the point of the maximum pressure by the expanding plate theory, i.e. be located by the abscissa $\bar{x}$. The velocity V is now the velocity of propagation of the stagnation point along the surface of the wedge. This velocity is evaluated as:

$$\dot{\bar{x}} = \frac{d}{dt}(\bar{x}) = \frac{d}{dt}\left(\frac{\bar{x}}{c}c\right)$$

observing that although $\bar{x}$ is a function of time, the ratio $\bar{x}/c$ is constant:

$$\dot{\bar{x}} = \frac{\bar{x}}{c}\dot{c} \qquad (143)$$

evaluating $\bar{x}/c = \sqrt{1-\lambda^2}$ by Eq. (141) and $\dot{c} = v_0/\lambda$ by Eq. 139 gives:

$$\dot{\bar{x}} = v_0\frac{\sqrt{1-\lambda^2}}{\lambda}$$

and

$$p_{max} = \tfrac{1}{2}\rho\dot{\bar{x}}^2 = \frac{\rho v_0^2}{2\lambda^2}(1-\lambda^2) \qquad (144)$$

Actually $\dot{\bar{x}}$ is only the horizontal component of the velocity of the stagnation point. It also has the vertical component due to its

Exp. Plate vs Spray Root

rate of rise above keel $\dot{\bar{X}} \tan\beta$, less the velocity of penetration v_o, i.e.

$$v = v_o \frac{\sqrt{1-\lambda^2}}{\lambda} \tan\beta - v_o = v_o\left(\frac{\sqrt{1-\lambda^2}}{\lambda}\tan\beta - 1\right)$$

For instance for 20° deadrise, $\tan\beta = .364$, $\lambda = .232$, $\dot{\bar{X}} = 4.2\, v_o$ and $v = .53$. The error in the estimate of the maximum pressure due to the neglect of the vertical component v is $(.53/4.2)^2 = 1.6\%$.

By comparing Eq. 144 with Eq. 142, we see that max. pressure is expressed by

$$p_{max} = \frac{\rho v_o^2}{2\lambda^2} k \qquad (145)$$

where:

from the expanding plate theory $k = 1 + 2\lambda^2$

from the spray root theory $k = 1 - \lambda^2$

The comparison of values of these coefficients for several deadrises is given below

Table IV

Deadrise in degrees	λ	The Coefficient Exp. Plate	Spray root
15	.171	1.06	.97
20	.232	1.11	.95
25	.297	1.18	.91
30	.367	1.27	.87
40	.535	1.50	.71

The experimental determination of the maximum pressure is very difficult, and the reliable data are difficult to find. The direct experiment by dropping the wedge onto water surface is difficult because the pressure peak travels over the pressure pick-up so rapidly that the pressure pulse of very short duration has to be recorded. This procedure usually leads to large instrument errors. The other source of error is often (if not usually) the large area of the pressure pick up, which therefore records the mean pressure over this area, rather than the true peak pressure. The data given by Fig. 42 of the first semester notes were obtained by this method. Experimental pressures were shown to be much lower than theoretical (presumably from the expansion

plate theory). While this deficiency of the pressure may be partly due to the experimental difficulties mentioned above, it is probably due mostly to the fact that very small deadrise angle of 9.5 degrees was used. As has been stated already (on p. 28) the expanding plate theory necessarily fails at the zero deadrise, and this applies equally to the spray root theory. The failure of both theories, connected with the fact that the velocities of the stagnation point $\dot{\bar{X}}$ approaches infinity as the deadrise β approaches zero, apparently becomes noticeable for the deadrise below 15 degrees, and the pressure deficiency at the deadrise angle of 10 degrees is quite pronounced.

A more reliable method of obtaining the experimental pressures is obtained by taking advantage of the similarity between the immersing wedge, and the planing of the prismatic Vee surface as shown by Figs. 18 and 19. The pressures are measured at a number of orifices on the bottom of a Vee surface planing at a steady speed. The instrumentation is simpler because the pressures are steady instead of being impulsive, and the pressure orifice can be much smaller than the diaphragm of a dynamic pressure pick up. There is a difficulty of making sure that the peak of the pressure is at the orifice, and the pressure is also very sensitive to the conditions at the orifice edges. Ref. 7, based on such a test for the 20 degree deadrise surface gives the max. pressure values a little smaller than those resulting from the expansion plate theory, and higher than given in the table IV for the spray root theory. The analysis of the pressures measured on Vee surfaces by Sottorf indicates the ratio of maximum experimental pressures to the spray root analysis pressures to be as follows:

For 5° deadrise-----	0.50
10°	0.65
15°	0.77
20°	0.85
30°	0.95

It is interesting to note that the factor of 0.65 for 10° deadrise very nearly agrees with Fig. 42 of the first semester notes.

We expect to return to the question of pressures again later in the course, but for the present it can be stated that the theory is well ahead of the experimental data, that the discrepancy between the expanding plate and the spray root theories is smaller than the uncertainty of the experi-

mental data, and that for the present, at least, the spray root data are recommended for use for the deadrise of 20 degrees and over.

16. The Flow at a Flat Planing Surface

In the article 14 we examined the flow in the vicinity of a doubly infinite flat plate at a zero angle of trim.

The attention was concentrated specifically on the flow in the vicinity of the spray root, and no other boundary conditions were introduced. As a result, a kinematic picture of the spray root region was obtained, and from the knowledge of velocities the pressure distribution was computed. The failure to introduce enough boundary conditions, however made the picture incomplete, and even inconsistent from the dynamic point of view. Thus we observe that in the part of the water turned into spray, the momentum of water is changed from $-\rho\delta V$ to $+\rho\delta V$, and therefore the drag force must be produced. Yet with the horizontal plate and the frictionless fluid, there is no mechanism of developing such a drag force.

We will apply now the methods of the previous chapter to the more realistic problem of the flow at a flat planing surface set at an angle of trim τ, and possessing a trailing edge g as shown on Fig. 33. The plate is of infinite span, so that the flow is two dimensional. It is assumed to extend infinitely in the forward direction, but this is just a way of saying that we are interested only in the formation of a spray sheet, and are not interested in what happens to it thereafter. As a matter of fact, in absence of the gravity and of frictional forces, once formed it will exist forever, i.e. will extend to infinity in the forward and upward direction.

Fig. 33 shows a flat plate with the trailing edge g, set at an angle of attack τ. The water flow is horizontal at infinity from right to left, both in front and aft of the plate. At the trailing edge the water leaves the plate tangentially, i.e. the velocity vector V is deflected downwards through the angle τ. There is a dividing streamline near the surface, which comes to a stagnation point, and above and in front of which the water is turned forward. We have now two sections of the free boundary--in the spray root b-c, and aft of the trailing edge gh. Both of these are in contact with the atmosphere, and are subjected to the uniform atmospheric pressure, and therefore at both the velocity has the uniform value V_1 which we will take as $V = 1$.

As in the previous case, we rotate the figure to such a position that the surface of the plate is horizontal, and the flow is above it, as on Fig. 34, which represents the Z plane. The direction of the velocity vector at the free boundary is $\theta = \pi + \tau$ at infinity both in the front at c, and in the rear at h. Along the free streamline bc it changes from $\theta = \pi + \tau$ to $\theta = 2\pi$, and along the free streamline gh from $\theta = \pi$ to $\theta = \pi + \tau$. The origin of the axes of coordinates is now taken at the trailing edge.

As before, we form the functions $\zeta = dz/dw$ and $\Omega = \ln \zeta$, and draw the w plane (Fig. 35), ζ plane (Fig. 36), Ω plane (Fig. 37) and t plane (Fig. 38). The important step, of course, is the assignment of the values of t, corresponding to the corners of the Ω plane. The value t = -1 is assigned to the trailing edge point g, t = +1 to the points c and d at infinity in the spray sheet, and t = m to the stagnation point ef. The value of m lies in the interval $-1 < m < 1$, and the determination of it is one of the important objectives of the analysis. The other objectives are the shape of the free streamlines, and the velocities and pressure distributions along the plate (the rigid boundary).

We proceed to establish the relation $d\Omega/dt$ by applying the Schwarz Christoffel theorem to the Ω plane and t plane, assuming, as before, the polygon of Fig. 37 to be split at h and b:

$$d\Omega = A\,(t-1)^{-\frac{1}{2}}(t-m)^{-1}(t+1)^{-\frac{1}{2}} = A\,\frac{dt}{(t-m)\sqrt{t^2-1}} \qquad (146)$$

In order to integrate this, the substitution is made t = u + m, dt = du, so that Eq. (146) becomes:

$$d\Omega = A\,\frac{du}{u\sqrt{u^2+2um+(m^2-1)}}$$

This is of the form

$$d\Omega = A\,\frac{du}{u\sqrt{au^2+bu+c}}$$

where $a = 1$

$b = 2m$

$c = m^2 - 1$

The integral of the above is found in the short tables of integrals* as:

$$\int f(u) = -\frac{1}{\sqrt{c}} \ln\left(\frac{\sqrt{au^2+bu+c}+\sqrt{c}}{u} + \frac{b}{2\sqrt{c}}\right)$$

and upon substitution of the values of coefficients and of u = t - m:

$$\Omega = -\frac{A}{\sqrt{m^2-1}} \ln\left(\frac{\sqrt{t^2-1}+\sqrt{m^2-1}}{t-m} + \frac{m}{\sqrt{m^2-1}}\right) + B$$

or bringing to the common denominator:

$$\Omega = -\frac{A}{\sqrt{m^2-1}} \ln \frac{\sqrt{t^2-1}\sqrt{m^2-1}+(m^2-1)+m(t-m)}{(t-m)\sqrt{m^2-1}} + B$$

The factor $1/\sqrt{m^2-1}$ under the ln sign can be brought out:

$$\Omega = -\frac{A}{\sqrt{m^2-1}}\left[\ln\frac{1}{\sqrt{m^2-1}} + \ln\frac{\sqrt{(t^2-1)(m^2-1)}+(mt-1)}{t-m}\right] + B$$

The additive constant term

$$\frac{A}{\sqrt{m^2-1}} \ln\frac{1}{\sqrt{m^2-1}}$$

m = constant in t plane

can be absorbed in the constant of integration β. Multiplying subsequently the numerator and the denominator under the ln sign by

$$-\sqrt{(t^2-1)(m^2-1)}+(mt-1)$$

gives

$$\Omega = -\frac{A}{\sqrt{m^2-1}} \ln\frac{t-m}{mt-1-\sqrt{(t^2-1)(m^2-1)}} + B$$

and finally, taking the reciprocals of the quantity under ln sign:

$$\Omega = \frac{A}{\sqrt{m^2-1}} \ln\frac{mt-1-\sqrt{(t^2-1)(m^2-1)}}{t-m} + B \qquad (147)$$

In order to evaluate the constant B, substitute the values corresponding to the point g, i.e. $\Theta = \pi$, U = 1 and t = -1, which make the ln on the right hand side vanish.

$$\Omega = \ln\frac{dz}{dw} = \ln\frac{1}{U} + i\Theta = i\pi = B \qquad (148)$$

In order to determine the constant A, substitute the values corresponding to the point b,h where U = 1, $\Theta = \pi + \tau$ and $t = \infty$. First rewrite the expression under the ln sign by dividing the numerator and denominator by t:

$$\ln\frac{m-\frac{1}{t}-\sqrt{(1-\frac{1}{t^2})(m^2-1)}}{1-\frac{m}{t}}$$

*For instance Burrington p. 71 No. 169

for $t = \infty$ this becomes

$$\ln(m - \sqrt{m^2-1})$$

and

$$\ln \frac{dz}{dw} = i(\pi+\tau) = \frac{A}{\sqrt{m^2-1}} \ln(m - \sqrt{m^2-1}) + 2i\pi$$

or

$$A = \frac{2i\tau\sqrt{m^2-1}}{\ln(m-\sqrt{m^2-1})}$$

and finally

$$\ln \frac{dz}{dt} = 2i \frac{\tau}{\ln(m-\sqrt{m^2-1})} \ln \frac{mt-1-\sqrt{(t^2-1)(m^2-1)}}{t-m} + 2i\pi \quad (149)$$

Determination of m

Now the quantity m can be determined. Since m was defined as a real number such that $-1 < m < 1$, it can be conveniently defined as

$$m = \cos\gamma$$

In order to evaluate γ substitute this value of m into Eq. (149), and at the same time substitute the values corresponding to the points c,d in the spray sheet at infinity, i.e. $U = 1$, $\theta = 2\pi$ and $t = +1$:

$$2i\pi = \frac{2i\tau}{\ln(m-\sqrt{m^2-1})} \ln \frac{m-1}{1-m} + 2i\pi$$

$$2\pi = \frac{\tau}{\ln(\cos\gamma - i\sin\gamma)} \ln(-1) + \pi$$

$\ln(\cos\gamma - i\sin\gamma) = \ln(e^{-i\gamma}) = -i\gamma$

$$2\pi = \frac{\tau}{-i\gamma}(-i\pi) + \pi$$

and

$$\gamma = \tau$$

so that m is defined as

$$m = \cos\tau \quad (150)$$

The coefficient of Eq. (149) now becomes

$$\frac{2i\tau}{\ln(m-\sqrt{m^2-1})} = \frac{2i\tau}{\ln(\cos\tau - i\sin\tau)} = \frac{2i\tau}{\ln e^{-i\tau}} = \frac{2i\tau}{-i\tau} = -1$$

and Eq. (149) becomes

$$\ln \frac{dz}{dw} = -\ln \frac{t\cos\tau - 1 - i\sin\tau\sqrt{t^2-1}}{t-\cos\tau} + i\pi$$

Substituting $i\pi = \ln e^{i\pi} = \ln(-1)$, and taking the reciprocal:

$$\ln \frac{dz}{dw} = \ln\left(-\frac{t-\cos\tau}{t\cos t - 1 - i\sin\tau\sqrt{t^2-1}}\right)$$

Multiplication of the numerator and denominator by

$$t\cos\tau - 1 + i\sin\tau\sqrt{t^2-1}$$

check into elimination of $i\pi$

gives

$$\ln \frac{dz}{dw} = \ln - \frac{t\cos\tau - 1 + i\sin\tau\sqrt{t^2-1}}{t-\cos\tau}$$

and taking anti-logarith of both sides:

$$\frac{dz}{dw} = -\frac{t\cos\tau - 1 + i\sin\tau\sqrt{t^2-1}}{t-\cos\tau} \qquad (151)$$

The Transformation dw/dt

We proceed now to apply the Schwarz-Christoffel theorem to the transformation of the lower half of the w plane (Fig. 35) onto the upper half of the t plane, considering the internal angle of 0 at the point c, d at which $\phi = \infty$ and t = 1, and the point e,f at which the internal angle is $\partial\pi$, ϕ = 0 and t = m:

$$\frac{dw}{dt} = C(t-1)^{\frac{0}{\pi}-1}(t-m)^{\frac{2\pi}{3\pi}-1} = C\frac{t-m}{t-1} \qquad (152)$$

$$w = C\left[\int \frac{t}{t-1}dt - \int \frac{m}{t-1}dt\right]$$
$$= C\left[t + \ln(t-1) - m\ln(t-1)\right] + D$$

or

$$w = C\left[t + (1-m)\ln(t-1)\right] + D \qquad (153)$$

We observe that at the points c and d, where t = 1, we have ln 0, and we write the expressions for the point c on the free boundary at which t > 1 and (t-1) approaches zero from positive values; and point d on the solid boundary for which t < 1 and (t-1) approaches zero from the negative values:

$\phi_0 + 0 =$

$$w = 0 = C\left[1 + (1-m)\ln(t-1)\right] + D \qquad (154)$$
$$(t-1) \to 0$$

$\ln(1-t)(-1)$
$= \ln(1-t) + \ln(-1)$
$= \ln(1-t) + i\pi$

$= \phi_0 - i\delta =$

$$w = -i\delta = C\left[1 + (1-m)\ln\left(\frac{1-t}{t-1}\right) + (1+m)i\pi\right] + D \qquad (155)$$
$$(1-t) \to 0$$

and subtracting Eq. (154) from Eq. (155):

$$-i\delta = C\, i\pi(1-m)$$

and

$$C = -\frac{\delta}{\pi(1-m)} \qquad (156)$$

so that

$$w = -\frac{\delta}{\pi(1-m)}\left[t + (1-m)\ln(t-1)\right] + D \qquad (157)$$

Now, at the stagnation point ef, w = o - $i\delta$, and t = m, so that Eq. (157) becomes:

$$-i\delta = -\frac{\delta m}{\pi(1-m)} - \frac{\delta}{\pi}\ln(m-1) + D \qquad (158)$$

Since by definition $m < 1$:

$$-i\delta = -\frac{\delta m}{\pi(1-m)} - \frac{\delta}{\pi}\ln(1-m) - \frac{\delta}{\pi} i\pi + D$$

and

$$D = \frac{\delta m}{\pi(1-m)} + \frac{\delta}{\pi}\ln(1-m)$$

and Eq. (158) becomes:

$$w = -\frac{\delta}{\pi}\frac{1}{1-m}\left[t + (1-m)\ln(t-1) - m - (1-m)\ln(1-m)\right] \qquad (159)$$

Substitution of Eq. (156) into Eq. (152) gives

$$\frac{dw}{dt} = -\frac{\delta}{\pi(1-m)}\,\frac{t-m}{t-1} \qquad (160)$$

or substituting $m = \cos\tau$:

$$\frac{dw}{dt} = -\frac{\delta}{\pi(1-\cos\tau)}\,\frac{t-\cos\tau}{t-1} \qquad (161)$$

Transformation dz/dt

The Equation (151)

$$\frac{dz}{dw} = -\frac{t\cos\tau - 1 + i\sin\tau\sqrt{t^2-1}}{t-\cos\tau}$$

together with Eq. (161) above, gives

$$\frac{dz}{dt} = \frac{dz}{dw}\,\frac{dw}{dt} =$$

$$= \frac{\delta}{\pi(1-\cos\tau)}\,\frac{t\cos\tau - 1 + i\sin\tau\sqrt{t^2-1}}{t-1} \qquad (162)$$

and

$$dz = \frac{\delta}{\pi(1-\cos\tau)}\left(\cos\tau\int\frac{t\,dt}{t-1} - \int\frac{dt}{t-1} + i\sin\tau\int\frac{\sqrt{t^2-1}\,dt}{t-1}\right) \qquad (163)$$

It will be convenient to modify the integrand of the last term as follows:

$$\frac{\sqrt{t^2-1}}{t-1} = \frac{\sqrt{t+1}}{\sqrt{t-1}} = \frac{\sqrt{t+1}\sqrt{t+1}}{\sqrt{t-1}\sqrt{t+1}} = \frac{t+1}{\sqrt{t^2-1}} = \frac{t}{\sqrt{t^2-1}} + \frac{1}{\sqrt{t^2-1}}$$

With this modification Eq. (163) can be easily integrated:

$$Z = \frac{\delta^2}{\pi(1-\cos\tau)}\left[\cos\tau\,(t+\ln(t-1)) - \ln(t-1) + \right.$$
$$\left. + i\sin\tau\sqrt{t^2-1} + i\sin\tau\,\ln\left(t+\sqrt{t^2-1}\right)\right] + E$$

and regrouping the terms:

$$Z = \frac{\delta^2}{\pi(1-\cos\tau)}\left[t\cos\tau - (1-\cos\tau)\ln(t-1) + \right. \qquad (164)$$
$$\left. + i\sin\tau\sqrt{t^2-1} + i\sin\tau\,\ln\left(t+\sqrt{t^2-1}\right)\right] + E$$

To evaluate the constant of integration E, substitute the values corresponding to the point g, i.e. z = 0, t = -1

$$0 = \frac{\delta^2}{\pi(1-\cos\tau)}\left[-\cos\tau - (1-\cos\tau)\ln(-2) + \right.$$
$$\left. + i\sin\tau\,\ln(-1)\right] + E$$

or

$$E = \frac{\delta^2}{\pi(1-\cos\tau)}\left[\cos\tau + (1-\cos\tau)(\ln 2 + i\pi) + \right. \qquad (165)$$
$$\left. + \pi\sin\tau\right]$$

With slight rearrangement of terms, Eq. (164) now can be written as:

$$\frac{z\pi}{\delta^2} = \frac{1}{1-\cos\tau}\left[(t+1)\cos\tau - (1-\cos\tau)\ln\frac{t-1}{2} + \right.$$
$$+ i\sin\tau\sqrt{t^2-1} + i\sin\tau\ln\left(t+\sqrt{t^2-1}\right) + \qquad (166)$$
$$\left. + i\pi(1-\cos\tau) + \pi\sin\tau\right]$$

5-2-50

Shape of the free boundary

All points on the free boundary in the spray root region b-c correspond to the real values of $t > 1$. The separation of the real

and imaginary variables is therefore a straight-forward process:

SHAPE OF SPRAY ROOT BOUNDARY

$$\frac{x\pi}{\delta} = \frac{1}{1-\cos\tau}\left[(t+1)\cos\tau - (1-\cos\tau)\ln\frac{t-1}{2} + \pi\sin\tau\right]$$

$$\frac{y\pi}{\delta} = \frac{1}{1-\cos\tau}\left[\sin\tau\sqrt{t^2-1} + \sin\tau\ln(t+\sqrt{t^2-1}) + \pi(1-\cos\tau)\right] \quad (167)$$

The variation of the shape of the free surface with trim is shown on Fig. 39, where the curves are plotted for the same wetted length. It will be observed that the thickness of spray and the ordinates of the spray root curve increase with the angle of trim τ .

The points on the free boundary aft of the trailing edge g-h correspond to the real values of $t < -1$. We will denote therefore $|t| = \xi$ and will consider separately several terms of Eq. (166).

The first term in square brackets becomes $(1-\xi)\cos\tau$

In the second term:

$$\ln\frac{t-1}{2} = \ln\frac{-\xi-1}{2} = \ln\frac{\xi+1}{2}(-1) = \ln\frac{\xi+1}{2} + i\pi$$

In the third term

$$t^2 = \xi^2 > 1 \qquad \text{and} \qquad \sqrt{t^2-1} = \sqrt{\xi^2-1}$$

In the fourth term $t^2-1 = \xi^2-1 \geq 1 \quad \xi > \sqrt{\xi^2-1}$

$$\ln(t+\sqrt{t^2-1}) = \ln(-\xi+\sqrt{\xi^2-1}) = \ln(\xi-\sqrt{\xi^2-1})(-1) =$$
$$= \ln(\xi-\sqrt{\xi^2-1}) + i\pi$$

Substitution of the above values into Eq.(166) yields:

$$\frac{z\pi}{\delta} = \frac{1}{1-\cos\tau}\left[(1-\xi)\cos\tau - (1-\cos\tau)\ln\frac{\xi+1}{2} - i\pi(1-\cos\tau)\right.$$
$$+ i\sin\tau\sqrt{\xi^2-1} + i\sin\tau\ln(\xi-\sqrt{\xi^2-1})$$
$$\left. - \pi\sin\tau + i\pi(1-\cos\tau) + \pi\sin\tau\right] \qquad (168)$$

SHAPE OF WAVES

And separating the real and imaginary variables:

$$\frac{x\pi}{\delta} = \frac{1}{1-\cos\tau}\left[(1-\xi)\cos\tau - (1-\cos\tau)\ln\frac{\xi+1}{2}\right]$$

$$\frac{y\pi}{x} = \frac{\sin\tau}{1-\cos\tau}\left[\sqrt{\xi^2-1} + \ln\left(\xi - \sqrt{\xi^2-1}\right)\right] \qquad (169)$$

In above equations all terms are real and $\xi = |t| > 1$ is always taken as positive. The shape of the water surface aft of the trailing edge, shown by above equations, is plotted on Fig. 39.

Velocity and Pressure Distribution on the Solid Boundary (the Planing Surface).

The points on the solid boundary correspond to real values of t in the range $-1 < t < +1$. We will again examine each term of Eq. (166) separately for this range of t values.

The first term does not call for any comments. In the second term $(t-1)$ is always negative, since $|t| \leq 1$, and therefore

$$\ln\frac{t-1}{2} = \ln\frac{1-t}{2} + i\pi$$

In third term $t^2 \leq 1$, and

$$\sqrt{t^2-1} = \sqrt{(1-t^2)(-1)} = i\sqrt{1-t^2}$$

Likewise in fourth term:

$$\ln\left(t + \sqrt{t^2-1}\right) = \ln\left(t + i\sqrt{1-t^2}\right)$$

Even this rearrangement does not put this term into the form suitable for separation of the real and imaginary variables. To accomplish this, make substitution $t = \cos\theta$, and $\sqrt{1-t^2} = \sin\theta$

$$\ln\left(t + i\sqrt{1-t^2}\right) = \ln\left(\cos\theta + i\sin\theta\right) = \ln e^{i\theta} = i\theta = i\cos^{-1}t$$

The Eq. (166) can be written now for $-1 < t < +1$:

$$\frac{2\pi}{\delta} = \frac{1}{1-\cos\tau}\left[(t+1)\cos\tau - (1-\cos\tau)\ln\frac{1-t}{2} - \pi(1-\cos\tau) - \sin\tau\sqrt{1-t^2} - \cos^{-1}t\sin\tau + \pi(1-\cos\tau) + \pi\sin\tau\right] \qquad (170)$$

In the above equation all terms are real, so that Z can be immediately replaced by x, and $y = 0$, conforming to the definition of the solid boundary.

In order to obtain the velocities corresponding to different values of the parameter t (and therefore the coordinate x) take the reciprocal of the Eq. (151), together with the definition of dw/dz from Eq. (67) and from the top of page 30:

$$\frac{dw}{dz} = u - iv = \frac{-t-\cos\tau}{t\cos\tau - 1 + i\sin\tau\sqrt{t^2-1}}$$

Upon substitution $\sqrt{t^2-1} = i\sqrt{1-t^2}$, all terms on the R. H. side become real. Furthermore inserting the velocity V in place of 1 used in the analysis, we get:

$$\frac{u}{V} = \frac{t-\cos\tau}{1-t\cos\tau+\sin\tau\sqrt{1-t^2}} \qquad (171)$$

and by Bernoulli's equation (Eq. 135)

$$\frac{p}{\frac{1}{2}\rho V^2} = 1-\left(\frac{u}{V}\right)^2 \qquad (172)$$

At the trailing edge g, $t = -1$, and $u/V = 1$. On the forward part of the boundary at d, $t = +1$, and likewise $u/V = 1$. At stagnation point e, f $t = m = \cos\tau$, $u = 0$ and $p = 1/2\ \rho V^2$.

In order to compare the pressure distribution for several dead-rises, it is necessary to establish some standard of the length over which the pressure is distributed, since the values of x corresponding to the given value of t will vary widely for different values of the angle of trim τ. A convenient length for this purpose is the dimension x_m given on Fig. 34, which may be called "wetted length" in the sense already used in Art. 11 (page 24). Mathematically it is defined as the minimum value of x of the free boundary curve b-c, and can be obtained by differentiating Eq. 167 with respect to t, and

and setting the dx/dt = 0: for minimum values on spray boundary

$$\frac{\pi}{\delta}\frac{dx}{dt} = \frac{1}{1-\cos\tau}\left[\cos\tau - (1-\cos\tau)\frac{1}{t-1}\right]$$

and equating the expression in square brackets to zero:

$$\cos\tau = (1-\cos\tau)\frac{1}{t-1}$$

or

$$t = 1/\cos\tau \qquad (173)$$

Substitution of this value into the first of Eqs. (167) yields:

$$\frac{x_m\pi}{\delta} = \left[\frac{1+\cos\tau}{1-\cos\tau} - \ln\left(\frac{1-\cos\tau}{2\cos\tau}\right) + \frac{\pi\sin\tau}{1-\cos\tau}\right] \qquad (174)$$

The pressures computed from Eqs. 171 and 172 can be conveniently plotted now against the ratio x/x_m, as this has been done on Fig. 40. It will be observed that as the angle of trim τ increases, the pressure peak becomes broader, and the point of the maximum pressure moves aft. It is interesting to observe that at the leading edge of the wetted area, at the $x/x_m = 1$, the pressure is approximately 3/4 of the maximum pressure for all angles of trim.

The total pressure on the plate is obviously represented by the area under the pressure distribution curve on Fig. 40. It evidently increases with the angle of trim, and it is clear from the visual inspection that the center of pressure (the center of gravity of the area under a curve) moves aft with increase of τ. The maximum pressure does not depend on the angle τ, but only on the velocity V. This is clear from Eq. (171) when $t = m = \cos\tau$ is substituted into it.

In case of the flow about doubly infinite horizontal plate, the spray thickness δ was the only length parameter available. In the present case of the plate with the trailing edge placed at an angle of attack τ, there are two length parameters δ and x_m, and the non-dimensional parameter τ. The solution expressed by Eq. (174) gives therefore the ratio δ/x_m as the function of τ.

Total Normal Force Acting on a Planing Surface.

The total normal force acting on a planing surface can be obtained by integrating the area under the pressure distribution curve of Fig. 40, i.e. by writing:

$$F = \int_{x=0}^{x=\infty} p\,dx = \int_{t=-1}^{t=+1} p \frac{dx}{dt}\,dt \tag{175}$$

The pressure p is given by Eqs. 172 and 171 as:

$$\frac{p}{\frac{1}{2}\rho V^2} = 1 - (u/V)^2 \tag{176}$$

and

$$\frac{u}{V} = \frac{t - \cos\tau}{1 - t\cos\tau + \sin\tau\sqrt{1-t^2}} \tag{177}$$

The derivative dx/dt is given by Eq. 162

$$\frac{dz}{dt} = \frac{\delta}{\pi(1-\cos\tau)} \frac{-1 + t\cos\tau + i\sin\tau\sqrt{t^2-1}}{t-1}$$

For the solid boundary, $Z = X$, and $|t| \leq 1$, so that $i\sqrt{t^2-1} = -\sqrt{1-t^2}$, and above becomes

$$\frac{dx}{dt} = \frac{\delta}{\pi(1-\cos\tau)} \frac{-1 + t\cos\tau - \sin\tau\sqrt{1-t^2}}{t-1} \tag{178}$$

Substitution of Eq's. 176, 177 and 178 into Eq. 175 gives:

$$F = \frac{\rho V^2 \delta}{2\pi(1-\cos\tau)} \int_{-1}^{+1} \left[1 - \left(\frac{t-\cos\tau}{1 - t\cos\tau + \sin\tau\sqrt{1-t^2}}\right)^2\right] \left[\frac{-1 + t\cos\tau - \sin\tau\sqrt{1-t^2}}{t-1}\right] dt$$

$$= \frac{\rho V^2 \delta}{2\pi(1-\cos\tau)} \int_{-1}^{+1} \left[\frac{-1 + t\cos\tau - \sin\tau\sqrt{1-t^2}}{t-1} - \right.$$

$$\left. - \frac{(t-\cos\tau)^2(-1 + t\cos\tau - \sin\tau\sqrt{1-t^2})}{(t-1)(1 - t\cos\tau + \sin\tau\sqrt{1-t^2})^2}\right] dt \tag{179}$$

The second term in square brackets becomes

$$+ \frac{(t-\cos\tau)^2}{(t-1)(1 - t\cos\tau + \sin\tau\sqrt{1-t^2}}$$

Multiplication of the numerator and denominator by $(1 - t\cos\tau - \sin\tau\sqrt{1-t^2})$ puts the denominator in the form

$$(t-1)(t-\cos\tau)^2$$

So that cancelling $(t - \cos\tau)^2$, leaves

$$+\frac{1-t\cos\tau-\sin\tau\sqrt{1-t^2}}{t-1}$$

Inserting this value of the second term into Eq. 179 gives

$$F=\frac{\rho V^2\delta^2}{2\pi(1-\cos\tau)}\int_{-1}^{+1}-\frac{2\sin\tau\sqrt{1-t^2}}{t-1}dt$$

$$=\frac{\rho V^2\delta^2\sin\tau}{2\pi(1-\cos\tau)}\int_{-1}^{+1}\frac{\sqrt{1-t^2}}{t-1}dt$$

or with the algebraic change of the form similar to one of the integrand given by Eq. (163a):

$$F=\frac{\rho V^2\delta^2}{\pi}\frac{\sin\tau}{1-\cos\tau}\left[\int_{-1}^{+1}\frac{t\,dt}{\sqrt{1-t^2}}+\int_{-1}^{+1}\frac{dt}{\sqrt{1-t^2}}\right]$$

$$=\frac{\rho V^2\delta^2}{\pi}\frac{\sin\tau}{1-\cos\tau}\left[\sin^{-1}t-\sqrt{1-t^2}\right]_{-1}^{+1}$$

and finally

$$F=\rho V^2\delta^2\frac{\sin\tau}{1-\cos\tau}=\rho V^2\delta\cot\frac{\tau}{2} \qquad (180)$$

Application of the **Momentum** Theory

If the determination of the total force F were the only object of the analysis, the Eq. (179) could be derived directly by the consideration of the changes of **momenta.** With reference to Fig. 42, consider the sum of momenta of the fluid at infinite distance up stream and down stream of the plate, and at infinite distance from the spray root. The velocity at infinity is everywhere equal to V, and therefore the changes of momenta occur only due to changes in the direction of the flow. Below the streamline $\psi = -\delta V$, there is no change in the direction, and therefore no change in the momentum of the fluid. The

fluid between the streamlines $\psi = 0$ and $\psi = -\delta V$ undergoes the change of direction through the angle of $\pi - \tau$, as shown by the vector diagram on Fig. 42. The sum of the horizontal components of the momenta is

$$\rho\delta^2V^2 + \rho\delta V^2\cos\tau = \rho\delta^2V^2(1+\cos\tau)$$

The above represents the change of the horizontal momentum per second and is equal to the drag force D. Since in the frictionless fluid the total force F is normal to the plate, we have

$$F = D/\sin\tau = \rho\delta V^2\frac{1+\cos\tau}{\sin\tau} = \rho\delta V^2\cot\frac{\tau}{2} \qquad (181)$$

The vertical components of the force F and of the momenta add to

$$F\cos\tau + \rho\delta^2V^2\sin\tau =$$

This represents the vertical reaction produced by the infinitessimal pressure over the infinite area at some streamline $\psi = -\infty$, as for instance at the bottom at a great depth. The boundary conditions set for the present problem, however, do not permit further study of the vertical reaction.

Total Normal Force in Terms of the Wetted Length χ_m.

The expression (180) is misleading, as it gives the appearance of the decrease of the normal force with the increase of the τ. As a matter of fact the normal force increases with the angle of trim τ, and Eq. (180) will indicate this if the proper values of δ increasing with τ were inserted. It is desirable therefore to eliminate the spray thickness δ, and to express the force F in terms of the wetted length χ_m by using the definition of δ given by Eq. (174):

$$\delta = \frac{\pi\chi_m}{\frac{1+\cos\tau}{1-\cos\tau} - \ln\frac{1-\cos\tau}{2\cos\tau} + \frac{\pi\sin\tau}{1-\cos\tau}} \qquad (182)$$

Substitution of Eq. (182) into Eq. (180) gives:

$$F = \frac{\rho V^2\chi_m}{2}\,\frac{2\pi\sin\tau}{1+\cos\tau-(1-\cos\tau)\ln\left(\frac{1-\cos\tau}{2\cos\tau}\right)+\pi\sin\tau} \qquad (183)$$

or

$$F = \frac{\rho V^2\chi_m}{2}\,f(\tau) \qquad (184)$$

$$F = \rho V^2 \delta f(\tau)$$

The above expression applies to the unit width of the plate of infinite span, so that we have the area = $\lambda_m \times 1$, and the expression is found to be dimensionally correct. The $f(\tau)$ is, of course, non-dimensional.

It will be noted that the quantity under the ln sign in the denominator is less than one, and the entire term becomes positive when the numerical values are substituted. This term has very small magnitude, and the pair of terms

$$\cos\tau + (1-\cos\tau)\ln\left(\frac{1-\cos\tau}{2\cos\tau}\right)$$

can be taken as unity.

For the angles τ commonly used in planing, say $\tau \leq 20^\circ$, the $f(\tau)$ can be expressed therefore as

$$f(\tau) = \frac{2\pi \sin\tau}{2 + \pi \sin\tau} \qquad (185)$$

with the error not exceeding 3 per cent.

The expressions (184) and (185) apply to the plate of infinite span, and to the fluid devoid of weight.

Before attempting the comparison with the experimental data, it will be necessary to evaluate the effects of the finite span, and to give at least some consideration to the effects of gravity.

17. Effect of the Finite Span of a Planing Surface.

When the lift force is generated by a planing surface of a finite span, the downward velocity w is given to the fluid, and in a uniform motion, the lift is equal to the momentum imparted to the fluid per second. The object of this section is to evaluate the vertical downwash velocity w, and to trace the consequences of its occurence.

The horizontal velocity V of the fluid with respect to the planing surface can be resolved in the components parallel and normal to the surface. The parallel component determines the amount of the fluid flowing past the surface, while the normal component forms the pattern of the flow identical with the flow about a plate placed normally in the stream, as it has been defined in Section 9, page 18. Consider a pair of planes in the fluid oriented normally to the planing surface and spaced small distance apart, and consider the two-dimensional flow between these two planes. Initially these planes are located in the undisturbed water forward of the planing surface and the vertical velocity w is zero. Finally they are found to be well aft of the planing surface and the vertical velocity of downwash is w. At the center of pressure of the planing surface, the vertical velocity is kw, where the coefficient k is yet to be determined. In the passing of a planing surface over a certain portion of the fluid, this fluid is accelerated downwards from the velocity zero to the velocity w. Since the acceleration is involved, we have to consider the virtual mass associated with the flow about a flat plate. This is shown in hydrodynamics to be equal to the mass of a cylinder, the diameter of which is equal to the width or the span of the surface. The sectional area of the cylinder is $1/4\,\pi\, b^2$, and the length traversed by this sectional area in a second is $V \cos\tau$ so that the virtual mass acted upon per second is $1/4\,\pi\rho\, b^2\, V \cos\tau$. Since the angle of trim is small, the cosine of it will be taken as unity and V will be used instead of $V \cos\tau$. Since in the planing process only the lower half of the flow about a plate is considered, half of the above mass is to be taken. Finally we get the change of the momentum per second, equal to the lift L as:

$$L = \tfrac{1}{8}\pi\rho b^2 V w \qquad (186)$$

or

$$w = \frac{8L}{\pi \rho b^2 V} \tag{187}$$

In order to determine the coefficient k, defining the velocity at the center of pressure of the plate, consider the energy imparted to the fluid. The energy imparted by the lift L and fluid velocity kw is:

$$kwL = \frac{1}{8}\pi\rho b^2 V k w^2 \tag{188}$$

On the other hand the energy left in the mass of fluid moving with the velocity w is (mass)$\times w^2/2$, or

$$\frac{1}{8}\pi\rho b^2 V w^2/2 \tag{189}$$

Since the energy left in the fluid is equal to the work done by the lift force, the expressions (188) and (189) are evidently equal, and it follows that k = 1/2 I.e. downwash velocity at the plate is half of the final or total downwash velocity. The angle of downwash ϵ at the center of pressure of the plate is therefore:

$$\epsilon = \frac{1}{2}\frac{w}{V} = \frac{4L}{\pi\rho b^2 V^2} \quad *) \tag{190}$$

Eq. (184) gives the normal force F per unit of span. For the span b, letting cos τ = 1, we have

$$L = bF = \frac{\rho b V^2 \chi_m}{2} f(\tau) \tag{191}$$

Dividing Eq. (191) by $\frac{1}{2}\rho b \chi_m V^2$ gives:

$$C_\ell = \frac{L}{\frac{1}{2}\rho b \chi_m V^2} = f(\tau) \tag{192}$$

and Substitution of the value of the lift L from Eq. (191) into Eq. (190) gives:

$$\epsilon = \frac{2}{\pi}\frac{\chi_m}{b} f(\tau) = \frac{2}{\pi}\lambda f(\tau) = \frac{2}{\pi}\lambda C_\ell \tag{193}$$

or, in degrees:

$$\epsilon = 36.5\,\lambda\, C_\ell$$

*) AS GIVEN IN REF. 13

18. Comparison of the Experimental and Theoretical Data for the Lift Coefficient.

The value of the lift coefficient, based on Wagner's theory of the planing surface with a finite trailing edge, is given by a very simple expression (193), where f (τ) is given by Eq. (185) as

$$f(\tau) = \frac{2\pi \sin\tau_e}{2+\pi \sin\tau_e} \tag{195}$$

The angle τ entering into this expression is the effective angle of trim measured from the direction of the velocity vector, and will be designated thereafter as τ_e . The velocity vector, however, is inclined by the angle ϵ , so that the angle of trim τ measured with respect to the undisturbed water level, or with respect to the direction of motion is

$$\tau = \tau_e + \epsilon \tag{196}$$

The calculations of the C_L are given in Table V , for a series of the arbitrarily assigned values of τ_e , on the basis of Eqs. (193) and (195). The angle ϵ is subsequently computed on basis of C_L by Eq. (194), then τ by Eq. (196), and finally C_L is plotted vs. τ for several values of λ .

The average values of the experimental data for the flat planing surfaces are given by the empirical formulae taken from Ref. 8 and 14 :

Sedov's Formula:

$$C_L = \frac{\tau}{57.3}\left[\frac{0.7\pi\lambda}{1+1.4\lambda} + \lambda(0.92\lambda - 0.38)/C_v^2\right] \tag{197}$$

Stevens Experimental Towing Tank formula:

$$C_L = \tau^{1.1}\left[0.0120\lambda^{1/2} + 0.0095(\lambda/C_v)^2\right] \tag{198}$$

In above the angle τ is in degrees.

Theoretical data are based on the fluid devoid of gravity, and with experimental data this corresponds to sufficiently high values of C_v, at which the forces of gravity can be neglected in comparison with the dynamic forces, and second terms in both of the above expressions vanish.

Furthermore, it is desired to express the coefficients in the form C_ℓ based on the wetted area $b\lambda m$, rather than C_L based on the beam squared. Substitution of $C_L = \lambda C_\ell$, and omission of the second terms puts Eqs. (197) and (198) into the form:

$$C_\ell = \frac{\tau}{57.3} \frac{0.7\pi}{1+1.4\lambda} \tag{199}$$

and

$$C_\ell = 0.0120\tau^{1.1}/\lambda^{\frac{1}{2}} \tag{200}$$

The data computed on basis of the above equations, representing the summary of the experimental data, are plotted on Fig. 43 for comparison with the theoretical data. Good agreement is shown for $\lambda = 1$ and 2, with greater discrepancy for $\lambda = 3$. It should be noted that disagreement at $\lambda = 3$ or higher is not as important as it appears at first sight, as at these values of λ, and the speed coefficients C_V commonly used, the second terms of Eqs. (197) and (198) become important, and mask the discrepancies between theoretical and experimental data in the first term.

TABLE V

τ_ℓ Degrees	$\pi \sin\tau$	C_ℓ	ϵ in degrees			$\tau = \tau_\ell + \epsilon$ in degrees		
			$\lambda = 1$	$\lambda = 2$	$\lambda = 3$	$\lambda = 1$	$\lambda = 2$	$\lambda = 3$
.25	.0137	.0136	.41	.83	1.24	.66	1.08	1.49
.50	.0274	.0270	.98	1.97	2.95	1.48	2.47	3.45
1.0	.0550	.0535	1.95	3.91	5.86	2.95	4.91	6.86
1.5	.0822	.0792	2.89	5.78	8.67	4.39	7.28	10.17
2.0	.1095	.1038	3.79	7.68	11.40	5.79	9.68	13.40
2.5	.1370	.1282	4.68	9.36	14.04	7.18	11.86	16.54
3.0	.1642	.1518	5.54	11.08	16.65	8.54	14.08	19.65
3.5	.1915	.175	6.38	12.76	---	9.88	16.26	---
4	.219	.1975	7.21	14.42	---	11.21	18.42	---
5	.274	.241	8.80	---	---	13.8	---	---
6	.328	.282	10.30	---	---	16.3	---	---
7	.383	.322	11.75	---	---	18.75	---	---

Attention should be called to the magnitude of the downwash angle ϵ. In Aerodynamics, the downwash angle is an important corrective term, but does not assume the controlling proportions, because the span/chord ratio

is high, and because the virtual mass is based on the cylinder of the diameter equal to the span. In a planing surface, the virtual mass is taken on the basis of the half of the cylinder, and the beam/wetted length ratios are usually small. These two factors make the downwash angle ϵ a predominating factor in determining the C_ℓ or $C_L = f(\tau)$ relation, and make the errors in the relation $C_\ell = f(\tau_e)$ relatively unimportant.

Slope of the Lift Coefficient vs. angle of trim curve.

It will be instructive to cast the above analysis into the form common in aerodynamics - the determination of the $dC_\ell/d\tau$ as a function of the length/beam ratio λ. It was shown in the previous article that τ_e is relatively small compared to $\tau = \tau_e + \epsilon$. This being the case, a further and a more radical simplification of the Eq. (195) is permissible in neglecting the value of $\pi \sin \tau$ in the denominator $2 + \pi \sin \tau$, and in rewriting the Eq. (195) as:

$$C_\ell = f(\tau_e) = \pi \sin \tau_e \cong \pi \tau_e$$

and

$$a_o = \frac{dC_\ell}{d\tau_e} = \pi \qquad (201)$$

This compares with the airfoil theory in which $a_o = 2\pi$, since the virtual mass is represented by the complete cylinder;

Differentiating Eq. (196) with respect to C_ℓ gives:

$$\frac{d\tau}{dC_\ell} = \frac{d\tau_e}{dC_\ell} + \frac{d\epsilon}{dC_\ell}$$

Substituting the value of $d\tau_e/dC_\ell$ as the reciprocal of Eq. (201), and obtaining $d\epsilon/dC_\ell$ from Eq. (193) as $2\lambda/\pi$, gives:

$$\frac{d\tau}{dC_\ell} = \frac{1}{\pi} + \frac{2\lambda}{\pi} = \frac{1+2\lambda}{\pi}$$

and taking the reciprocal:

$$\frac{dC_\ell}{d\tau} = \frac{\pi}{1+2\lambda} \qquad (202)$$

This compares with the form given in the airfoil theory (Ref. 16):

$$\frac{dC_\ell}{d\alpha} = \frac{\pi}{\frac{1}{2} + \frac{1}{A}} \qquad (203)$$

$\tau = 10°$

$\lambda =$	.5	1	2	3	4	5
Qual C_L	.226	.159	.106	.083	.070	.062
Exp. C_L	.240	.155	.110	.090	.078	.070

$$C_L = \frac{.07}{1+\lambda}\tau + .000262\tau^2$$

Since the reciprocal of the aspect ratio $\frac{1}{A} = \lambda$.

Eq. (202) gives the rate of change of C_ℓ per radian. Expressing it per degree makes the numerator $\pi/57.3$. However, C_ℓ was slightly exaggerated in using the denominator of 2 instead of $2 + \pi \sin\tau$, and the slope given by Eqs. (202) and (203) in the maximum, corresponding to the elliptic pressure distribution along the span, and in practive can be expected to be lower. Rounding the $\pi/57.3$ to 0.05 gives finally $dC_\ell/d\tau$ per degree as:

For a planing surface:

$$\frac{dC_\ell}{d\tau} = \frac{0.05}{1+2\lambda} \tag{204}$$

For an airfoil:

$$\frac{dC_\ell}{d\alpha} = \frac{0.05}{\frac{1}{2}+\frac{1}{A}} = \frac{0.10\,A}{2+A} \tag{205}$$

as given by Von Mides in Ref. 17.

The values of $dC_\ell/d\tau$ for a planing surface are given in table VI for comparison with the experimental data.

The average experimental data are obtained by differentiating the empirical Eqs. (199) and (200):

Sedov's

$$dC_\ell/d\tau = \frac{0.7}{57.3}\,\frac{\pi}{1+1.4\lambda} = \frac{.038}{1+1.4\lambda} \tag{206}$$

Stevens E.T.T.

$$dC_\ell/d\tau = 1.1 \times 0.0120\,\tau^{0.1}/\lambda^{\frac{1}{2}} = .0132\,\tau^{0.1}/\lambda^{\frac{1}{2}} \tag{207}$$

TABLE VI

The Values of $dC_\ell/d\tau = f(\lambda)$

Method used:	$dC_\ell/d\tau$ for λ =			
	0.5	1.0	2.0	3.0
Theoretical - Eq. (204)	0.0250	0.0166	0.0100	0.0071
Empirical:				
Sedov's - Eq. (206)	0.0223	0.0158	0.0100	0.0073
Stevens E.T.T. - Eq. (207)	0.0219	0.0155	0.0109	0.089

*)

*) This equation gives $dC_\ell/d\tau$ as a function slowly varying with τ. For the purpose of comparison in Table VI, the value of $\tau = 5^\circ$ was used, as giving approximately the mean rate in determining the C_ℓ at $\tau = 10^\circ$.

The linear form of $C_\ell = f(\tau)$, or the constant value of $dC_\ell/d\tau$ given by Eqs. (204) and (205) results from the analysis based on a "lifting line" theory, which applies to the large span/chord ratio. For the small span airfoils, or for the planing surfaces in which the wetted length/beam ratio λ is large (the aspect ratio A is small) it is shown by Siler - Ref. 15 - that the lift coefficient is expressed by the form:

$$C_\ell = A\alpha + B\alpha^2 \tag{208}$$

and therefore

$$dC_\ell/d\alpha = A + 2B\alpha$$

In derivation of the Stevens E.T.T. Formula, Eq. (198) the plot resulting from the above polynomials was in effect approximated by the exponential curve

$$C_\ell = C\alpha^{1.1}$$

and the resultant formula was demonstrated in Ref. 8 to agree with experimental data at high values of C_V and λ.

The nonlinear form of $C_L = f(\alpha)$ given by Eq. (208) is furthermore clearly shown in all tests on the slender bodies such as airship hulls and ship hulls.

References:

1. L. M. Milne-Thomson--"Theoretical Hydrodynamics"--2nd Edition, MacMillan and Co. Ltd., London, 1949. (Obtainable in New York through Stechert-Hafner, Inc., 31 East 10th Street, New York 3, New York).

2. Louis A. Pipes--"Applied Mathematics for Engineers and Physicists", McGraw Hill Co., Inc., New York, 1949.

3. H. W. Reddick and F. H. Miller--"Advanced Mathematics for Engineers", John Wiley and Sons, Inc., New York, 2nd Edition.

4. Victor L. Streeter--"Fluid Dynamics", McGraw Hill Book Co., Inc., New York, First Edition, 1948.

5. W. L. Cowley and H. Levy--"Aeronautics in Theory and Experiment", Edward Arnold, London, 1918.

6. Herbert Wagner--"Landing of Seaplanes", Zeitschript fur Flugtechnik and Motorluftschiffahrt, Vol. 22, No. 1, Jan. 14, 1931, English Translation N.A.C.A. T.M. No. 622, May 1931.

7. John D. Pierson--"On the Pressure Distribution for a Wedge Penetrating a Fluid Surface" Stevens Institute of Technology, Experimental Towing Tank Rep. No. 336, Institute of Aeronautical Science, Sherman M. Fairchild Publication Fund Paper No. 167.

8. B. V. Korvin-Kroukovsky, Daniel Savitsky and William F. Lehman--"Wetted Area and Center of Pressure of Planing Surfaces", Stevens Institute of Technology, Experimental Towing Tank Rep. No. 360; Sherman M. Fairchild Publication Fund Paper No. 244, Institute of Aeronautical Science, New York.

9. (a) H. Lamb-"Hydrodynamics," 6th Revised Edition, Art. 20, Dover Publications, New York, 1945.

9. (b) Ditto--Art. 78.

10. John D. Pierson--"On the Pressure Distribution for a Wedge Penetrating a Fluid Surface", Stevens Institute of Technology, Experimental Towing Tank Rep. No. 336, Sherman M. Fairchild Publication Fund Paper No. 167, Institute of Aeronautical Sciences, New York.

11. B. V. Korvin-Kroukovsky and Faye R. Chabrow--"The Discontinuous Fluid Flow Past an Immersed Wedge", Stevens Institute of Technology, Experimental Towing Tank Rep. No. 334, Sherman M. Fairchild Publication Fund Paper No. 169, Institute of Aeronautical Sciences, New York.

12. John D. Pierson and Samuel Leshnover--"An Analysis of the Fluid Flow in the Spray Root and Wake Regions of Flat Planing Surfaces", Stevens Institute of Technology, Experimental Towing Tank, Rep. No. 335, Sherman M. Fairchild Publication Fund Paper No. 166, Institute of Aeronautical Sciences, New York.

13. Herbert Wagner--"Planing of Watercraft", Jahrbuch der Schiffblautechnik, Vo. 34, 1933, English Translation NACA T.M. No. 1139, April 1948.

14. L. I. Sedov--"Planing on a Water Surface", R.T.P. Translation No. 2506, Durand Reprinting Committee, California Institute of Technology, Pasadena 4, California.

15. Siler, William--"Lift and Moment of Flat Rectangular Low Aspect Ratio Lifting Surfaces", a thesis submitted in partial fullfillment of the requirements for the degree of Master of Science, Stevens Institute of Technology, 1949

16. L. M. Milne-Thomson--"Theoretical Aerodynamics", D. Van Nostrand Co., Inc., New York, N. Y., Art. 11.42, page 200.

17. Richard Von Mises--"Theory of Flight", McGraw-Hill Book Co., Inc., New York, N. Y., 1945, Sec. VII-2, page 149.

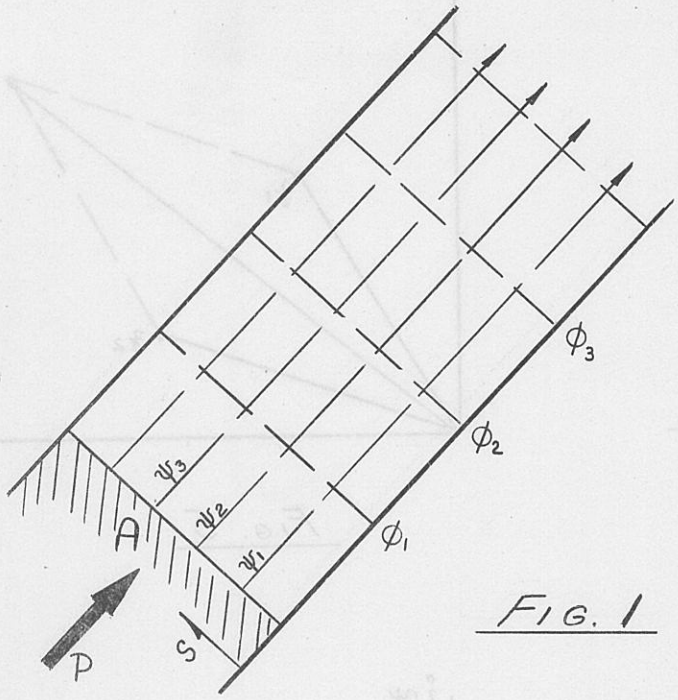

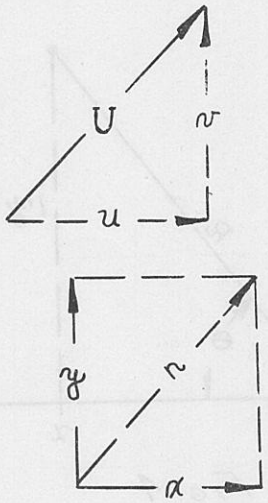

FIG. 1

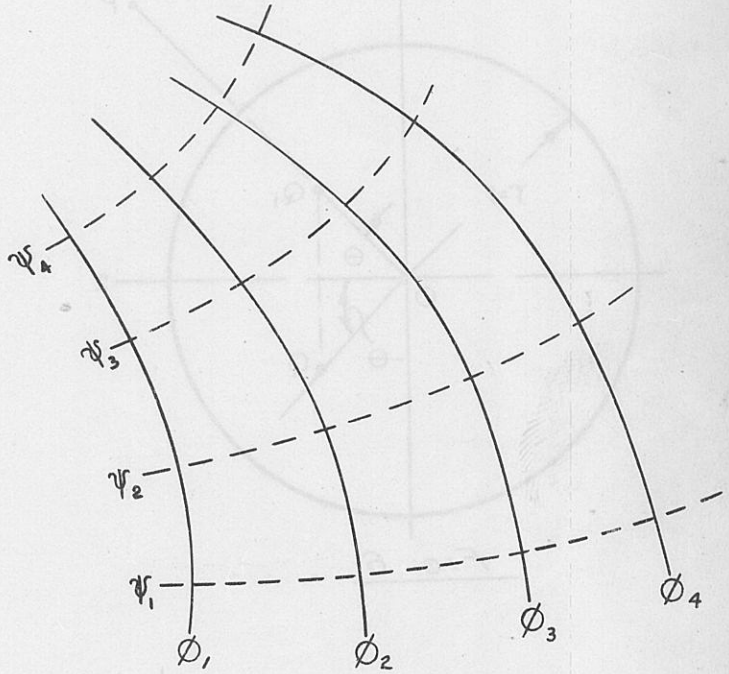

FIG. 2

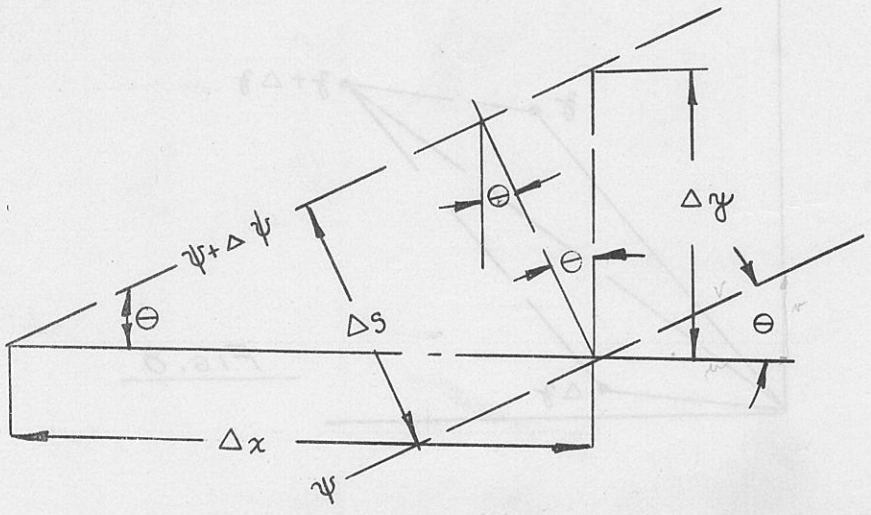

FIG. 3

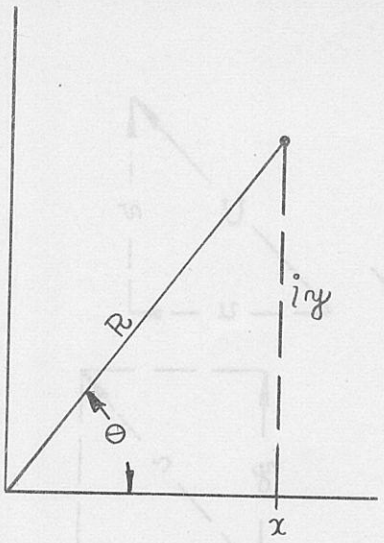

FIG. 4

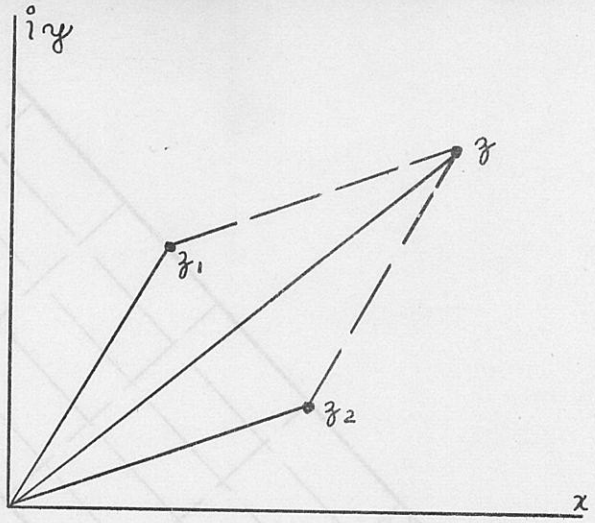

FIG. 5

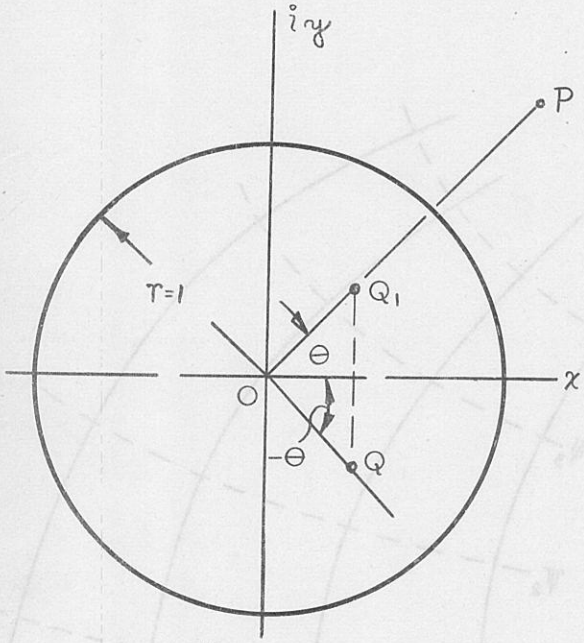

FIG. 6

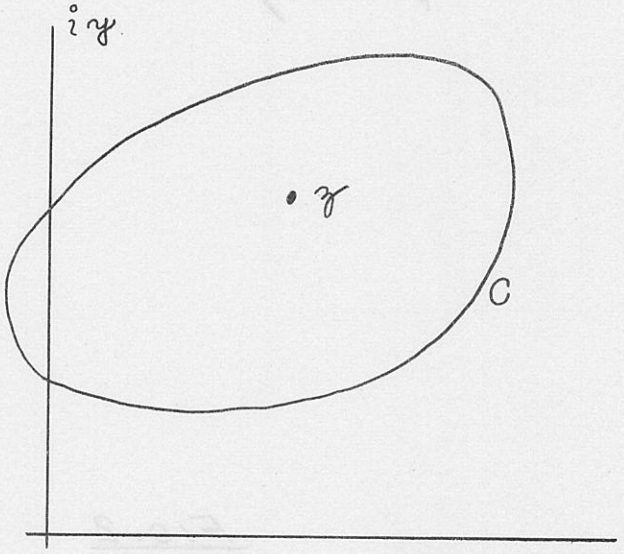

FIG. 7

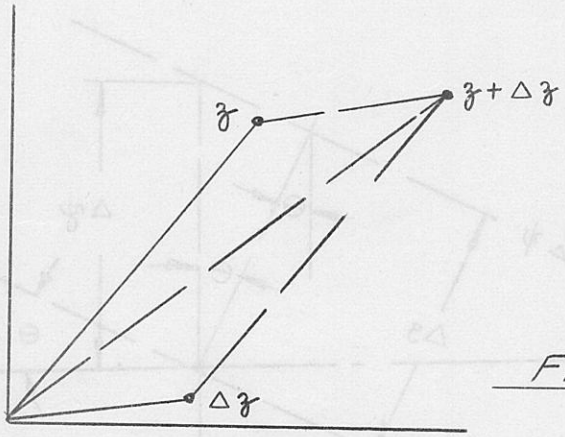

FIG. 8

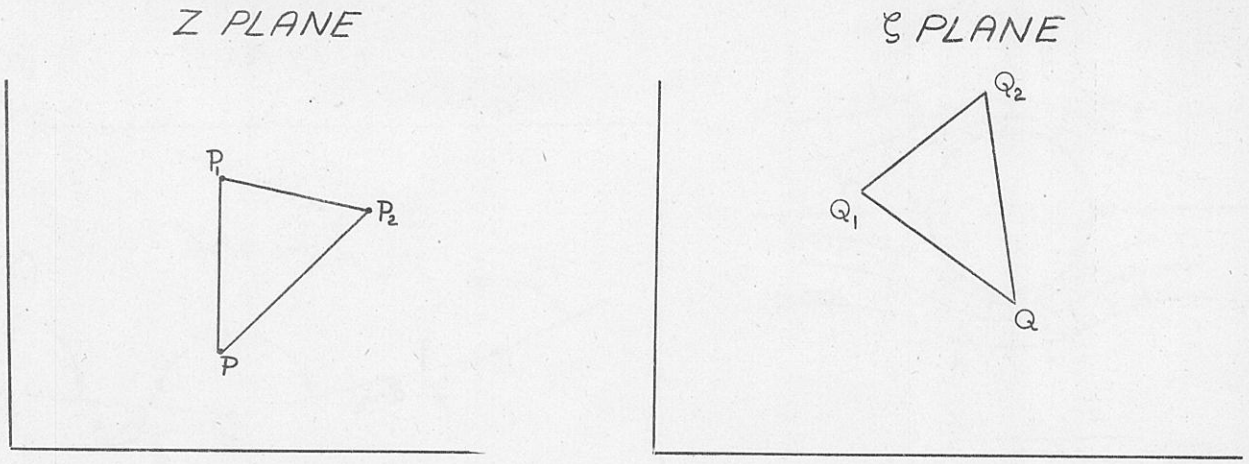

FIG. 9

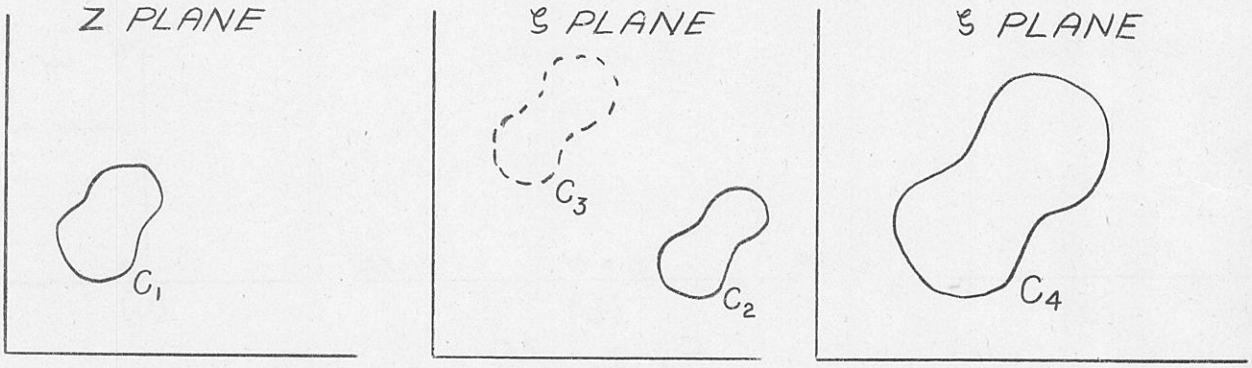

FIG. 10

FIG. 11

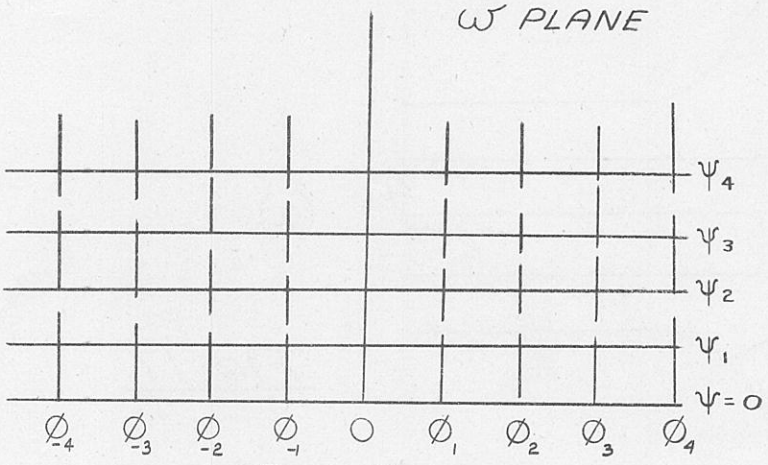

FIG. 12

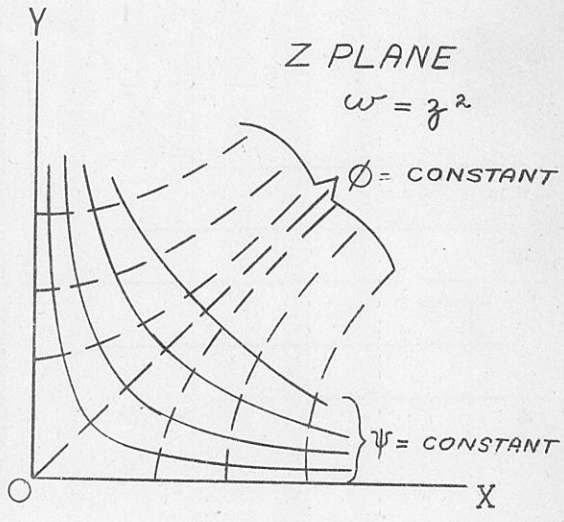

FIG. 13

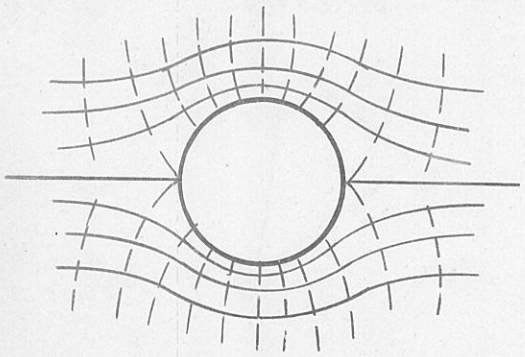

FIG. 14

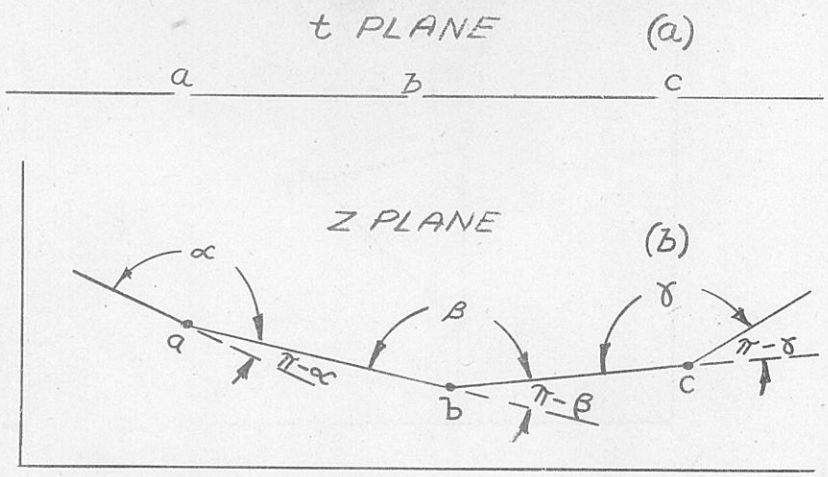

FIG. 15

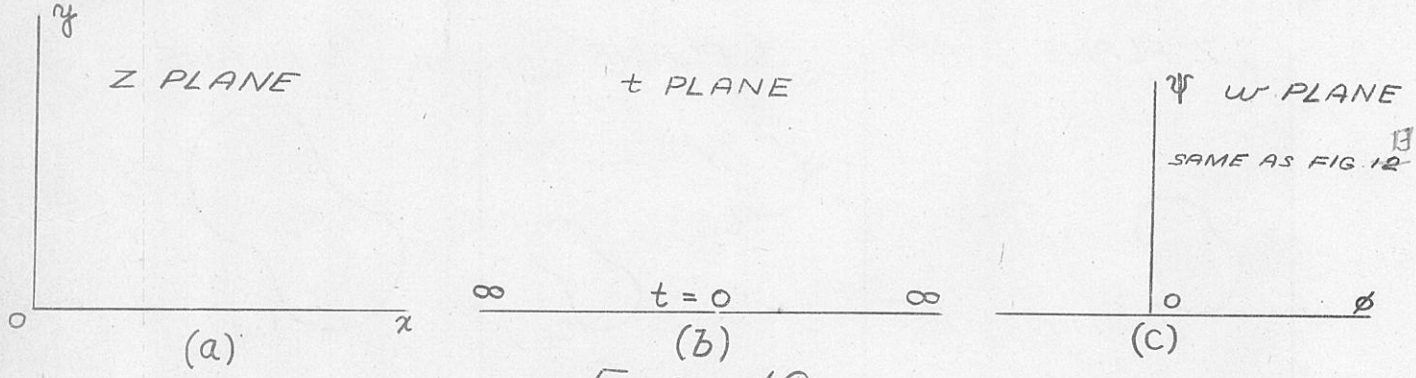

FIG. 16

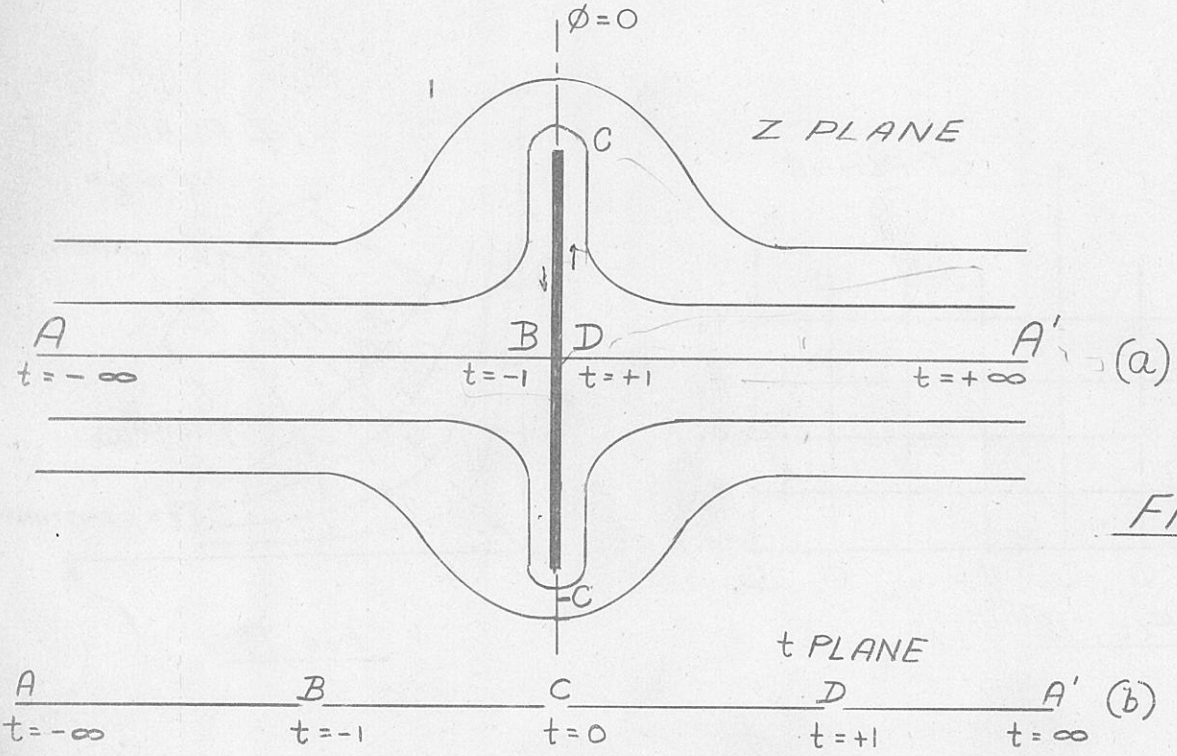

FIG. 17

FIGURE 22a

THEORETICAL PRESSURE ON WEDGE
CONSTANT VELOCITY PENETRATION
$\beta = 22.5°$

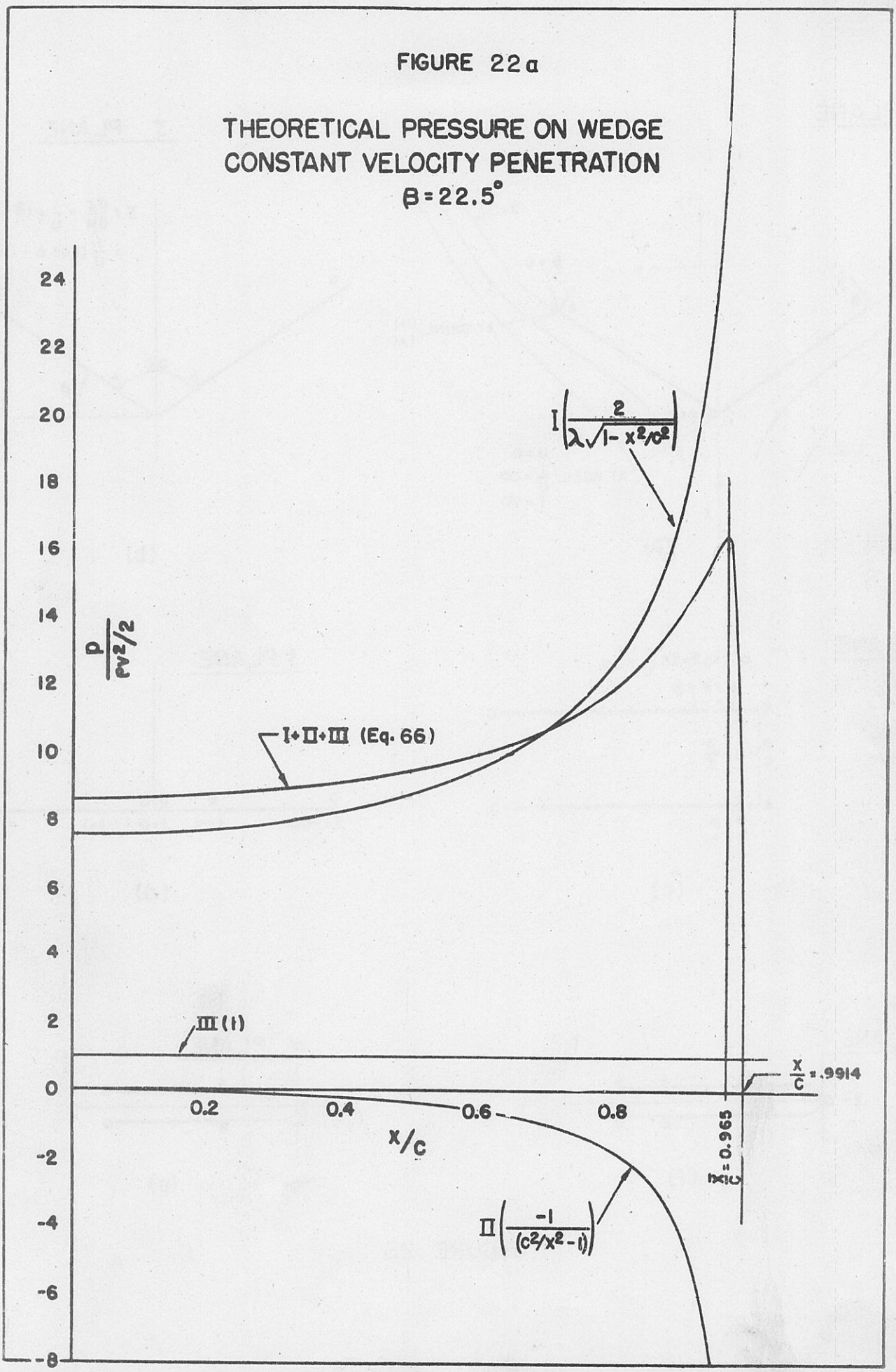

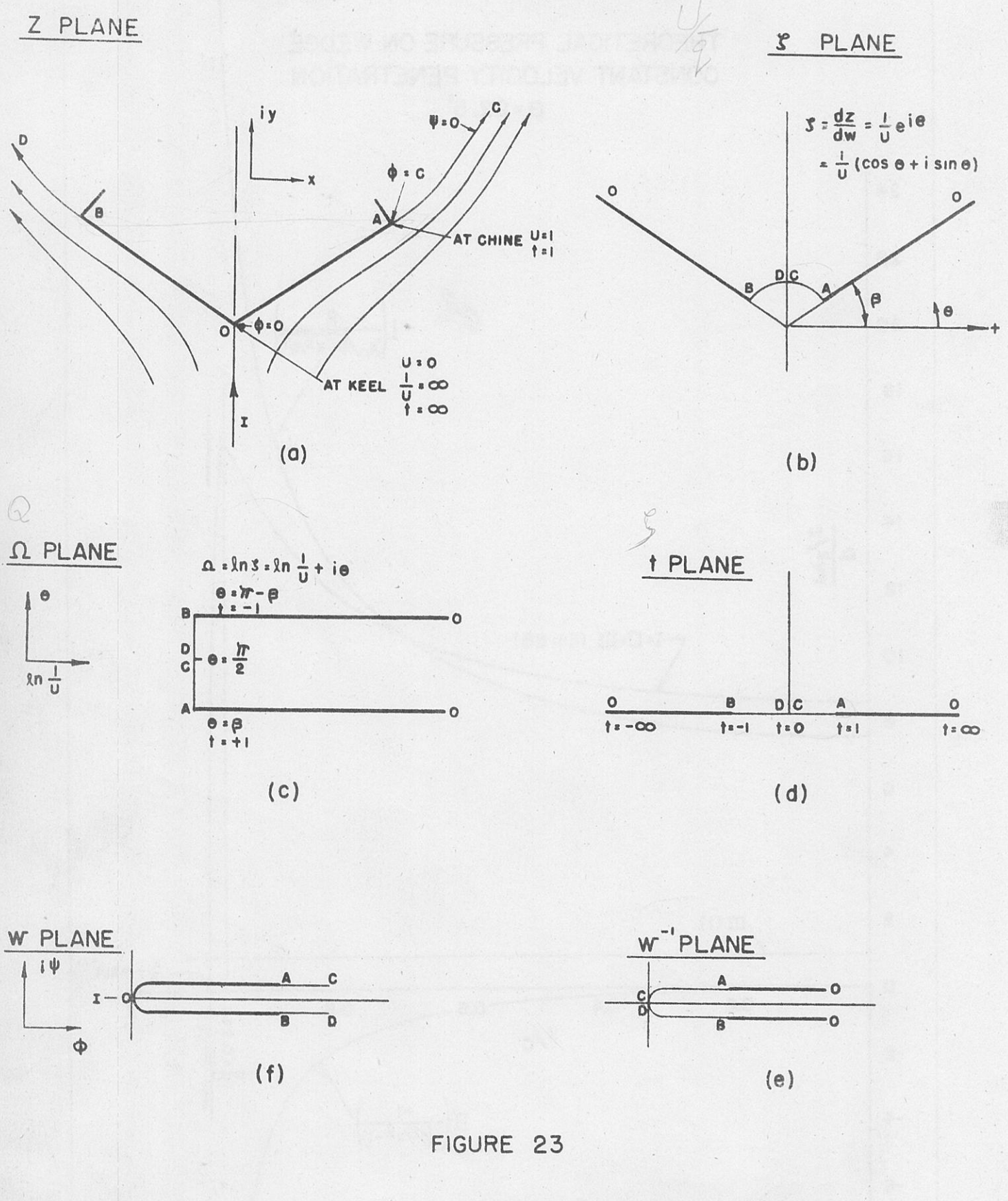
Z PLANE
iy
x
D
B
A
C
ψ=0
φ = C
AT CHINE U=1 t=1
O
φ=0
AT KEEL U=0 1/U=∞ t=∞
I
(a)
ζ PLANE
ζ = dz/dw = 1/U e^iθ
= 1/U (cos θ + i sin θ)
O
O
B
D C
A
β
θ
+
(b)
Ω PLANE
θ
ln 1/U
Ω = ln ζ = ln 1/U + iθ
θ = π - β
t = -1
B
O
D
C
θ = π/2
A
O
θ = β
t = +1
(c)
t PLANE
O
B
D C
A
O
t = -∞
t = -1
t = 0
t = 1
t = ∞
(d)
W PLANE
iψ
I
O
A
C
B
D
Φ
(f)
W^-1 PLANE
A
O
C
D
B
O
(e)

FIGURE 23

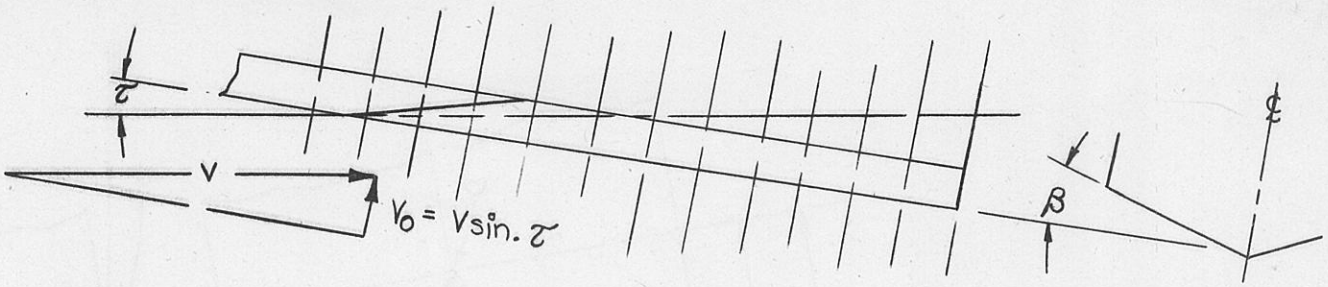

FIGURE 18

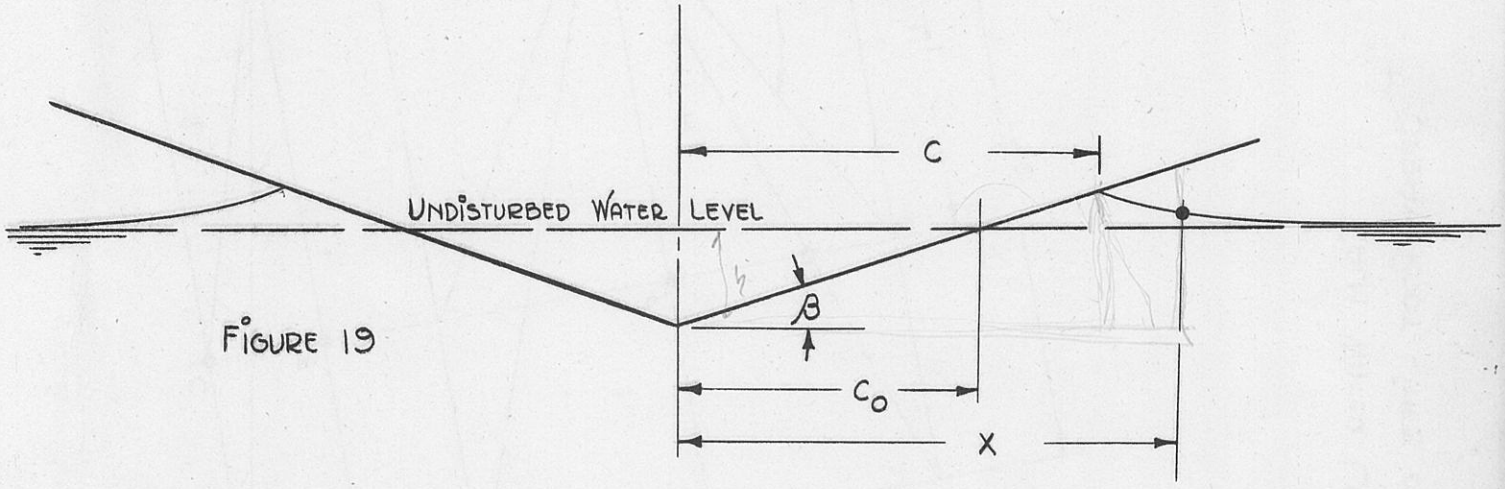

FIGURE 19

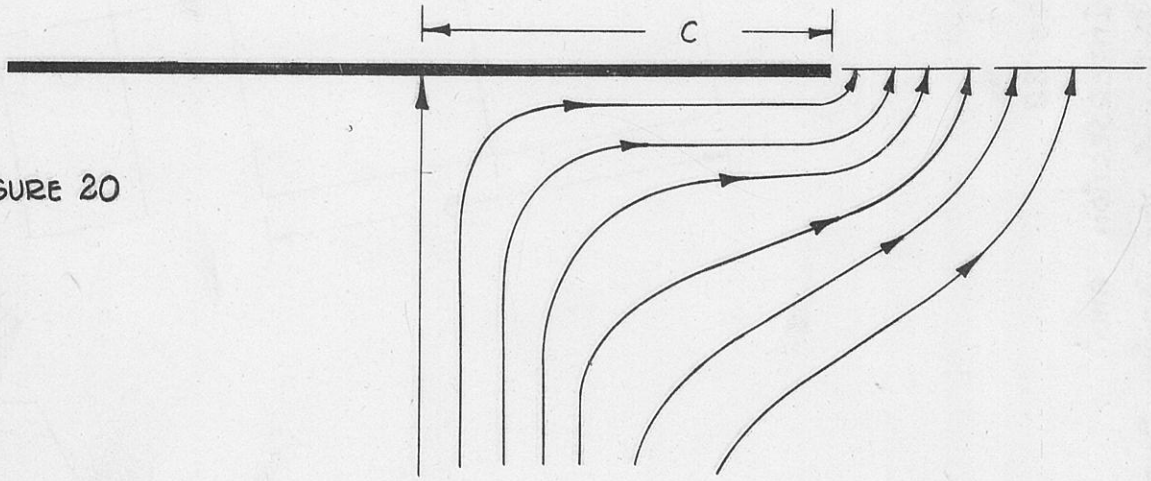

FIGURE 20

FIGURE 21

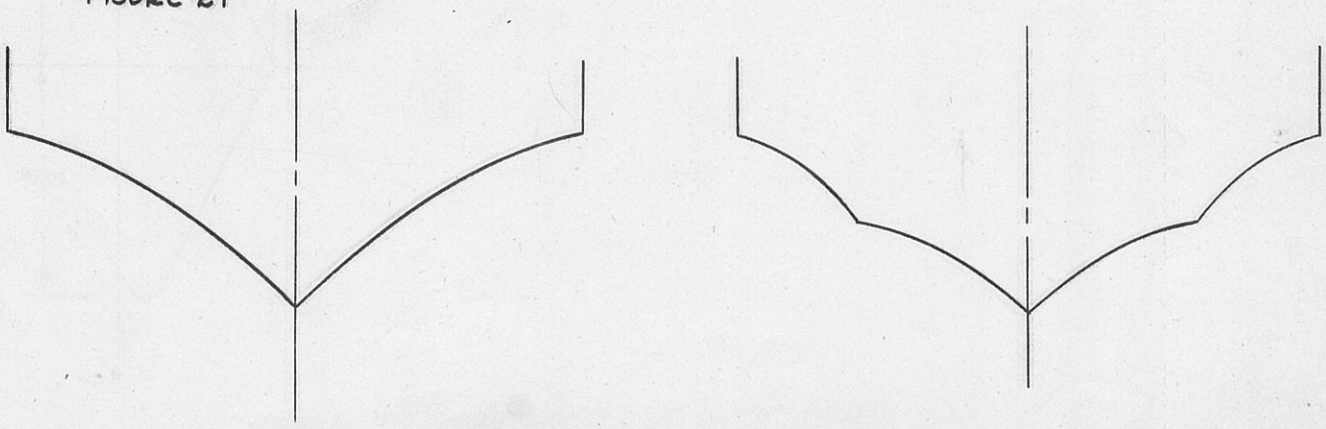

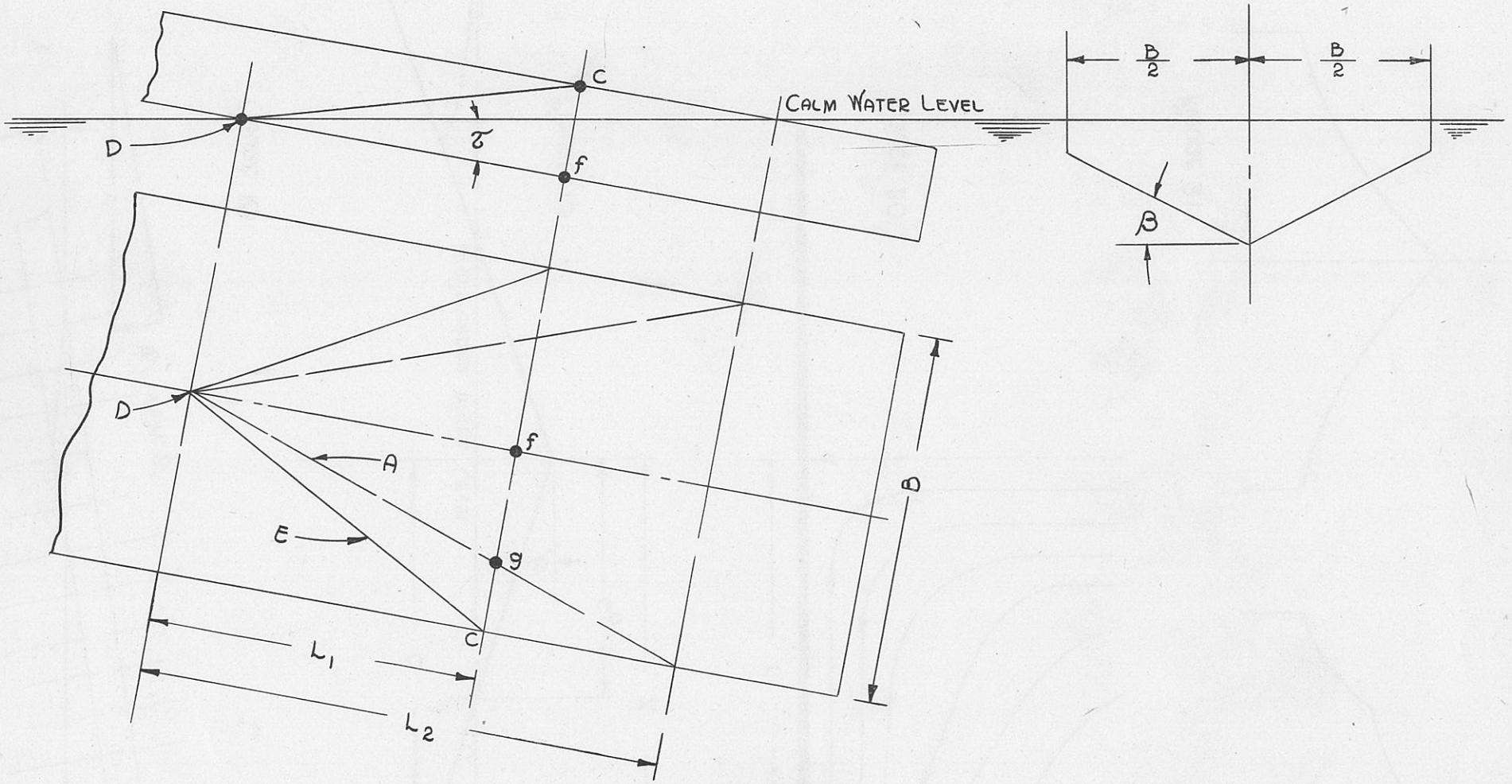

FIGURE 22

CALM WATER LEVEL INTERSECTION AND
SPRAY ROOT LINES ON A PRISMATIC VEE PLANING SURFACE

SHAPE OF
FREE STREAMLINE
FOR
IMMERSED V-BOTTOM

FIGURE 24

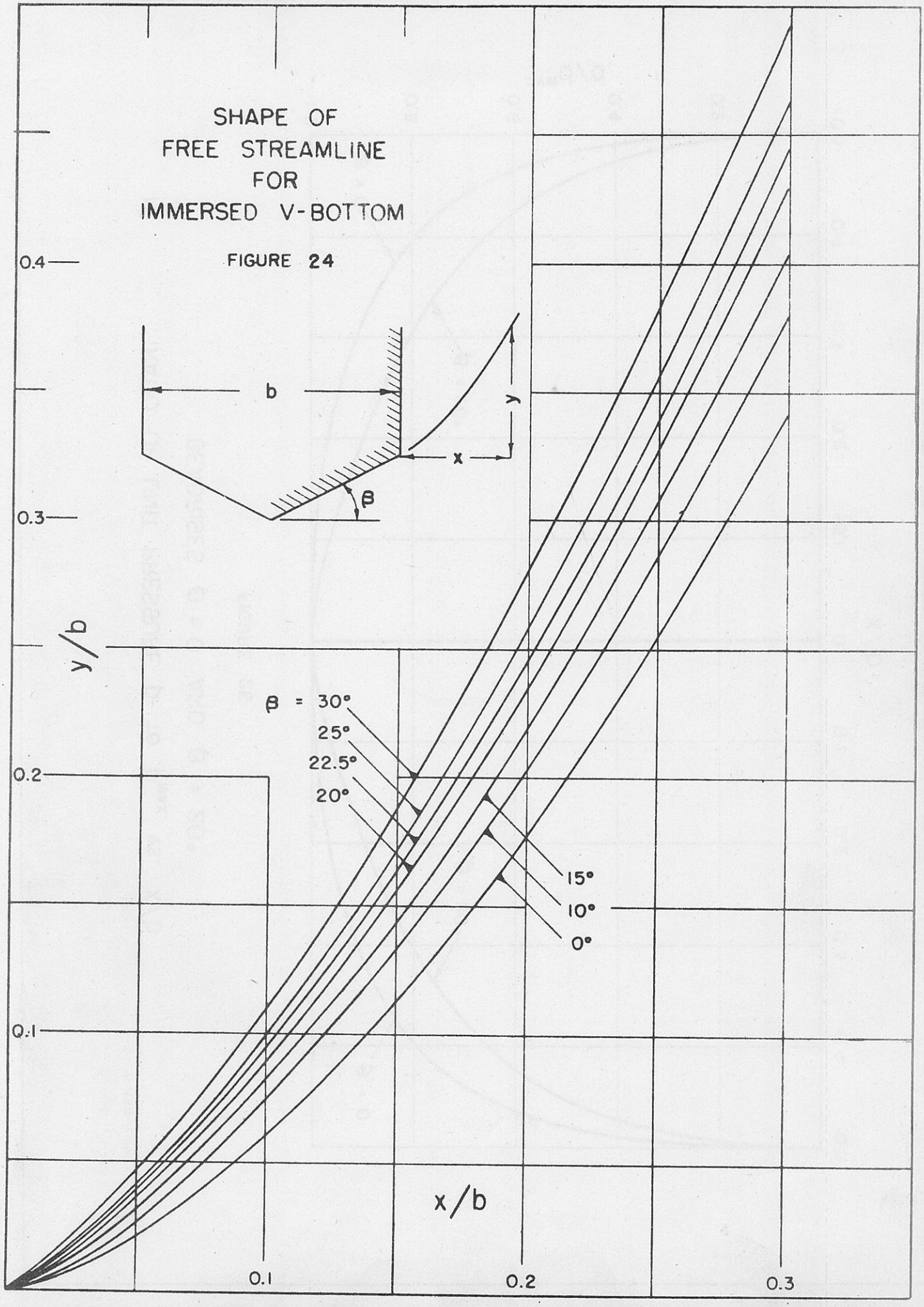

FLOW ABOUT
SUBMERGED PLATE

RATIO OF UNIT PRESSURE p TO $p_{MAX.}$ VS. x/b

DEADRISES $\beta = 0$ AND $\beta = 20°$

FIGURE 25

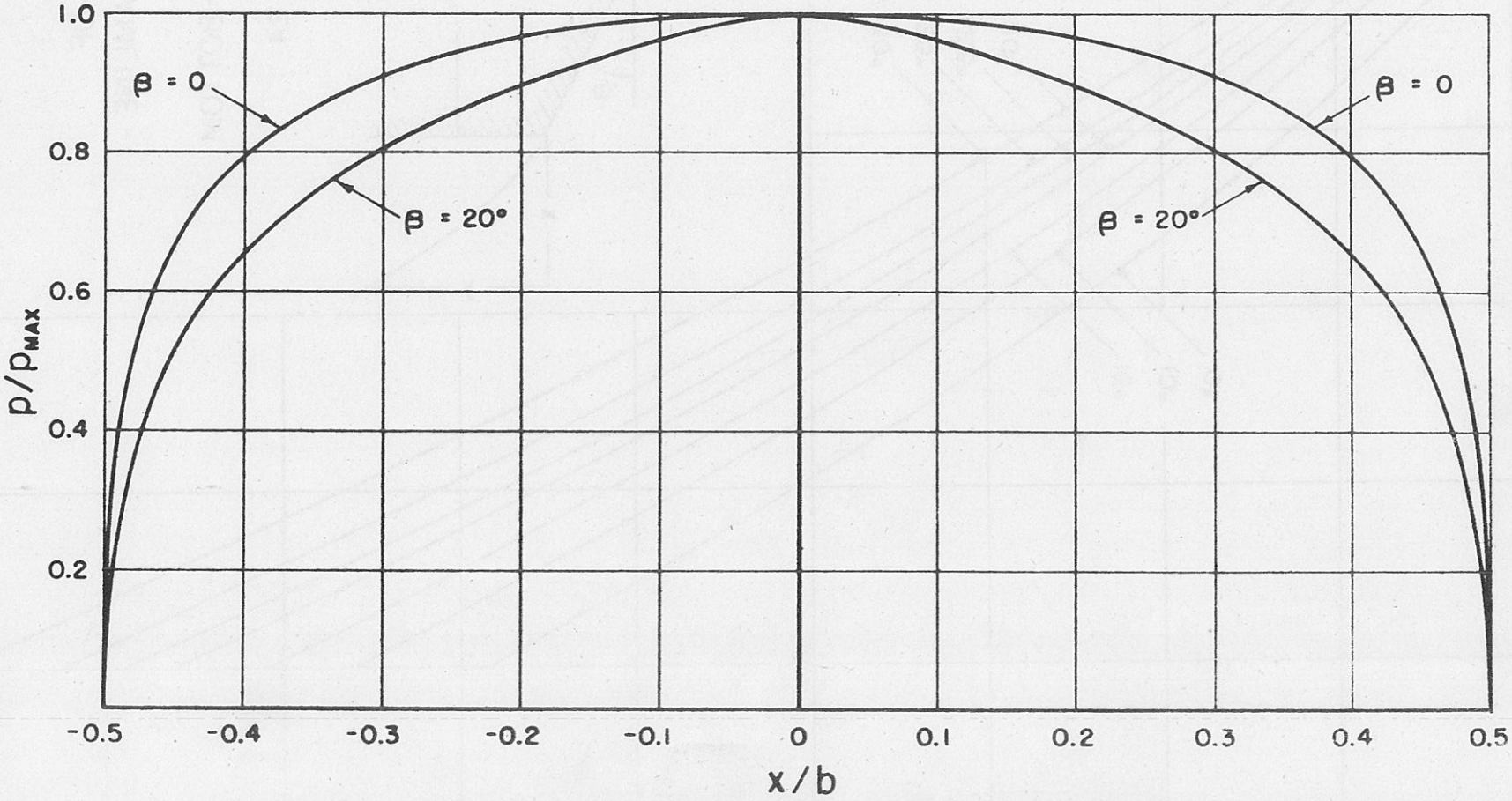

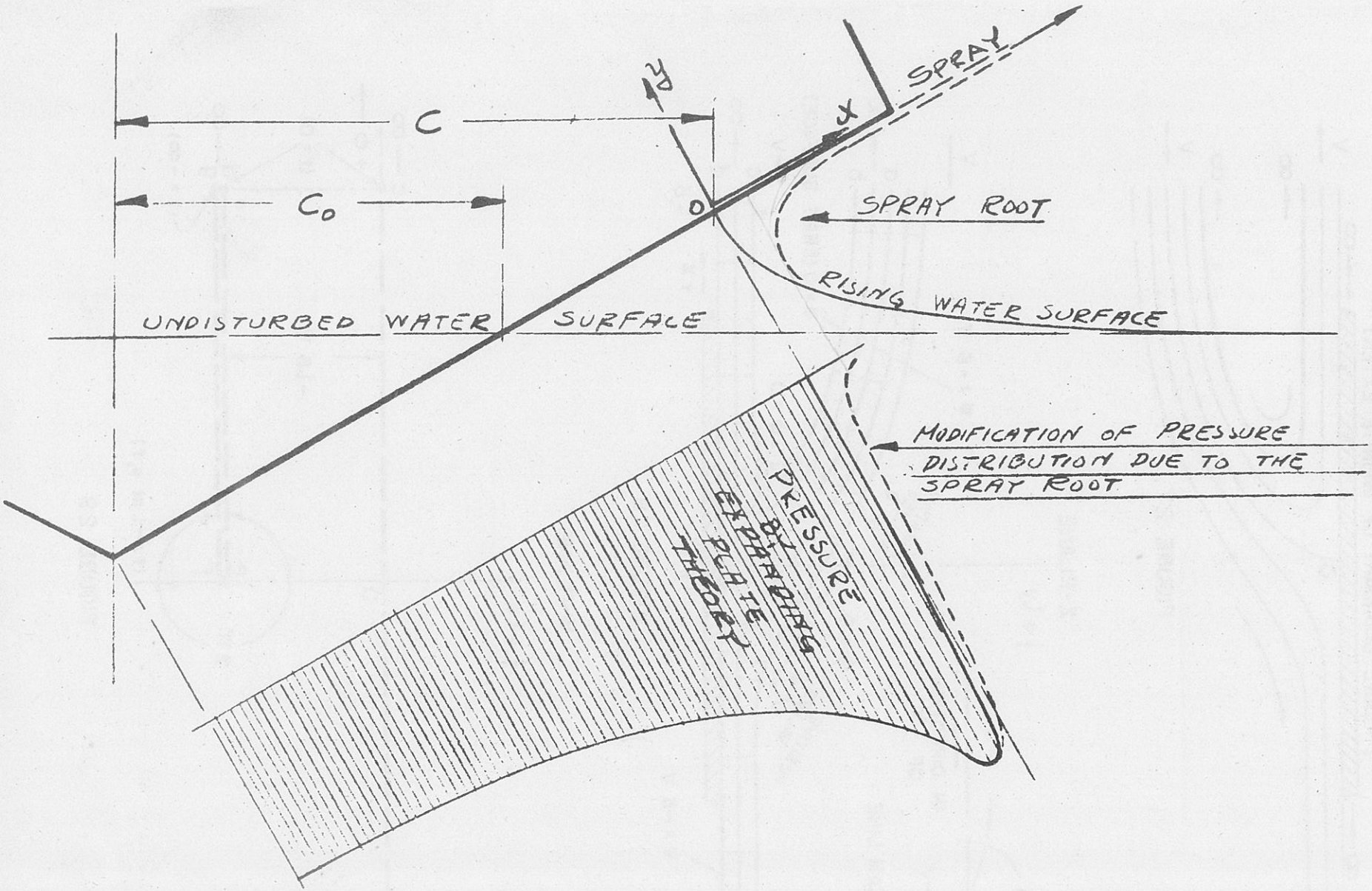

FIG. 26 FORMATION OF WATER SURFACE AND PRESSURE DISTRIBUTION AS DETERMINED BY EXPANDING PLATE AND BY SPRAY ROOT THEORIES

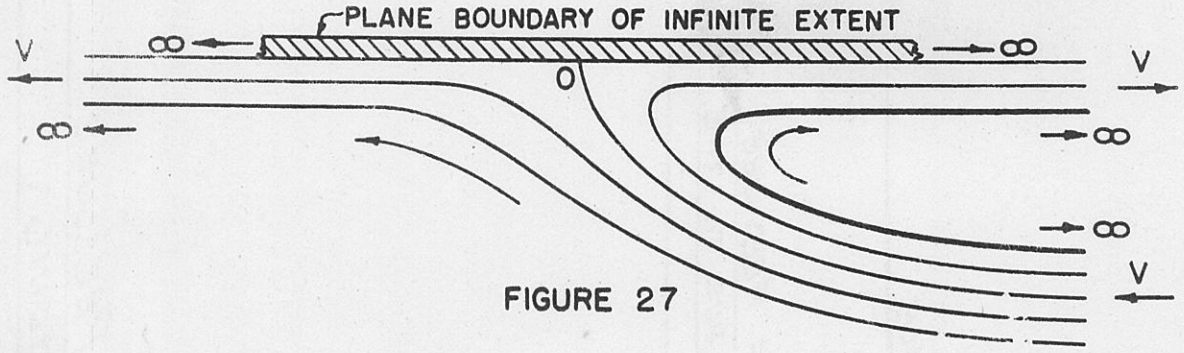

FIGURE 27

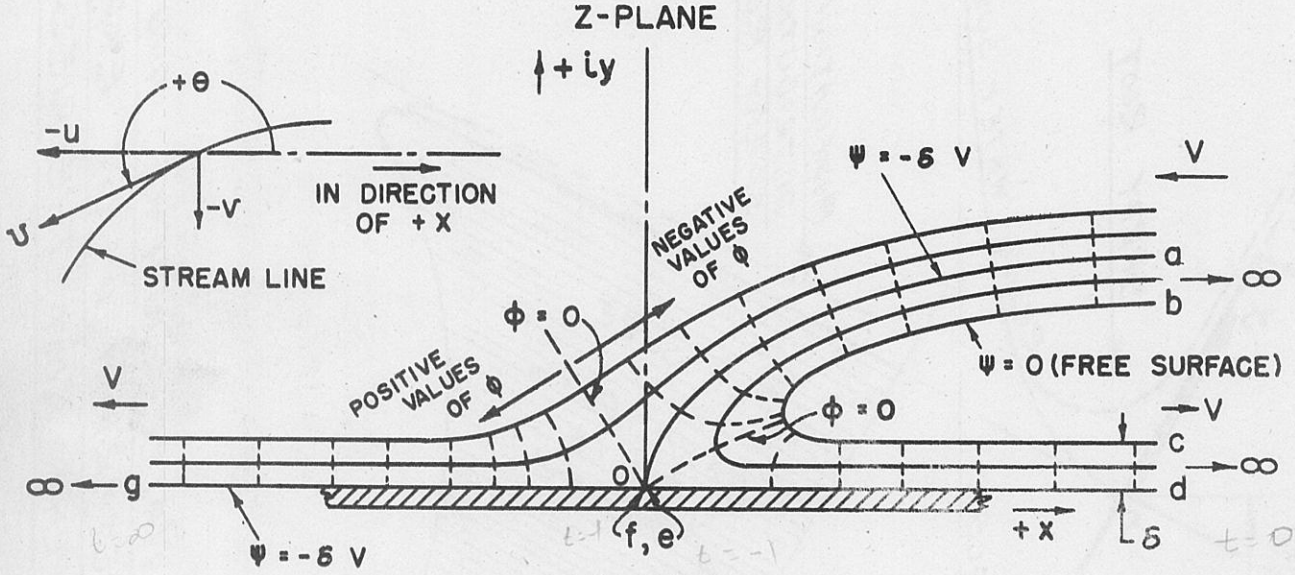

FIGURE 28

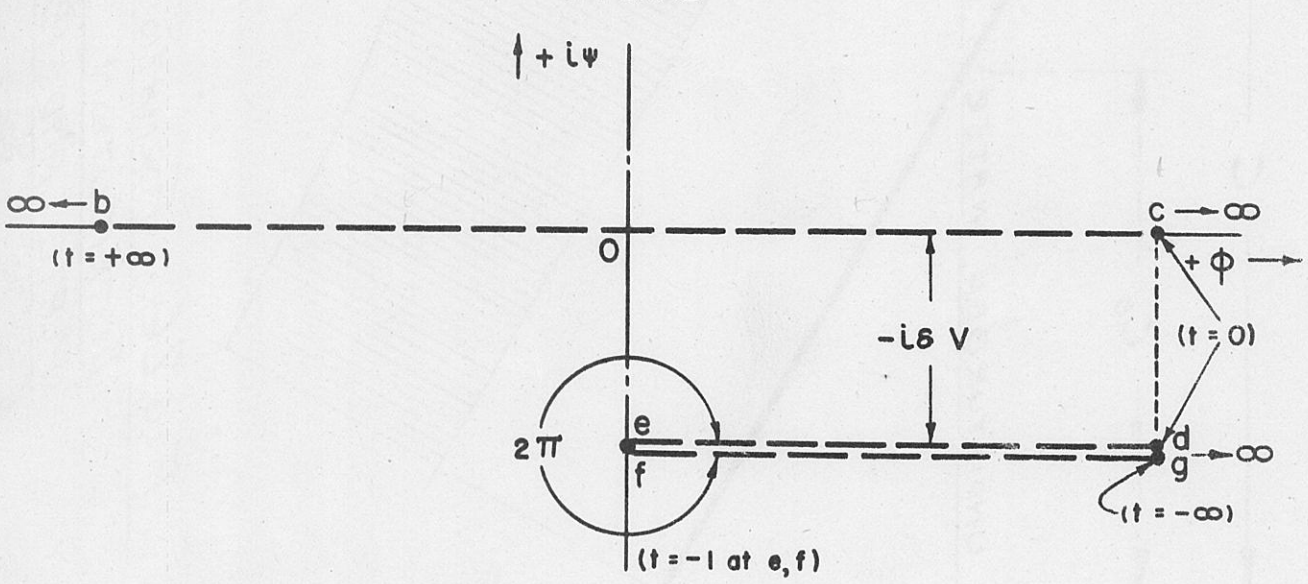

FIGURE 29

ζ PLANE

$$\zeta = \frac{dz}{dw} = \frac{1}{v} e^{i\theta}$$

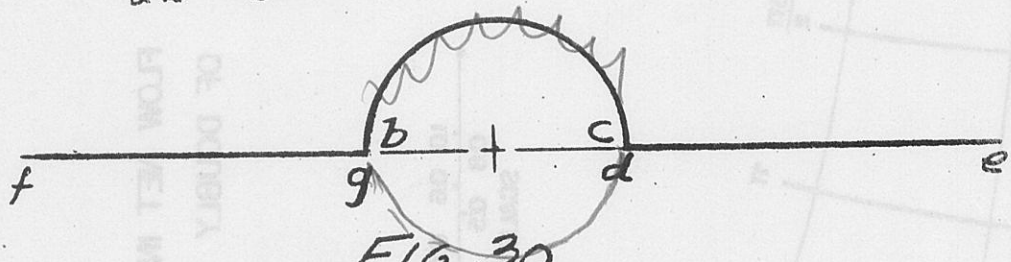

FIG. 30

Ω PLANE

$$\Omega = \ln \frac{dz}{dw} = \ln \frac{1}{v} + i\theta$$

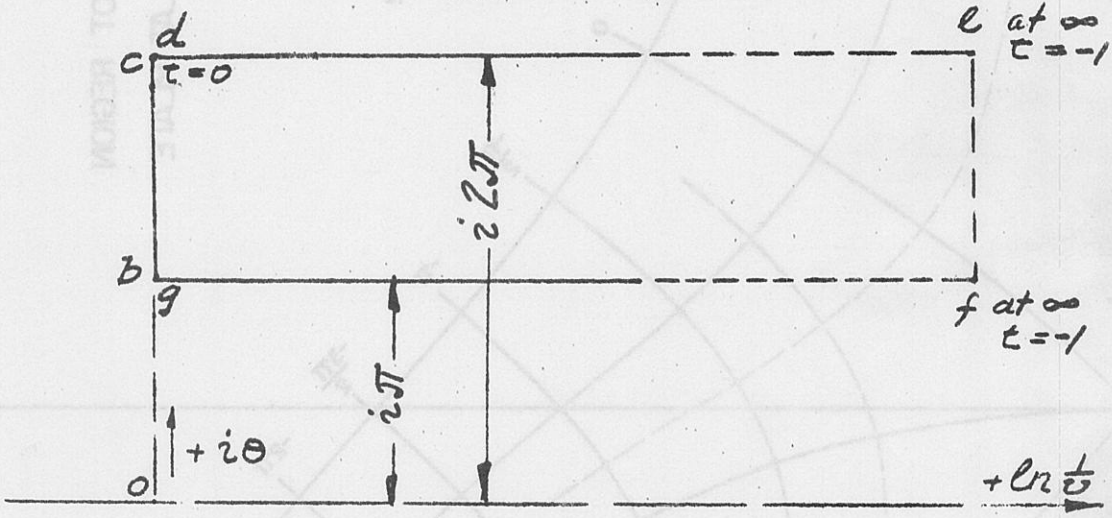

FIG. 31

t PLANE

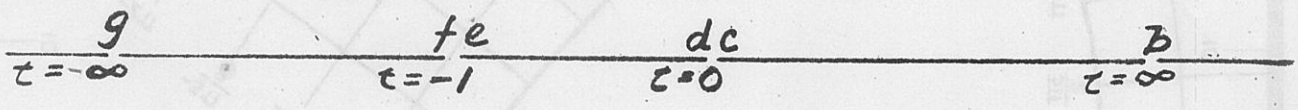

FIG. 32

FIGURE 33

FLOW NET IN SPRAY ROOT REGION
OF DOUBLY INFINITE FLAT PLATE

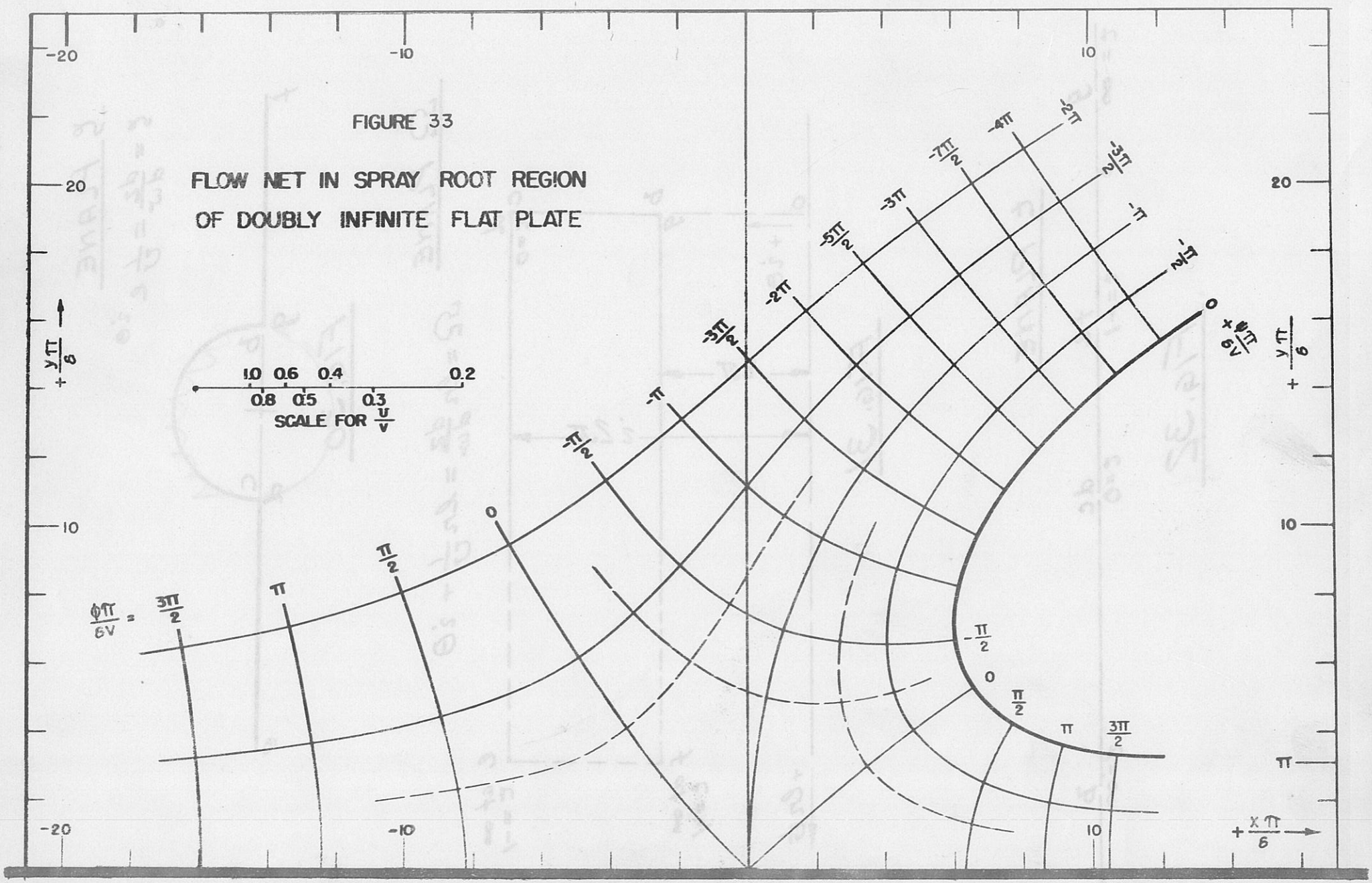

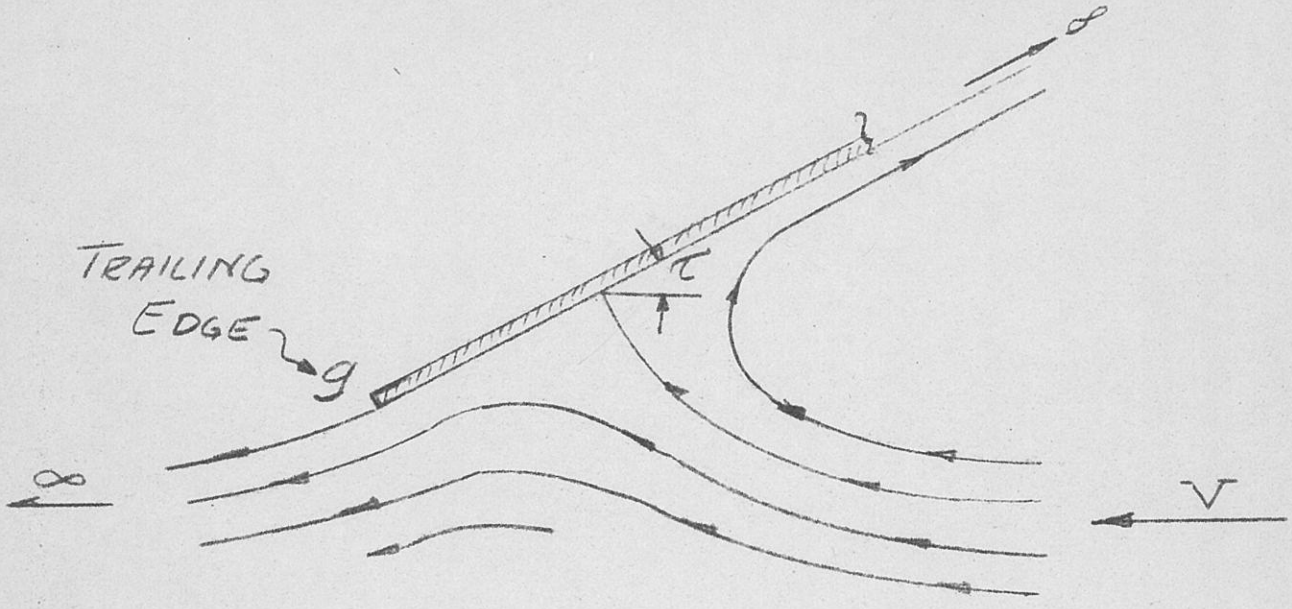

FIG. 35a

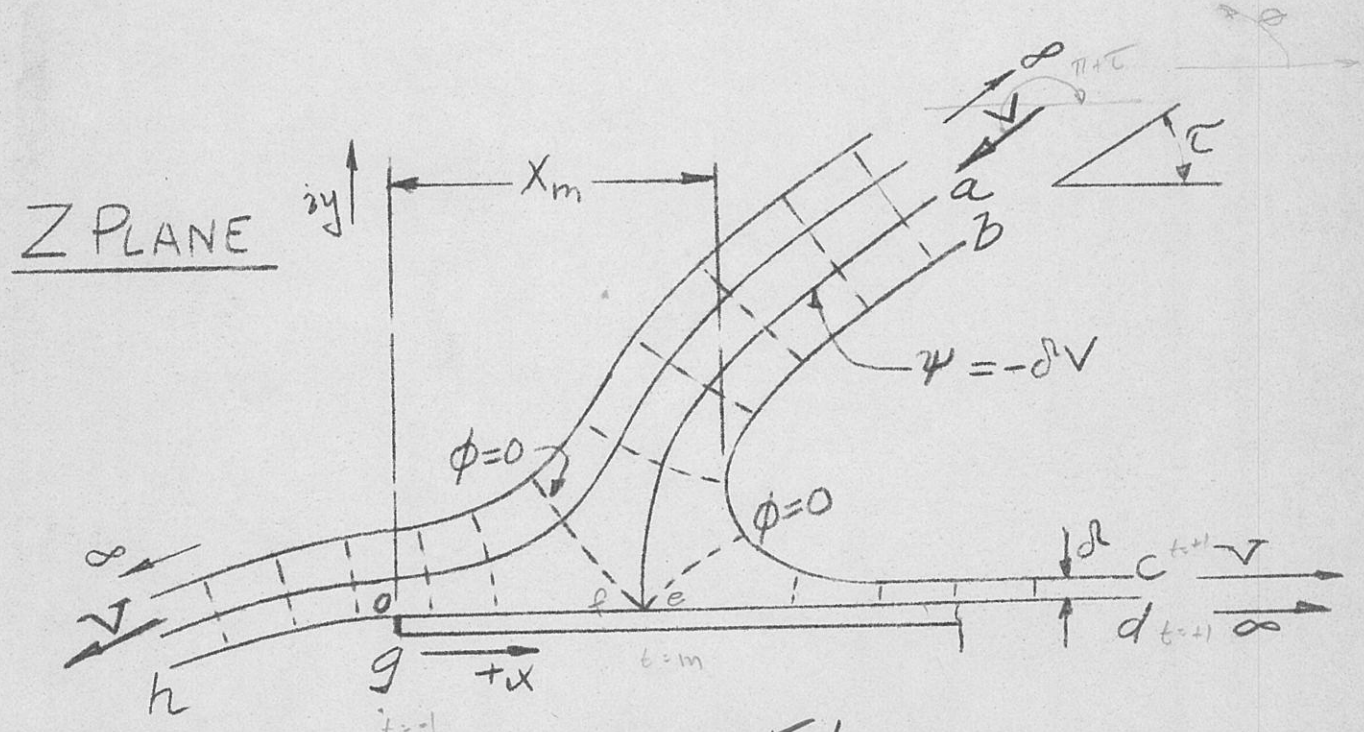

FIG. 35b

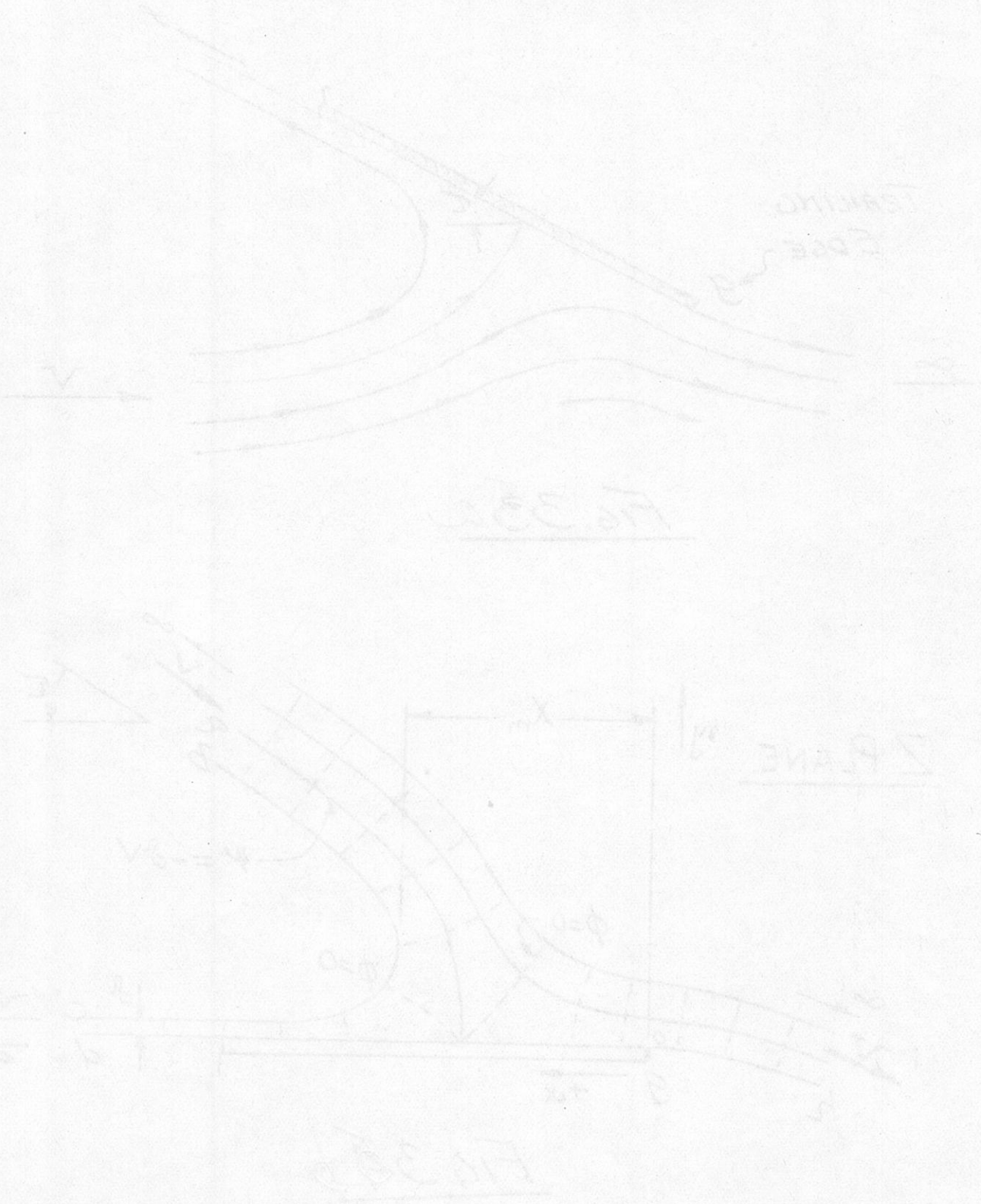

PRESSURE DISTRIBUTION ON A DOUBLY INFINITE PLANE BOUNDARY IN SPRAY ROOT REGION

FIGURE 34

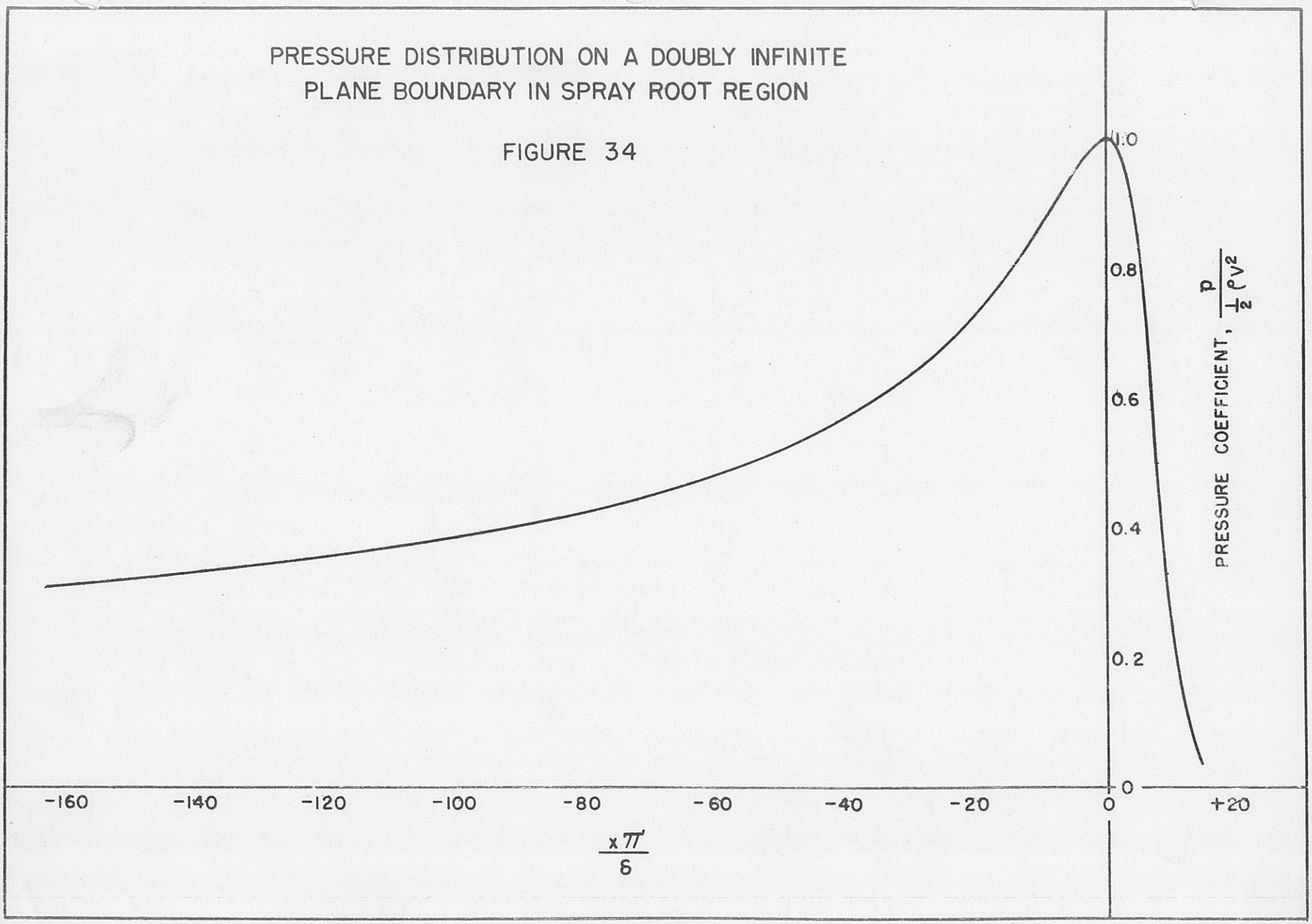

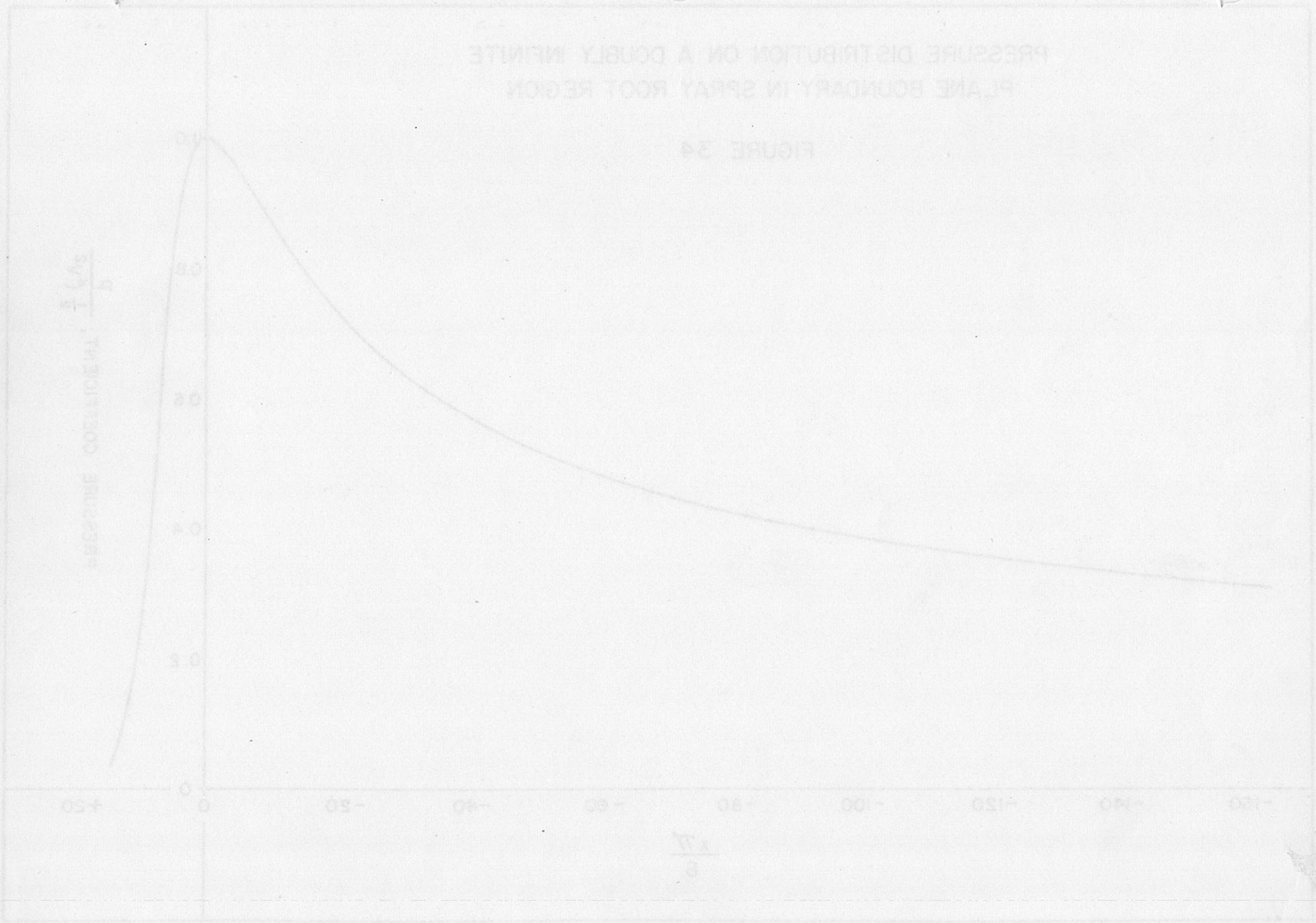

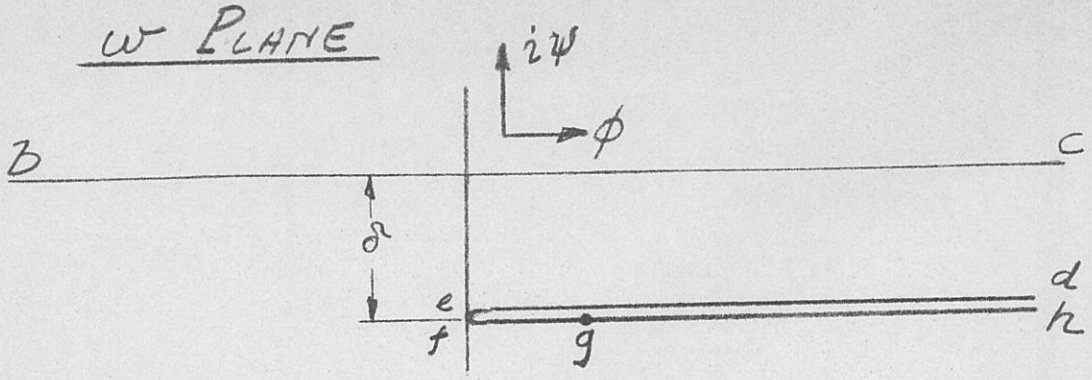

FIG. 35C

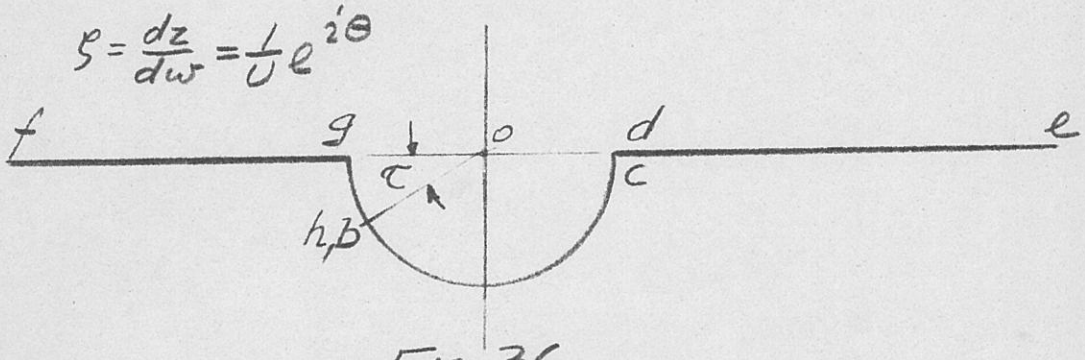

FIG. 36

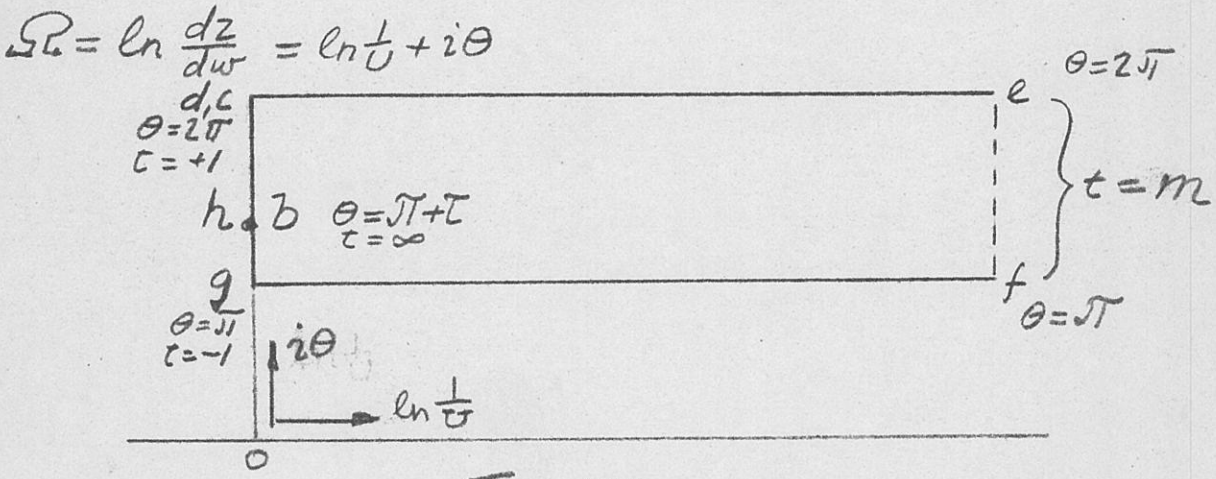

FIG. 37

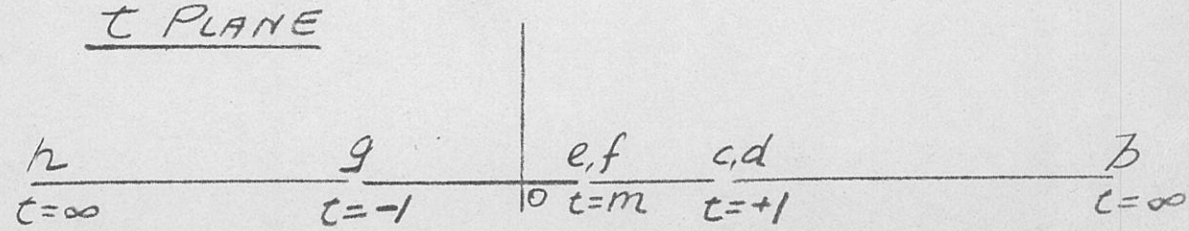

FIG. 38

VARIATION WITH TRIM ANGLE OF SPRAY AND WAKE SURFACE SHAPES AT CONSTANT WETTED LENGTH

FIGURE

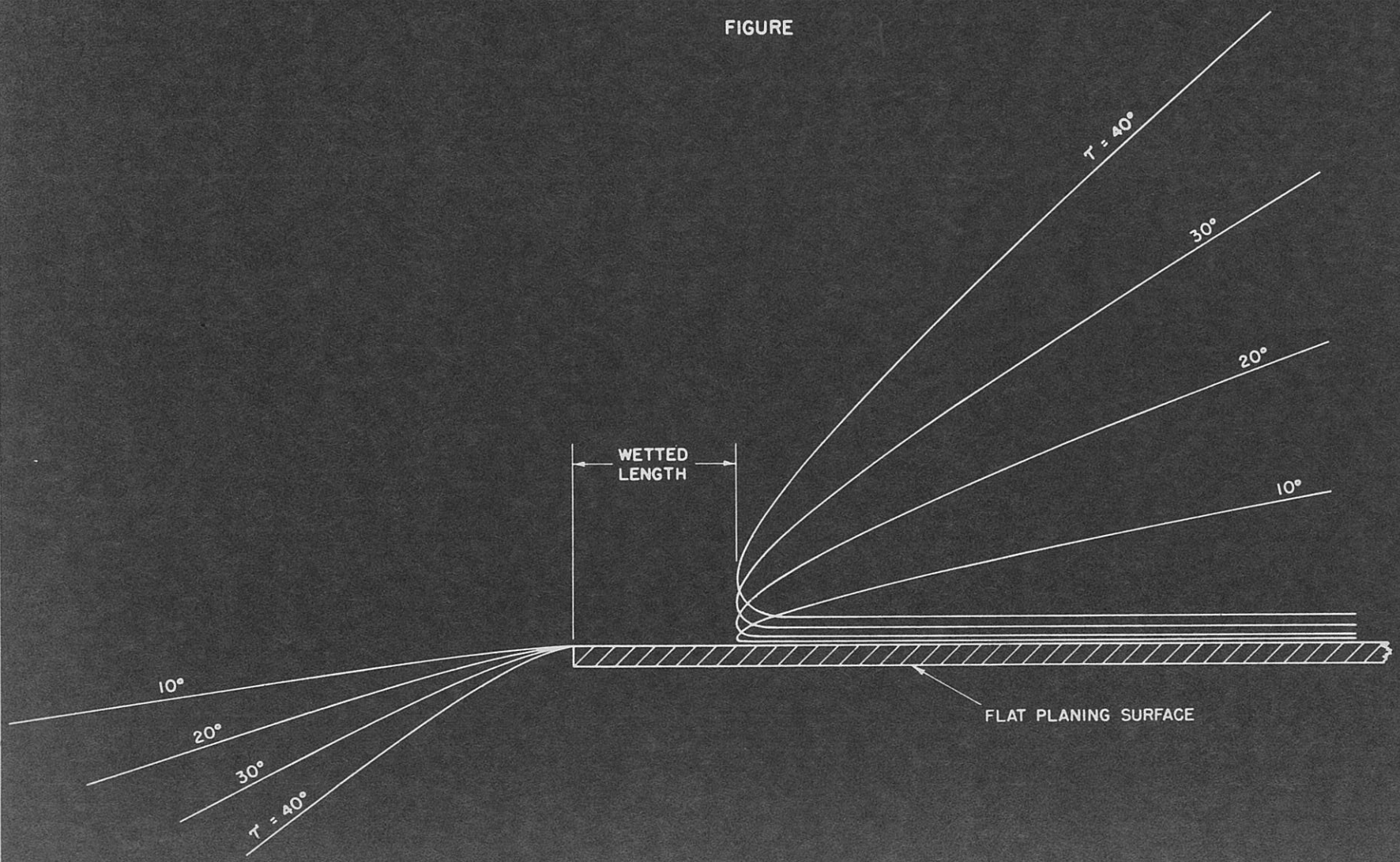

Figure 39

FIGURE

VARIATION WITH TRIM ANGLE OF PRESSURE DISTRIBUTION OVER FLAT PLANING SURFACE

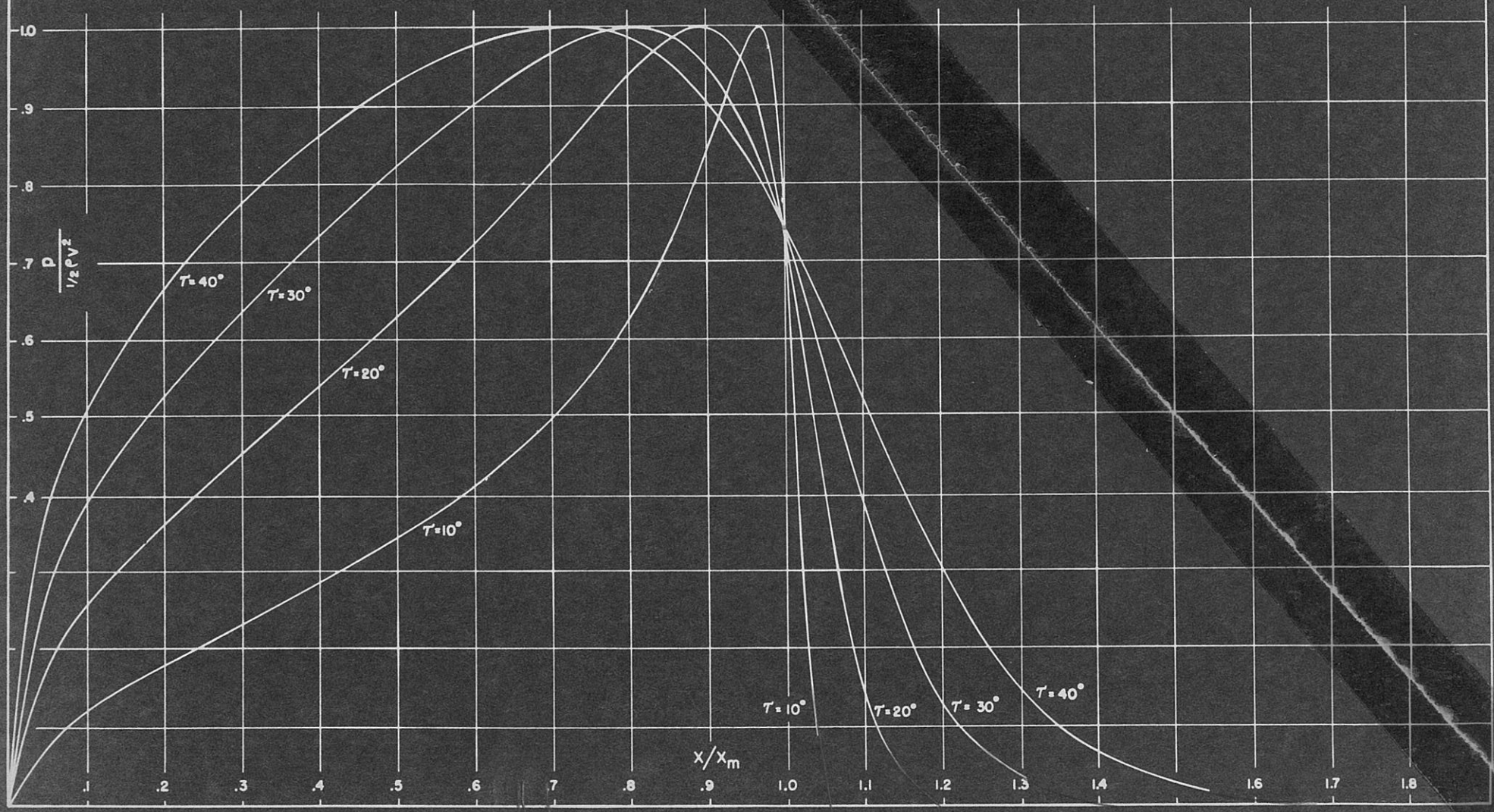

EXPERIMENTAL TOWING TANK
STEVENS INSTITUTE OF TECHNOLOGY
HOBOKEN, NEW JERSEY

Figure 40

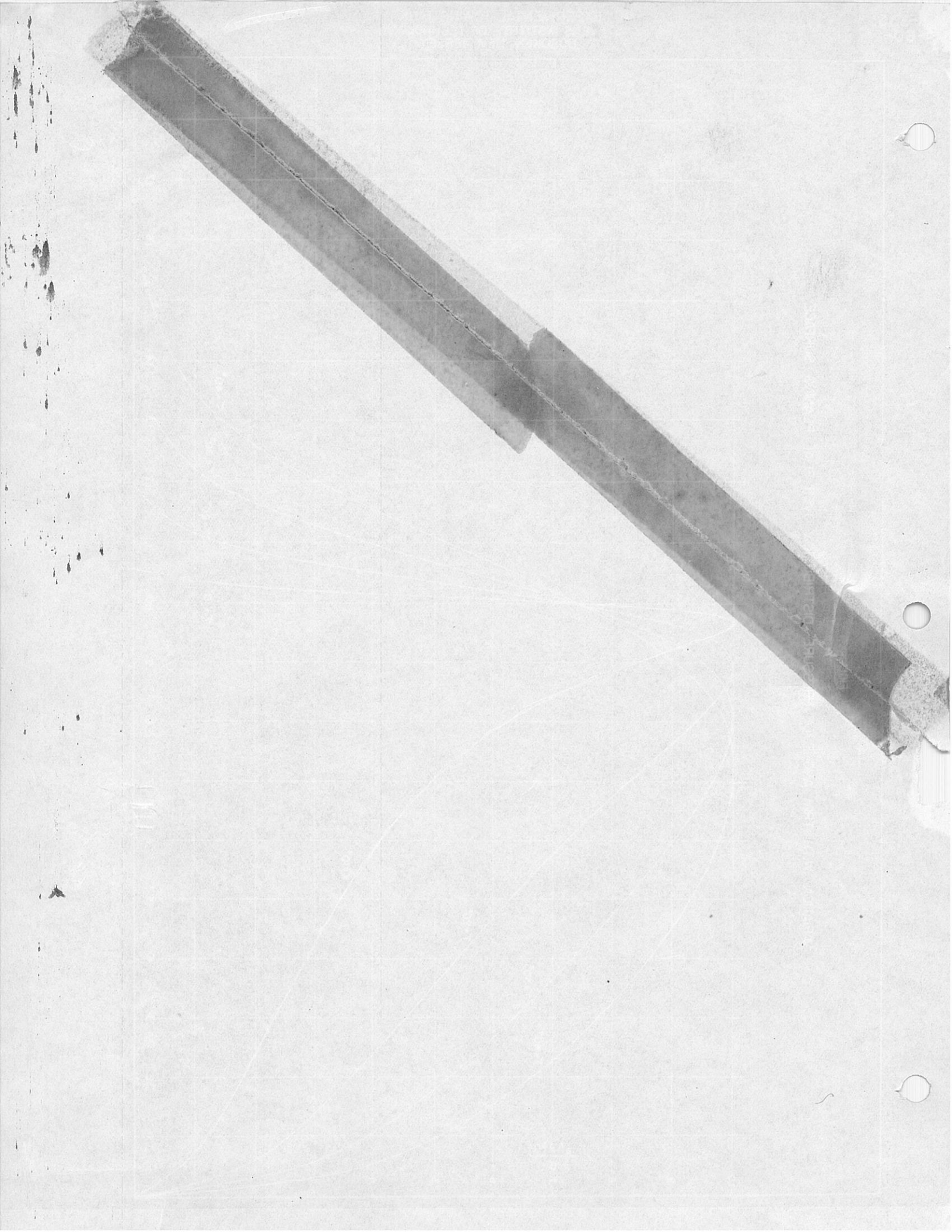

DATE _____ INITIALS _____ FILE _____

SPRAY THICKNESS AND WETTED LENGTH VARIATION WITH TRIM ANGLE

FIGURE

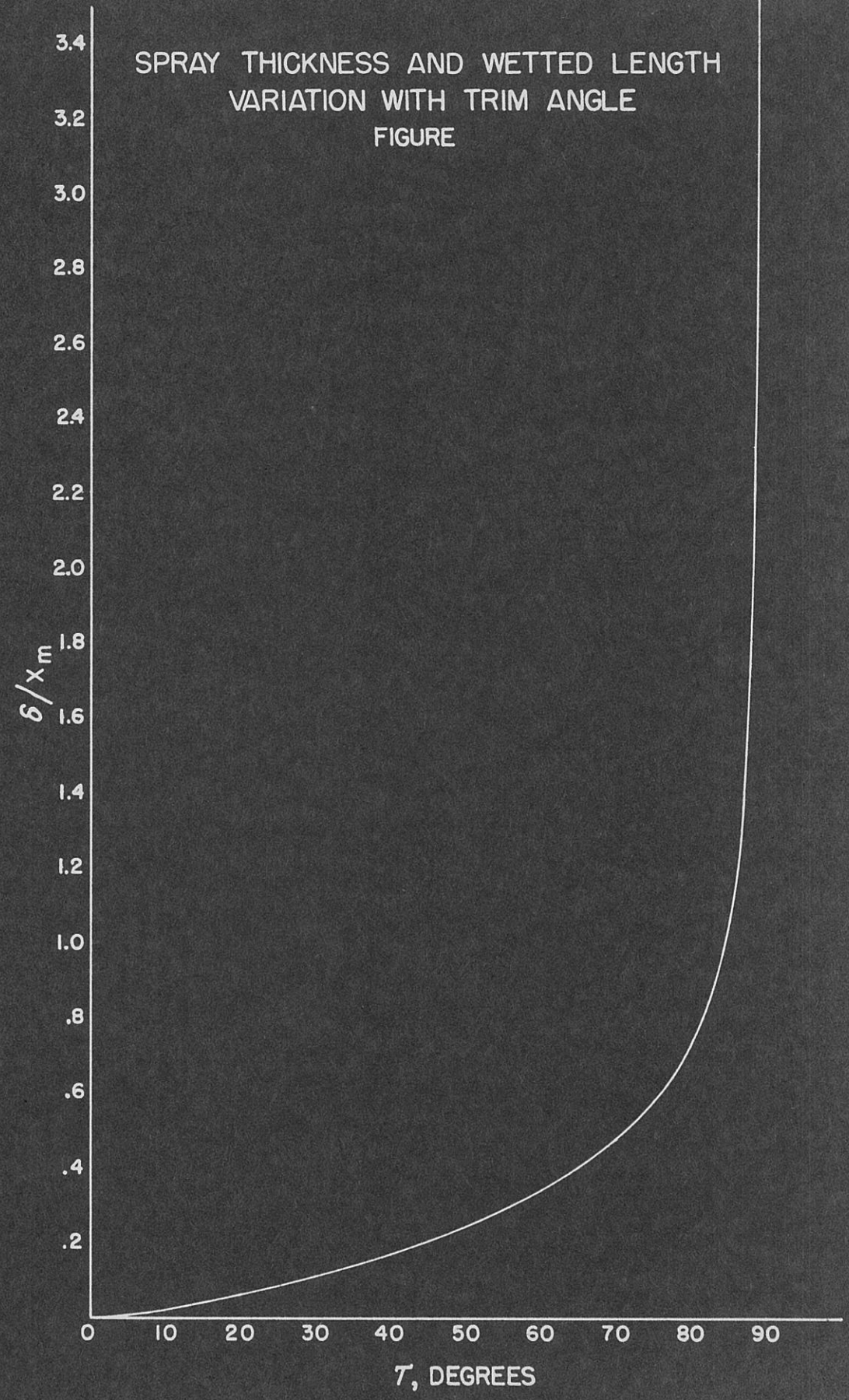

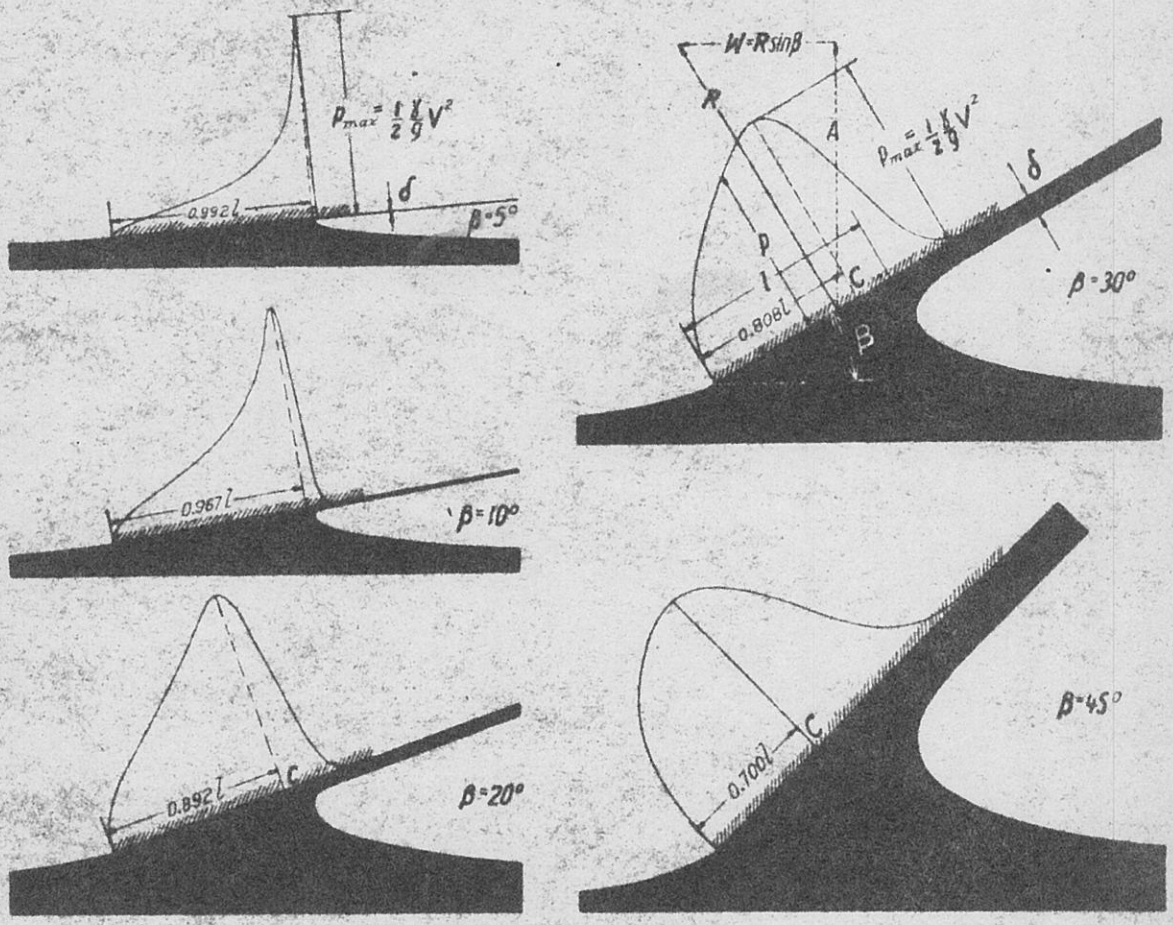

Figure 39a.– Surface of fluid and pressure distribution for flat plates of infinite width in gravity-free motion. For plates of finite width angle β would be replaced by β_w according to equation (18); for short plates of infinite width under gravity effect angle β is replaced by β_w according to equation (29).

NO. 359-11. 10 × 10 to the half inch, 5th lines accented.
Engraving, 7 × 10 in.
MADE IN U.S.A.
KEUFFEL & ESSER CO.

FIG. 43

COMPARISON OF THEORETICAL AND EXPERIMENTAL DATA ON THE LIFT COEFFICIENT

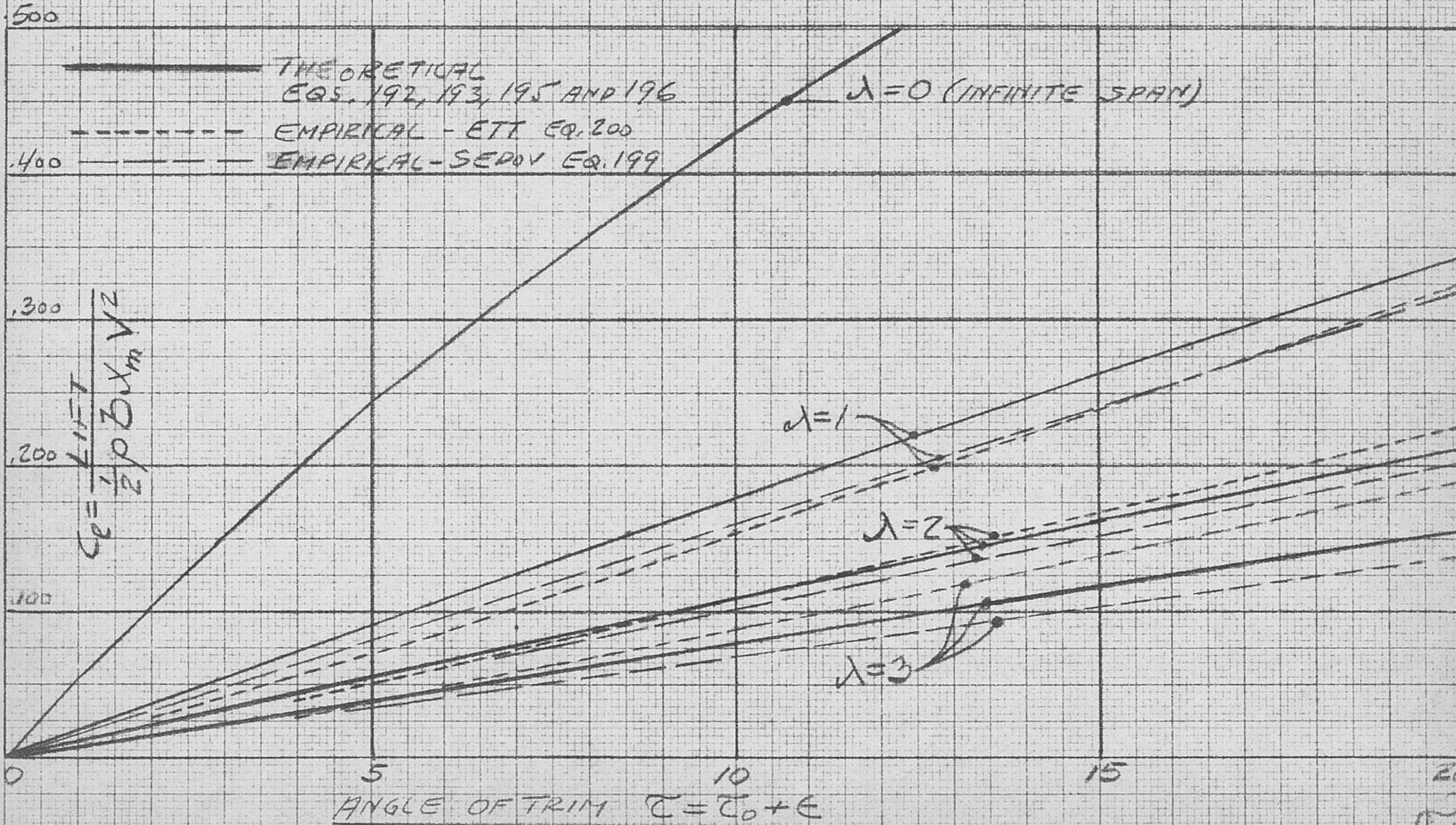

D.K.
5-2-1950

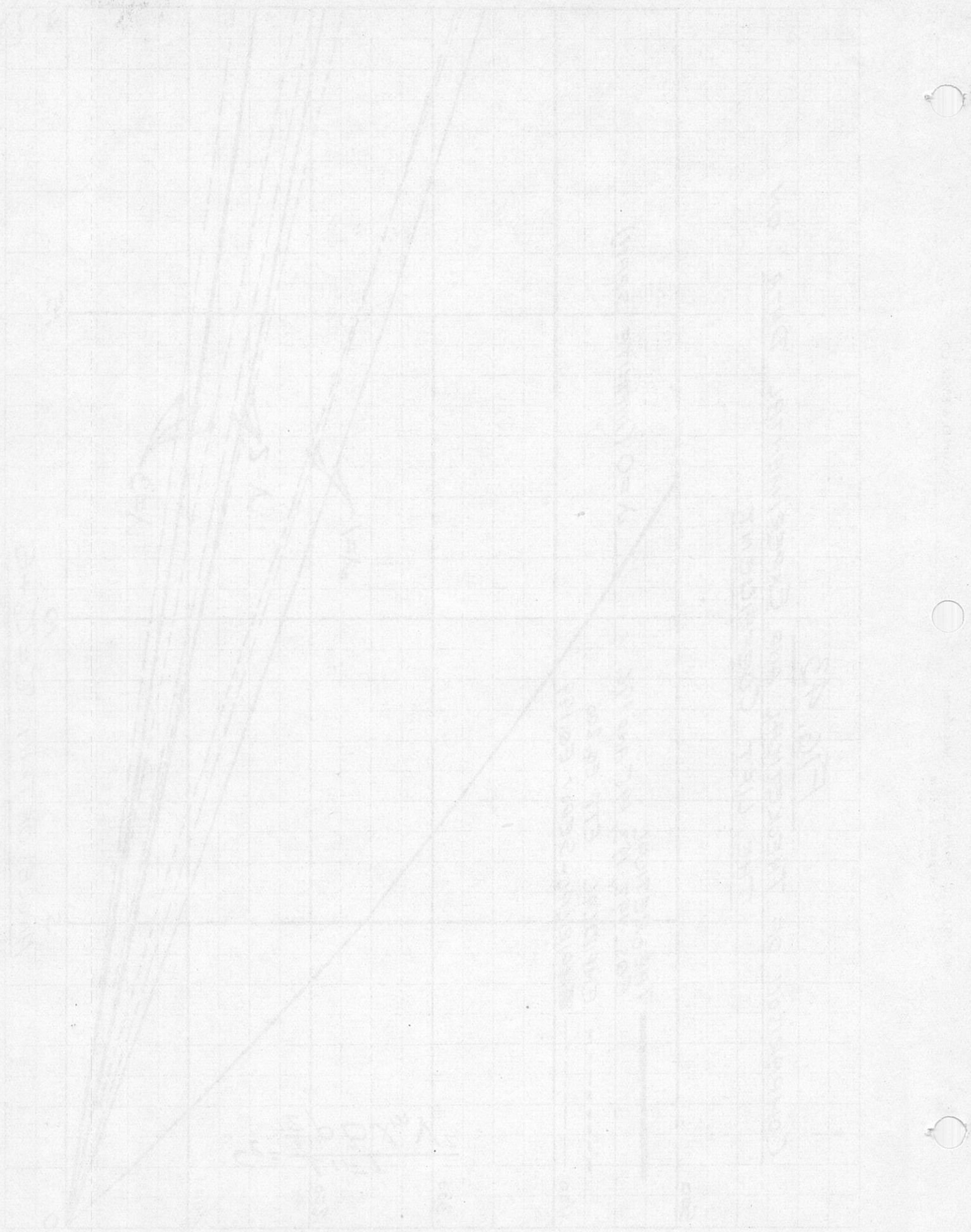

or

$$w = \frac{8L}{\pi \rho b^2 V} \tag{187}$$

In order to determine the coefficient k, defining the velocity at the center of pressure of the plate, consider the energy imparted to the fluid. The energy imparted by the lift L and fluid velocity kw is:

$$kwL = \frac{1}{8}\pi\rho b^2 V k w^2 \tag{188}$$

On the other hand the energy left in the mass of fluid moving with the velocity w is (mass)$\times w^2/2$, or

$$\frac{1}{8}\pi\rho b^2 V w^2/2 \tag{189}$$

Since the energy left in the fluid is equal to the work done by the lift force, the expressions (188) and (189) are evidently equal, and it follows that k = 1/2 I.e. downwash velocity at the plate is half of the final or total downwash velocity. The angle of downwash ϵ at the center of pressure of the plate is therefore:

$$\epsilon = \frac{1}{2}\frac{w}{V} = \frac{4L}{\pi\rho b^2 V^2} \quad *) \tag{190}$$

Eq. (184) gives the normal force F per unit of span. For the span b, letting cos τ = 1, we have

$$L = bF = \frac{\rho b V^2 \chi_m}{2} f(\tau) \tag{191}$$

and

$$\epsilon = \frac{2}{\pi}\frac{\chi_m}{b} f(\tau) = \frac{2}{\pi}\lambda f(\tau) \tag{192}$$

Also dividing Eq. (191) by $1/2\,\rho b^2 V^2$ gives:

$$C_L = \frac{\chi_m}{b} f(\tau) = \lambda f(\tau) \tag{193}$$

and

$$\left.\begin{aligned} \epsilon &= \frac{2}{\pi} C_L \\ \text{or in degrees:}\quad \epsilon &= 36.5\, C_L \end{aligned}\right\} \tag{194}$$

*) AS GIVEN IN REF. 13

18. Comparison of the Experimental and Theoretical Data for the Lift Coefficient.

The value of the lift coefficient, based on Wagner's theory of the planing surface with a finite trailing edge, is given by a very simple expression (193), where f (τ) is given by Eq. (185) as

$$f(\tau) = \frac{\pi\tau \sin\tau_e}{2+\pi \sin\tau_e} \tag{195}$$

The angle τ entering into this expression is the effective angle of trim measured from the direction of the velocity vector, and will be designated thereafter as τ_e . The velocity vector, however, is inclined by the angle ϵ , so that the angle of trim τ measured with respect to the undisturbed water level, or with respect to the direction of motion is

$$\tau = \tau_e + \epsilon \tag{196}$$

The calculations of the C_L are given in Table V , for a series of the arbitrarily assigned values of τ_e , on the basis of Eqs. (193) and (195). The angle ϵ is subsequently computed on basis of C_L by Eq. (194), then τ by Eq. (196), and finally C_L is plotted vs. τ for several values of λ .

The average values of the experimental data for the flat planing surfaces are given by the empirical formulae taken from Ref. 8 and 14 :

Sedov's Formula:

$$C_L = \frac{\tau}{57.3}\left[\frac{0.7\pi\lambda}{1+1.4\lambda} + \lambda(0.92\lambda - 0.38)/C_v^2\right] \tag{197}$$

Stevens Experimental Towing Tank formula:

$$C_L = \tau^{1.1}\left[0.0120\lambda^{1/2} + 0.0095(\lambda/C_v)^2\right] \tag{198}$$

In above the angle τ is in degrees.

Theoretical data are based on the fluid devoid of gravity, and with experimental data this corresponds to sufficiently high values of C_v, at which the forces of gravity can be neglected in comparison with the dynamic forces, and second terms in both of the above expressions vanish.

On Fig. 43 , theoretical curves from the Table V are shown by solid lines, the data from Sedov's formula by the dashed lines and Stevens E.T.T. by dotted lines.